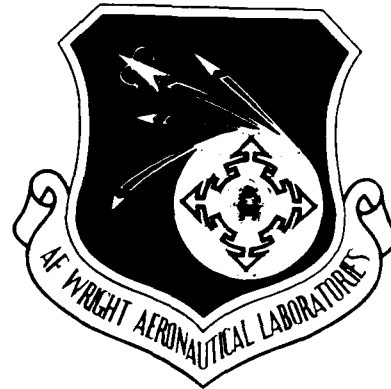


2

AFWAL-TR-88-2131



AD-A206 064

ELECTRICALLY COMPENSATED CONSTANT SPEED DRIVE
(MODEL No. 60 ECEPGS 02)

R. OLSON, K. ANDERSON, S. CHAJ-NAM NG,
B. DISHNER, C. FERREIRA - SUNDSTRAND
ATG RESEARCH AND DEVELOPMENT
SUNDSTRAND CORPORATION
4747 HARRISON AVENUE
ROCKFORD, ILLINOIS 61125-7002



20 JANUARY 1989

FINAL REPORT FOR THE PERIOD SEPTEMBER 1985 THROUGH JUNE 1988

Approved for public release; distribution is unlimited.

AERO PROPULSION LABORATORY
AIR FORCE WRIGHT AERONAUTICAL LABORATORIES
AERONAUTICAL SYSTEMS DIVISION (AFSC)
UNITED STATES AIR FORCE
WRIGHT-PATTERSON AFB OHIO 45433-6563

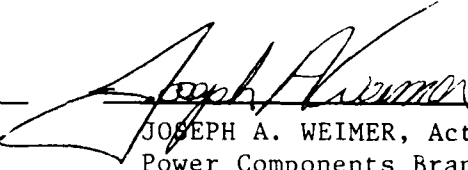
80 0 0 0 0 0

NOTICE

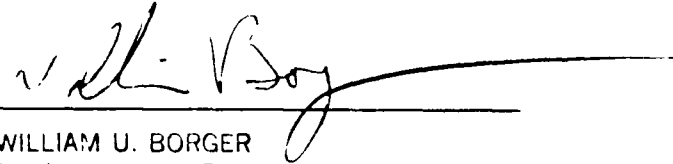
When Government drawings, specifications, or other data are used for any purpose other than in connection with a definitely Government-related procurement, the United States Government incurs no responsibility or any obligation whatsoever. The fact that the Government may have formulated or in any way supplied the said drawings, specifications, or other data, is not to be regarded by implication, or otherwise in any manner construed, as licensing the holder, or any other person or corporation; or as conveying any rights or permission to manufacture, use, or sell any patented invention that may in any way be related thereto.

This report has been reviewed by the Office of Public Affairs (ASD/PA) and is releasable to the National Technical Information Service (NTIS). At NTIS, it will be available to the general public, including foreign nations.

This technical report has been reviewed and is approved for publication.

	
ANGELA MORRIS, Project Engineer Power Components Branch Aerospace Power Division Aero Propulsion and Power Laboratory	JOSEPH A. WEIMER, Acting TAM Power Components Branch Aerospace Power Division Aero Propulsion and Power Laboratory

FOR THE COMMANDER


WILLIAM U. BORGER
Chief, Aerospace Power Division
Aero Propulsion & Power Laboratory

If your address has changed, if you wish to be removed from our mailing list, or if the addressee is no longer employed by your organization please notify AFWAL/POOC-1, W-PAFB, OH 45433-6523 to help us maintain a current mailing list.

Copies of this report should not be returned unless is required by security considerations, contractual obligations, or notice on a specific document.

UNCLASSIFIED

SECURITY CLASSIFICATION OF THIS PAGE

Form Approved
OMB No. 0704-0188

REPORT DOCUMENTATION PAGE

1a. REPORT SECURITY CLASSIFICATION Unclassified		1b. RESTRICTIVE MARKINGS	
2a. SECURITY CLASSIFICATION AUTHORITY		3. DISTRIBUTION / AVAILABILITY OF REPORT Approved for public release; distribution unlimited.	
2b. DECLASSIFICATION / DOWNGRADING SCHEDULE		4. PERFORMING ORGANIZATION REPORT NUMBER(S)	
4. PERFORMING ORGANIZATION REPORT NUMBER(S)		5. MONITORING ORGANIZATION REPORT NUMBER(S) AFWAL-TR-88-2131	
6a. NAME OF PERFORMING ORGANIZATION Sundstrand ATG	6b. OFFICE SYMBOL (If applicable)	7a. NAME OF MONITORING ORGANIZATION Aero Propulsion and Power Laboratory Air Force Wright Aeronauticals Laboratory, AFSC	
6c. ADDRESS (City, State, and ZIP Code) 4747 Harrison Ave Rockford, Illinois 61125-7002		7b. ADDRESS (City, State, and ZIP Code) AFWAL/POOC-1 WPAPB, OH 45433-6563	
8a. NAME OF FUNDING / SPONSORING ORGANIZATION Aero Propulsion & Power Lab.	8b. OFFICE SYMBOL (If applicable) AFWAL/POOC-1	9. PROCUREMENT INSTRUMENT IDENTIFICATION NUMBER F33615-85-C-2590	
8c. ADDRESS (City, State, and ZIP Code) Wright Patterson AFB, Ohio 45433-6563		10. SOURCE OF FUNDING NUMBERS	
		PROGRAM ELEMENT NO. 62203F	PROJECT NO. 3145
		TASK NO. 29	WORK UNIT ACCESSION NO. L3
11. TITLE (Include Security Classification) Electrically Compensated Constant Speed Drive			
12. PERSONAL AUTHOR(S) R. Olson, K. Anderson, S. Chaj-Nam NG, B. Dishner, C. Ferreira			
13a. TYPE OF REPORT Final	13b. TIME COVERED FROM 9/85 TO 6/88	14. DATE OF REPORT (Year, Month, Day) 1-20-89	15. PAGE COUNT 161
16. SUPPLEMENTARY NOTATION			
17. COSATI CODES		18. SUBJECT TERMS (Continue on reverse if necessary and identify by block number)	
FIELD	GROUP	SUB-GROUP	
01	03		
10	02		
		Aircraft electrical power, generators, power conversion, constant speed drive.	
19. ABSTRACT (Continue on reverse if necessary and identify by block number)			
<p>The concept of an electric constant speed drive is one of the approaches usable to overcome those barriers and issues for a 400-Hz power system.</p> <p>The principle of concept investigated is to use electronic controlled PM machines in conjunction with a summing differential to attain a constant speed from a variable speed input. An approach is identified, design analysis completed, and hardware of breadboard nature fabricated to demonstrate concept principle.</p>			
20. DISTRIBUTION / AVAILABILITY OF ABSTRACT <input checked="" type="checkbox"/> UNCLASSIFIED/UNLIMITED <input type="checkbox"/> SAME AS RPT. <input type="checkbox"/> DTIC USERS		21. ABSTRACT SECURITY CLASSIFICATION UNCLASSIFIED	
22a. NAME OF RESPONSIBLE INDIVIDUAL Angela Morris		22b. TELEPHONE (Include Area Code) (513) 255-6016	22c. OFFICE SYMBOL AFWAL/POOC-1

TABLE OF CONTENTS

SECTION		PAGE
1.0	INTRODUCTION	1
1.1	NOVEL TECHNIQUES IN 400 Hz ELECTRIC POWER GENERATION . .	1
1.2	THE ECCSD PROGRAM.	1
1.2.1	DESIGN CONSTRAINTS	2
1.2.2	STUDY TIMETABLE.	2
2.0	SYSTEM	5
2.1	ECCSD OPTIONS.	6
2.1.1	DIFFERENTIAL ALWAYS ABOVE OPTIONS.	7
2.1.1.1	CONTROLLER ABOVE STRAIGHT THROUGH.	8
2.1.2	MIDRANGE DIFFERENTIAL OPTIONS.	8
2.1.2.1	MIDRANGE OPTION CONTROLLER	9
2.1.3	DIFFERENTIAL ALWAYS BELOW OPTIONS.	11
2.1.3.1	ALWAYS BELOW CONTROLLER TOPOLOGY	12
2.1.4	PARALLEL DIFFERENTIAL OPTION	13
2.1.5	PM MOTOR/GENERATOR	13
2.1.5.1	SYSTEM SPEED	14
2.1.5.2	PM MOTOR TORQUE REQUIREMENTS	16
2.1.6	SYSTEM TRADE STUDY	18
2.1.6.1	TRADE ANALYSIS	21

n For	<input checked="" type="checkbox"/>
MI	<input type="checkbox"/>
	<input type="checkbox"/>
	<input type="checkbox"/>

Approved for Release by NSA on 05-08-2014 pursuant to E.O. 13526
 CONFIDENTIAL

A-1

TABLE OF CONTENTS (Continued)

SECTION	PAGE
2.1.6.2 CONTROLLER	22
2.1.6.3 PM MACHINES.	23
2.1.7 SYSTEM SELECTION	23
2.1.7.1 SELECTION CONSIDERATIONS	23
2.2 DESCRIPTION OF SELECTED SYSTEM CONFIGURATION	30
2.2.1 SPEED RANGE AND SYSTEM GEARING	30
2.2.2 SYSTEM POWER RATING.	31
2.2.3 ELECTRIC POWER PROCESSOR (CONTROLLER).	33
2.2.4 CONTROLS AND SIMULATION.	35
2.2.4.1 MODEL DESCRIPTIONS	35
2.2.4.2 CONTROLLER OBJECTIVES.	38
2.2.4.3 CONTROLLER FOR PMA/SCR BRIDGE.	39
2.2.4.4 CONTROLLER FOR PMB/INVERTER.	40
2.2.4.5 SIMULATION RESULTS	40
3.0 POWER ELECTRONICS.	45
3.1 AC/DC CONVERTER.	45
3.1.1 DETAILED DESCRIPTION	46
3.1.1.1 POWER MODULE ASSEMBLY.	46
3.1.1.2 SNUBBER CIRCUIT.	46

TABLE OF CONTENTS (Continued)

SECTION	PAGE
3.1.1.3 LC FILTER.	49
3.1.1.4 PHASE DELAY CONTROLS.	50
3.1.1.5 CONTROL ELECTRONICS.	55
3.1.1.6 GATE DRIVES.	55
3.1.2 PERFORMANCE VERIFICATION OF THE THYRISTOR CONVERTER. . .	56
3.1.2.1 OPEN LOOP TEST	56
3.1.2.2 DIODE REVERSE RECOVERY	56
3.1.2.3 HARMONIC INSTABILITY BETWEEN CONVERTER AND SOURCE. . . .	59
3.1.2.4 FREQUENCY RESPONSE TEST.	63
3.1.2.5 STEP RESPONSE TEST	66
3.1.2.6 IMPACT LOAD TEST	66
3.2 INVERTER/MOTOR DRIVE	68
3.2.1 MOTOR CONTROL STRATEGY	68
3.2.2 INVERTER SPECIFICS	72
3.2.3 INVERTER TESTING	76
4.0 PERMANENT MAGNET MACHINES.	85
4.1 DESIGN OBJECTIVES.	85
4.2 ELECTROMAGNETIC ANALYSIS	85
4.3 THERMAL ANALYSIS	97

TABLE OF CONTENTS (Continued)

SECTION	PAGE
4.4	BEARING ANALYSIS 104
4.5	ROTOR CRITICAL SPEED 105
4.6	ROTOR STRESS ANALYSIS. 107
4.7	TEST SETUP 116
5.0	GEARBOX. 119
5.1	DESIGN OBJECTIVES. 119
5.2	DESIGN PARAMETERS. 119
5.3	GEAR BOX INTERFACE 119
5.4	HOUSING DESIGN 119
5.5	GEAR DESIGN. 122
5.6	BEARING DESIGN 122
5.7	GEAR BOX LUBRICATION AND COOLING 123
5.8	GEAR BOX TEST HISTORY. 123
6.0	SYSTEM TEST. 141
6.1	TESTING WITH STATIC DC SUPPLY. 141
6.2	SCR BRIDGE AND INVERTER COMBINED TESTING 143
6.3	SYSTEM DEMONSTRATION : 146
7.0	CONCLUSIONS AND RECOMMENDATIONS. 149

TABLE OF CONTENTS (Concluded)

SECTION	PAGE
Appendix A DESIGN CONSTRAINTS	153
Appendix B ELECTROMAGNETIC DESIGN TRADE STUDY	159

LIST OF FIGURES

FIGURE		PAGE
1.1	ELECTRICALLY COMPENSATED CONSTANT SPEED DRIVE	1
1.1A	PROGRAM SCHEDULE.	3
2.1	DIFFERENTIAL.	5
2.2	INPUT DIFFERENTIAL ALWAYS ABOVE	7
2.3A	INPUT DIFFERENTIAL ALWAYS ABOVE CONTROLLER/SYSTEM	8
2.3B	CONTROLLER TOPOLOGY ALWAYS ABOVE OPTION	8
2.4	OUTPUT DIFFERENTIAL MIDRANGE.	9
2.5	CONTROLLER POWER TOPOLOGY	10
2.6	MIDRANGE CONFIGURATIONS	11
2.7	ALWAYS BELOW TOPOLOGY	12
2.8	OUTPUT DIFFERENTIAL ALWAYS BELOW.	12
2.9	PARALLEL DIFFERENTIAL	13
2.10	DIFFERENTIAL MAKEUP SPEED CHARACTERISTIC.	15
2.11	PMB TORQUE VS INPUT SPEED INPUT DIFFERENTIAL, 2.0 P.U. LOAD	16
2.12	TRIM POWER VS INPUT SPEED INPUT DIFFERENTIAL, 2.0 P.U. LOAD	17
2.13	PMA TORQUE VS INPUT SPEED OUTPUT DIFFERENTIAL, 2.0 P.U. LOAD	17
2.14	TRIM POWER VS INPUT SPEED OUTPUT DIFFERENTIAL, 2.0 P.U. LOAD	18

LIST OF FIGURES (CONTINUED)

FIGURE		PAGE
2.15	OUTPUT DIFFERENTIAL SIMPLIFIED MODEL FOR EFFICIENCY CALCULATIONS	18
2.16	INPUT DIFFERENTIAL SIMPLIFIED MODEL FOR EFFICIENCY CALCULATIONS	19
2.17	CONTROLLER LOSSES	19
2.18	MOTOR LOSSES.	20
2.19	SYSTEM EFFICIENCY	20
2.20	MODULAR SYSTEM STRUCTURAL SCHEMATIC	21
2.21	REAL TIME SIMULATION HARDWARE	22
2.22	OUTPUT DIFFERENTIAL MID RANGE	24
2.23	INPUT DIFFERENTIAL ALWAYS ABOVE	25
2.24	PARALLEL DIFFERENTIAL	26
2.25	OUTPUT DIFFERENTIAL ALWAYS BELOW.	26
2.26	SYSTEM WEIGHT TRADES.	27
2.27	RELIABILITY	28
2.28	SELECTED TOPOLOGY	29
2.29	SYSTEM BLOCK DIAGRAM.	30
2.30	ELECTRIC POWER PROCESSOR TOPOLOGY	34
2.31	CONTROLLER BLOCK DIAGRAM.	36
2.32	MACHINE DESIGN PARAMETERS USED IN MODEL	36
2.33	SPICE MODEL FOR SCR BRIDGE.	37

LIST OF FIGURES (CONTINUED)

FIGURE		PAGE
2.34	SCR BRIDGE OUTPUT CHARACTERISTICS.	37
2.35	EASY 5 INVERTER MODEL.	38
2.36	DESIRED TRANSIENT RESPONSE OF SYSTEM	39
2.37	DC LINK VOLTAGE.	39
2.38	5000 RPM LOAD-ON	42
2.39	9000 RPM DECEL W/OVERLOAD.	43
2.40	9000 RPM DECEL W/OVERLOAD.	44
3.1	BLOCK SCHEMATIC OF 3 ϕ SIX SCR FW BRIDGE REGULATOR. . . .	45
3.2	POWER CIRCUIT.	47
3.3	POWER MODULE ASSEMBLY.	48
3.4	BLOCK DIAGRAM OF PHASE DELAY CONTROL	50
3.5	TIMING DIAGRAM OF PHASE DELAY CONTROL CIRCUIT.	53
3.6	PHASE SHIFT CIRCUIT.	54
3.7A	THYRISTOR GATE CURRENT WAVEFORM.	55
3.7B	THYRISTOR GATE VOLTAGE AND CURRENT WAVEFORMS	56
3.8	BRIDGE INPUT VOLTAGE AND CURRENT	57
3.9	DIODE REVERSE RECOVERY	58

LIST OF FIGURES (CONTINUED)

FIGURE		PAGE
3.10	EFFECTS OF LOAD CURRENT AND IMPEDANCE ON HARMONIC INSTABILITY.	59
3.11	POWER SPECTRAL ANALYSIS OF FILTERED GENERATOR TERMINAL VOLTAGE (B)	61
3.12	HARMONIC INSTABILITY BETWEEN CONVERTER AND WEAK AC SOURCE	62
3.13	OPEN LOOP FREQUENCY RESPONSE EXCLUDING COMPENSATOR . . .	63
3.14	OVERALL OPEN LOOP FREQUENCY RESPONSE WITH P.I. COMPENSATION.	64
3.15	LINEAR APPROXIMATION TRANSFER FUNCTION OF SCR BRIDGE . .	65
3.16	OUTPUT RESPONSE OF CONVERTER FOR A STEP INPUT.	66
3.17	TRANSIENT TEST WITH STEP LOAD (30 A - 120 A)	67
3.18	INVERTER SCHEMATIC AND BLOCK DIAGRAM	68
3.19	MOTOR VECTOR DIAGRAMS.	69
3.20	HYSTERESIS CURRENT CONTROL WAVEFORM GENERATION	69
3.21	HYSTERESIS CURRENT CONTROL SIMULATION RESULT	70
3.22	COMMUTATION ANGLE CONTROL WAVEFORM	70
3.23	MOTOR CONTROL BLOCK DIAGRAM.	71
3.24	SWITCH MODULE.	72
3.25	SWITCH MODULE SCHEMATIC.	72

LIST OF FIGURES (CONTINUED)

FIGURE		PAGE
3.26	INVERTER SINGLE PHASE.	73
3.27	INVERTER PHOTO WITHOUT BASE DRIVES	74
3.28	INVERTER PHOTO WITH BASE DRIVES.	75
3.29	PMB SIMULATION RESULTS	76
3.30	STATIC TEST WAVEFORMS.	76
3.31	INTERIM TEST SET-UP.	77
3.32	INTERIM TEST MOTOR CURRENTS.	77
3.33	INPUT TO OUTPUT RESPONSE MEASUREMENT	78
3.34	OPEN LOOP BODE PLOTS, NO-LOAD.	80
3.35	OPEN LOOP BODE PLOTS, WITH LOAD.	81
3.36	OUTPUT SPEED CONTROL BLOCK DIAGRAM	82
3.37	CLOSED LOOP TRANSFER FUNCTION BODE PLOT.	83
4.1	PERMANENT MAGNET (PMA) GENERATOR	86
4.2	PERMANENT MAGNET (PMB) MOTOR	87
4.3	PMA/PMB REQUIRED OUTPUT POWER VS SPEED	88
4.4	PM MACHINE FLUX PLOTS AT NO-LOAD AND PEAK LOAD CONDITIONS	90
4.5	PMA NO-LOAD PHASE VOLTAGE WAVEFORM AT 25,000 RPM AND 150° F OIL.	92

LIST OF FIGURES (CONTINUED)

FIGURE		PAGE
4.6	PMA MEASURED NO-LOAD VOLTAGE FREQUENCY SPECTRUM AT 5,000 RPM AND 150° F OIL.	93
4.7	PMB MEASURED NO-LOAD VOLTAGE FREQUENCY SPECTRUM AT 5,000 RPM AND 150° F OIL	94
4.8	PMA PHASE VOLTAGE VS LOAD CURRENT AT 14,040 RPM AND 150° F INLET OIL.	96
4.9	PMA AND PMB PHYSICAL CROSS SECTIONAL VIEW.	98
4.10	LOCATIONS OF SINDA NODES FOR TYPICAL CROSS SECTION OF THE ROTOR AND STATOR ASSEMBLIES	99
4.11	LOCATIONS OF THE THERMAL NODES IN THE PATRAN GEOMETRIC MODEL - PMA GENERATOR.	100
4.12	PMA/PMB OIL FLOW SCHEMATIC AND FLOW RATES.	101
4.13	MACHINE BEARINGS TOTAL POWER LOSS FOR MIL-L-7808 OIL AT 275° F	106
4.14	ROTATING ASSEMBLY OF PMA STATION NUMBERS	108
4.15	MODE SHAPES OF THE PMA ROTOR	109
4.16	MODE SHAPES OF THE PMB ROTOR	110
4.17A	PMA VERTICAL VIBRATION FREQUENCY SPECTRUM - NO-LOAD. . .	111
4.17B	PMA LATERAL VIBRATION FREQUENCY SPECTRUM - NO-LOAD . . .	112
4.18A	PMB VERTICAL VIBRATION FREQUENCY SPECTRUM - NO-LOAD. . .	113
4.18B	PMB LATERAL VIBRATION FREQUENCY SPECTRUM - NO-LOAD . . .	114
4.19	ECCSD SYSTEM TEST SETUP.	117
5.1	GEAR BOX INPUT PAD	120
5.2	GEAR BOX, COVER REMOVED.	121

LIST OF FIGURES (CONTINUED)

FIGURE		PAGE
5.3	DIFFERENTIAL GEAR BOX.	124
5.4	DIFFERENTIAL GEAR SPEED DIAGRAM.	125
5.5	DIFFERENTIAL GEAR BOX.	126
5.6	PROPOSED PRODUCTION GEAR TRAIN	127
5.7	GEAR DESIGN.	128
5.8	GEAR PROFILE	131
5.9	GEAR PROFILE	132
5.10	GEAR PROFILE	133
5.11	GEAR PROFILE	134
5.12	GEAR PROFILE	135
5.13	GEAR PROFILE	136
5.14	DIFFERENTIAL GEAR BOX TEST SCHEMATIC	137
6.1	TYPICAL SYSTEM RESPONSE, 4200 RPM.	142
6.2	INVERTER CURRENT SHOWING MISFIRING	144
6.3	ONE PER REVOLUTION TRANSIENTS.	144
6.4	MOTOR CURRENT TRANSIENT.	145
6.5	MOTOR CURRENT IN RUN MODE.	145

LIST OF FIGURES (CONCLUDED)

FIGURE		PAGE
6.6	MOTOR CURRENT VARIATIONS	146
6.7	EXCESSIVE CURRENT CAUSES SHUT-DOWN	146
6.8	SYSTEM TEST AREA	148

LIST OF TABLES

TABLE		PAGE
1.1	DESIGN CONSTRAINTS	2
1.2	ECCSD DESIGN AND ANALYSIS.	2
2.1	EXAMPLES OF SEVERAL N COMP SPEED RATIOS.	31
2.2	STEADY STATE POWER FLOW.	32
2.3	SIMULATION RESULTS	41
2.4	SIMULATION RESULTS	41
4.1	PM AND PMB NO-LOAD PHASE VOLTAGES.	91
4.2	NO-LOAD VOLTAGE FREQUENCY SPECTRUM IN VOLTS (rms).	91
4.3	PMA LOAD PERFORMANCE: ANALYTICAL VS MEASURED VALUE	95
4.4	PMB ANALYTICAL LOAD PERFORMANCE.	95
4.5	ELECTROMAGNETIC DESIGN SUMMARY	97

LIST OF TABLES

TABLE		PAGE
4.6	THERMAL ANALYTICAL VS TEST RESULTS - 1 P.U. LOAD	102
4.7	TABULATION OF PREDICTED COMPONENT TEMPERATURES FOR MIL-L-7808 AND MIL-L-23699 LUBRICATION OIL PMA GENERATOR.	103
4.8	PMB MEASURED TEMPERATURES AT RATED CURRENT, 40,000 RPM AND 100°F INLET OIL.	104
4.9	PMA/PMB BEARING PARAMETERS	105
4.10	PM MACHINES CALCULATED CRITICAL SPEED.	107
4.11	CONTAINMENT RING CALCULATED STRESS FOR VARIOUS SPEED AND TEMPERATURES	115
4.12	MP35 TENSIL TEST RESULTS	116
5.1	GEAR SUMMARY DIFFERENTIAL GEAR BOX	124
5.2	GEAR LOAD.	130
5.3	GEAR TOOTH TIP MODIFICATION.	138
5.4	BEARING INFORMATION.	139
6.1	SYSTEM SPEC SUMMARY.	141
6.2	TEST RESULTS	142
A-1	TRANSIENT FREQUENCY LIMITS	157
A-2	FREQUENCY MODULATION LIMITS.	158

1.0 INTRODUCTION

1.1 NOVEL TECHNIQUES IN 400 Hz ELECTRIC POWER GENERATION

Future aircraft requirements have placed a strong emphasis on improving the method of electric power generation. The thrust of this program has been to develop technology required to overcome and identify barriers of a novel 400 Hz power generation system. The novel approach has as objectives, higher reliability, maintainability, and reduced attitude sensitivity to high gravitational forces. The Electrically Compensated Geared Differential Drive System investigated offers the potential to achieve these goals.

The Electrically Compensated Constant Speed Drive (ECCSD) consists of two permanent magnet machines, differential, gearing, and controller. The ECCSD program has been conducted by Sundstrand for AFWAL/POOC-1, WPAFB. The program includes monthly status reports, design reviews, final report, and delivery of breadboard, proof of principle hardware. The program establishes the feasibility of the ECCSD approach for constant frequency power generation, identifies the possible approaches, identifies system attributes and areas which require further development to arrive at a fully viable system.

This program is a Sundstrand/Air Force joint participation effort where an award has been made to Sundstrand to supply one set of breadboard hardware upon completion of the design, fabrication and feasibility demonstration.

1.2 THE ECCSD PROGRAM

The program consisted of two parts: first to design the permanent magnet machines, controller, and DC conversion, and second to design a gear box containing a standard differential and gearing necessary to couple the differential to the permanent magnet units and 12,000 rpm 400-Hz generator.

The arrangement of this equipment is illustrated in Figure 1.1.

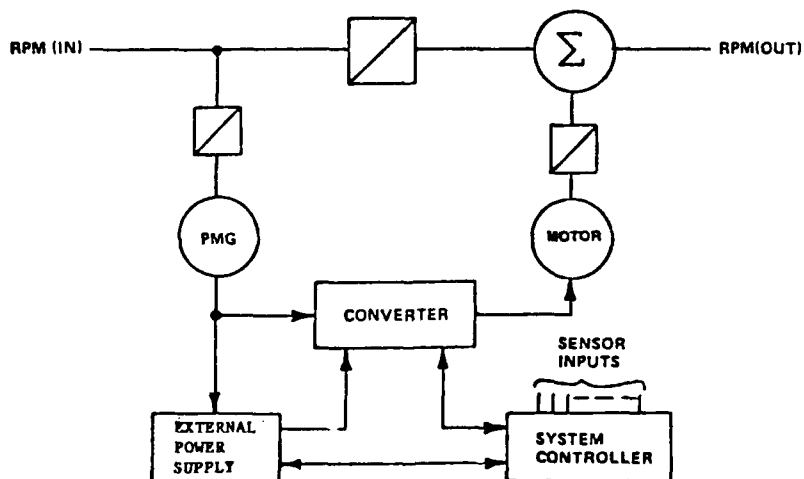


Figure 1.1. Electrically Compensated Constant Speed Drive

1.2.1 Design Constraints

General design constraints for performance were first identified. These have been selected to allow use of existing components, where possible, with a system goal having the capability as defined in Table 1.1.

Table 1.1. Design Constraints

SPEED RANGE	1.8/1
SYSTEM RATING	40/60 KVA
INPUT SPEED	5,000 - 9,000 RPM
OIL SYSTEM	MIL-L-7808 / MIL-L-23699
OIL TEMPERATURE	275°F MAX
MIL-G-21480A	ELECTRICAL PERFORMANCE

1.2.2 Study Timetable

Design and analysis for each part of the system has addressed the items listed in Table 1.2.

Table 1.2 ECCSD Design and Analysis

Specification

- o Performance Requirements
- o System Interfaces
- o Physical Arrangement
- o Cooling Requirements
- o Bearing Analysis
- o Critical Speed Analysis
- o Thermal and Cooling Requirements

Motor Controller Design

- o Preliminary Analysis
- o System Definition
- o Dynamic Analysis
- o TTopology Identification
- o Component Requirements
- o Performance Estimates
- o Topology Determination
- o Control Definition
- o Circuit Design
- o Thermal Analysis
- o Breadboard Layout

Generator Motor Design

- o Performance Analysis
- o Configuration Selection
- o Materials Definition
- o Definition of Losses
- o Stress Analysis
- o Layouts Required
- o Detail Drawings
- o Parts Procurement
- o Unit Assembly

Final Report

The schedule and timing of major tasks is given in Figure 1.1A.

PROGRAM SCHEDULE

TASK DESCRIPTION	1985				1986				1987				1988			
	I	II	III	IV												
1.0 SYSTEM STUDY																
2.0 DESIGN																
3.0 PROCUREMENT																
4.0 ASSEMBLY																
5.0 SUB ASSEMBLY TEST																
6.0 SYSTEM TEST																
7.0 DEMONSTRATION																
8.0 FINAL REPORT																

Figure 1.1A Program Schedule



Sundstrand Aviation
 Rockford, Illinois
 a unit of Sundstrand Corp.

ACTUALS	PLANNED	ESTIMATED	MILESTONE	DEPENDENT	CRITICAL	TASKS	AUTHOR	RUN DATE	VERSION	PAGE
			7	0	4	8			v1.23	1 of 1

2.0 SYSTEM

The approach being studied provides a means of obtaining constant output from a variable speed input shaft using a differential which is electrically compensated. The approach combines permanent magnet machines, electronic power controller, and differential to achieve this task.

The differential of Figure 2.1 is not part of this study, it is a standard well developed piece of hardware used in present constant frequency aircraft electrical systems. The following description of differential operation is included so that the operating relationship of motor/generator, differential, and controller can be better visualized.

The differential as illustrated in Figure 2.1 consists of carrier shaft, two planet gears, and two ring gears (trim ring gear and output ring gear). At any speed and load condition, the generator load is imposed on the output ring and the input torque is supplied by the input gear shaft turning the carrier shaft. In the ECCSD, motor/generators are geared to the carrier shaft and trim ring gear.

Mechanical summing is accomplished through the planetary gearing. In an ordinary gear train, the gears revolve about a fixed axis. In the planetary, the axes of planet gears are in motion and the carrier shaft is the fixed link.

Speed summing is accomplished in the differential by adding or subtracting the trim speed of the input ring gear to the meshing planet gear which is orbited as a function of input speed by the carrier shaft. The second planet is meshed with the first planet and with the output ring gear. The output ring gear is thereby made to rotate at constant speed. Since the output ring gear is meshed with the generator, the generator is driven at constant speed.

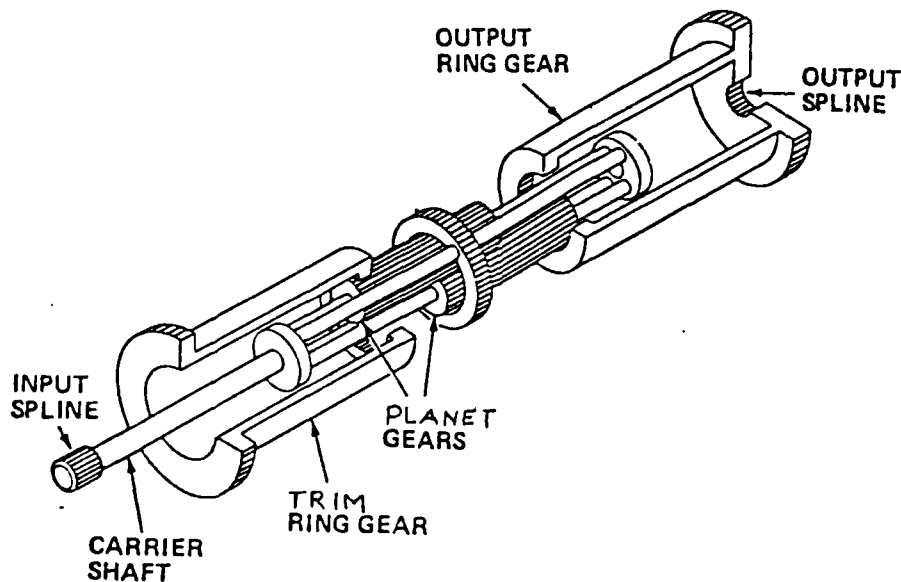


Figure 2.1. Differential

The controller functions to control motor/generator operation adding or subtracting speed and power at the differential to maintain output shaft speed of the system constant. For the output differential system, the power which is added to or subtracted from the differential is, respectively, taken from or returned to the input shaft. For the input differential system, the power which is added to or subtracted from the differential is, respectively, taken from or added to the output shaft.

The controller responds to the following operational conditions:

- (1) Changes in input (engine) speed to the system
- (2) Changes in load on the output shaft

Power which flows into or out of the differential is mechanical power. Power which is taken from or added to an input or output shaft is also mechanical power. Motors/generators PMA and PMB are integrated with the differential and input or output shaft. These machines will convert the mechanical power to electrical power. The controller which interfaces with PMA and PMB controls the flow of electrical power between the two machines.

Basically, the controller responds to a speed error signal. The speed error is derived by comparing a signal representing speed of the output shaft to a reference signal. Depending upon the polarity of this error signal, the control increases or decreases the amount of speed being added to or subtracted from the differential. This is accomplished by controlling the net torque present at the permanent magnet (PM) machine which is attached to the differential. Part of this torque comes from the average current which is fed to the PM machine when it is a brushless motor, or drawn from the PM machine when it is a generator. The rest of this torque is supplied by the differential, and is a result of the load on the output shaft.

The other PM machine is attached to the input or output shaft of the system depending upon the placement of the differential gear. The speed of this machine is fixed by the shaft to which it is attached. Therefore, the only way to control the power flow into or out of this machine is to control the magnitude of torque developed by this machine. This is done by controlling the current fed to or drawn from this machine.

2.1 ECCSD OPTIONS

Seven basic options were identified for inclusion in the design trade study. These options are output differential always above, output differential always below, output differential always midrange, input differential always above, input differential always below, input differential always midrange, and parallel differential.

Two options, the output differential always above and input differential always below, are dropped from the trade study at this point. In the case of the output differential always above the system components have higher power ratings, and the system has a lower efficiency than a system using an input differential. In the case of the input differential always below, system component size is larger and efficiency is lower than an output differential approach, and it is therefore dropped from consideration.

2.1.1 Differential Always Above Options

In this differential arrangement, Figure 2.2, Permanent Magnet Machine PMA is always a generator, and permanent magnet machine PMB always operates as a motor.

Because the motor (PMB) always runs at its maximum speed and voltage, the operating current required is relatively low. The speed of generator PMA increases with increasing input speed. As the speed of PMA increases, the power required from PMA also increases. This is a favorable relationship between the power drawn from PMA and the speed of PMA.

Because power flows from the trim gear on the differential, the losses in the controller components reduce the power which is transferred to the motor (PMB), thus reducing PMB motor size. In this option, controller losses work to reduce system size.

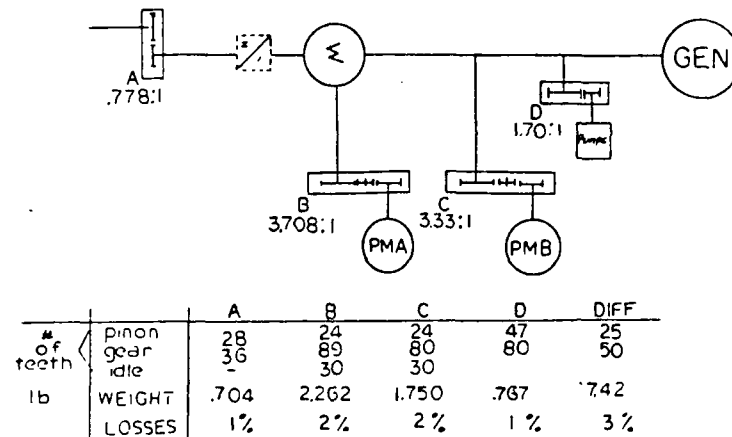


Figure 2.2. Input Differential Always Above

Power flow through the controller is in one direction. Input voltage need only be boosted for all operating speeds of the system. Controller system arrangement is shown in Figure 2.3A. The inductor required in this circuit carries mostly dc current. Losses due to alternating flux in the core will be low, and a high permeability material can be used for the inductor magnetic core, thus keeping the inductor small. The operating current of the controller does not show peaking anywhere in the operating speed range of the system. This characteristic keeps the power conversion requirements small, since components must be sized for worst case operating conditions. This offers a system size advantage. Because of the favorable relationships between speed and power of the permanent magnet machines, the power conversion is accomplished more efficiently than for any of the other options.

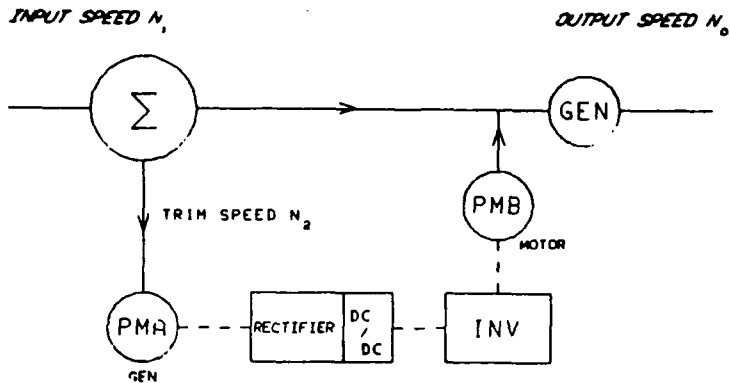


Figure 2.3A. Input Differential Always Above Controller/System

2.1.1.1 Controller Above Straight Through

For a speed range which is strictly above straight through, the PM machine attached to the differential will run as a generator. The other PM machine is run as a motor.

A full-wave bridge rectifier, a converter, and an inverter are required. Figure 2.3B shows a simplified schematic of the power circuitry. The output of the generator is rectified and fed to the converter. The converter shifts the voltage level as required and feeds the terminals of the inverter. Power flow through the power converter is unidirectional.

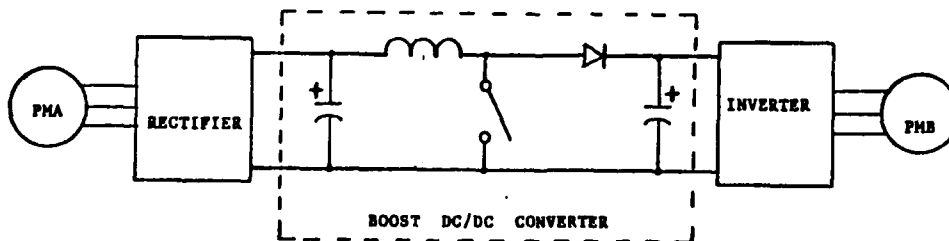


Figure 2.3B. Controller Topology Always Above Option

2.1.2 Midrange Differential Options

In the output differential midrange option of Figure 2.4 when system input speed is below straight through, the permanent magnet generator, PMA, supplies power to permanent magnet motor, PMB. When input speed of the system is above straight through, PMB supplies power to run PMA as a motor.

Below straight through, the speed and voltage of PMA are increasing as the system input speed increases. The motor speed and voltage, however, are decreasing, thus the voltage of PMA must be boosted at low input speeds but reduced at higher input speeds. This complicates the controller.

Above straight through the voltage output of PMB is always boosted to supply the voltage requirements of PMA.

Of the options using a single differential, this option requires the least amount of power to be processed by the controller. The controller for this option, however, must be fully bidirectional. The controller is required to boost or reduce the voltage output of a generator in order to supply motor voltage requirements. The complexity of this controller causes it to be large, even though the amount of power processed is relatively smaller than a single direction controller.

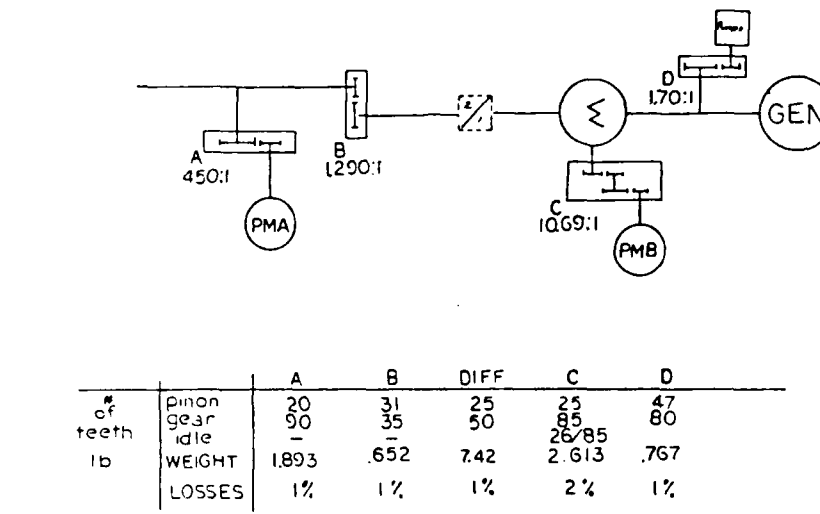


Figure 2.4. Output Differential Midrange

2.1.2.1 Midrange Option Controller

The controller for this speed option is the most general one. Each of the permanent magnet (PM) machines PMA and PMB will run as both motor and generator. The controller will be fully bidirectional. That is, the controller will have to handle power flow between PMA and PMB in either direction.

Normally, for speeds above straight through the PM machine attached to the differential will be a generator, and the other PM machine will be run as a motor. For speeds below straight through the PM machine attached to the differential will be run as a motor, and the other machine will function as a generator.

For speeds just slightly above straight through, the control scheme changes. Power must be subtracted from the differential, and normally the PM machine attached to the differential runs as a generator. However, this machine must be at a very low speed. The torque required at the differential cannot be obtained by simply loading the PM which is attached to the differential. Therefore, this machine must be run as a motor in the plugging mode.

Three distinct operating modes for the controller are now obvious. (1) Below straight through the PM machine attached to the differential is a motor. The other PM machine is a generator. (2) Slightly above straight through the PM machine attached to the differential is run as a motor in the plugging mode the other PM machine continues acting as a generator. (3) Above straight through the PM machine attached to the differential is a generator. The other PM machine is a motor.

The controller, for this option, is made up of three main functional blocks, two inverters and a converter. One inverter is required for each of the PM machines PMA and PMB. The simplified schematic of Figure 2.5 shows an inverter circuit. With all the switches of the inverter in the open (off) state, the circuit becomes a three phase full-wave bridge rectifier. Thus, when either of the permanent magnet machines is used as a generator, a voltage is produced by the circuit which performs as a bridge rectifier.

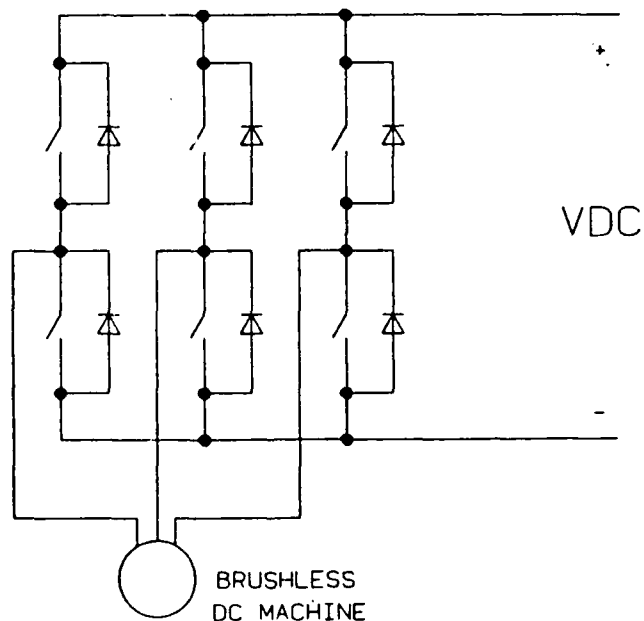


Figure 2.5. Controller Power Topology

Controller/system configuration for this option is given in Figure 2.6. In this configuration, controller switches and the internal transformer ratio are used to control converter output voltage to the required operation levels. A bidirectional switch network is used to direct power flow for the difference in operation between above and below straight through. Bidirectional operation requirements for the controller add to its complexity. As a result, it was determined that for this approach the controller would be less reliable and weigh more.

Figure 2.6 illustrates the input and output differential options for midrange operation. The controller for both options is bidirectional. In the output differential option both PMs operate over a speed range. In the case of the input differential, PMB is always operated at a constant speed. Both options, however, require a bidirectional controller and are dropped from further consideration on the basis of controller complexity.

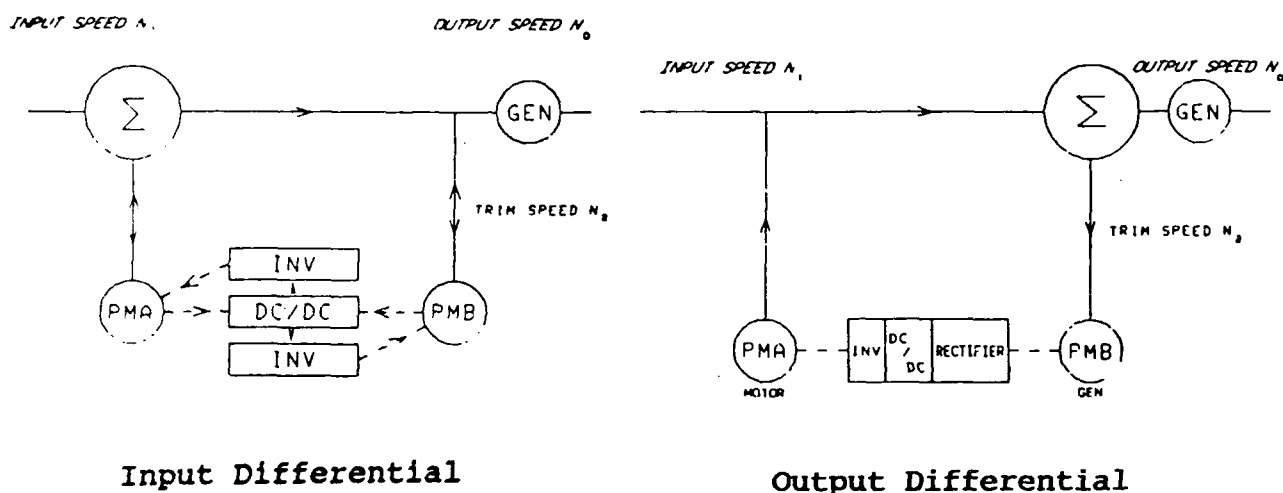


Figure 2.6. Midrange Configurations

Figure 2.6 illustrates the input and output differential options for midrange operation. The controller for both options is bidirectional. In the output differential option both PMs operate over a speed range. In the case of the input differential, PMB is always operated at a constant speed. Both options, however, require a bidirectional controller and are dropped from further consideration on the basis of controller complexity.

2.1.3 Output Differential Always Below Options

In the Output Differential Always Below, Figure 2.7, PMA is always generating power to drive the permanent magnet machine PMB as a motor. Speed and voltage of PMA increase as system input speed increases. The speed, voltage, and power required to drive the motor, PMB, decreases as system input speed increases. At low input speeds, PMA output voltage must be boosted to supply PMB. At higher input speeds, voltage output of PMA must be reduced to supply the power for the motor PMB.

The relationship between speed and power of PMA is unfavorable. Because maximum power is required from PMA at its minimum speed and voltage, the controller must be designed to handle relatively high currents.

2.1.3.1 Always Below Controller Topology

A buck-boost topology was found to be necessary for this option. The controller for this option is larger and less efficient than for any of the other options.

The losses of the controller components cause the power required from the generator PMA to be higher, thus the size of PMA is larger than if the controller were lossless. The losses of the controller work to increase the size of the system. System/controller arrangement of this option is illustrated in Figure 2.7.

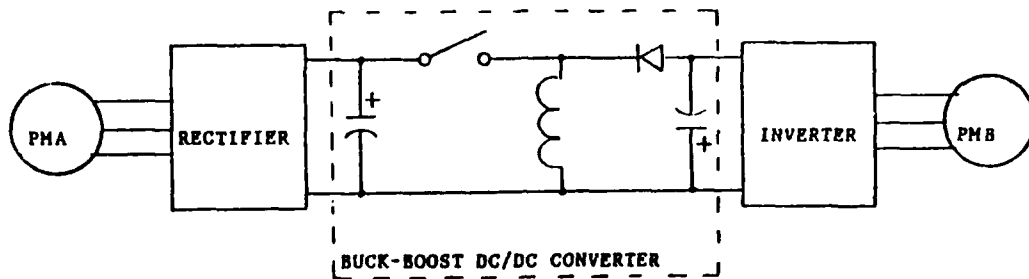


Figure 2.7. Always Below Topology

For a speed range which continually operates below straight through, the permanent magnet machine attached to the differential will operate as a motor. Thus the topology of the controller is like that illustrated in Figure 2.8.

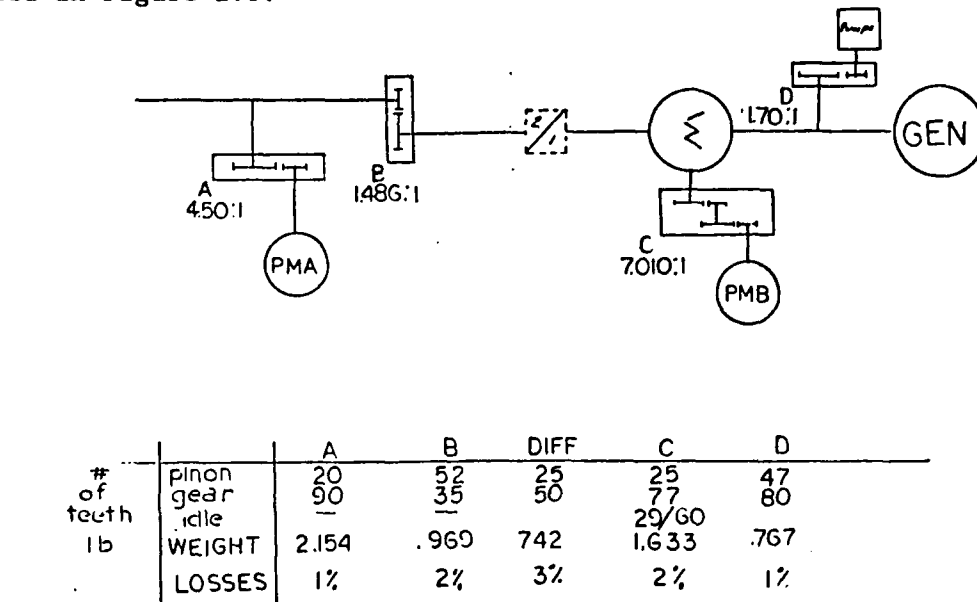


Figure 2.8. Output Differential Always Below

2.1.4 Parallel Differential Option

The Parallel Differential Option is illustrated in Figure 2.9. In this option, the permanent magnet machine attached to one of the differentials is always a generator. The permanent magnet machine attached to the other differential always runs as a motor. Thus power flow is unidirectional.

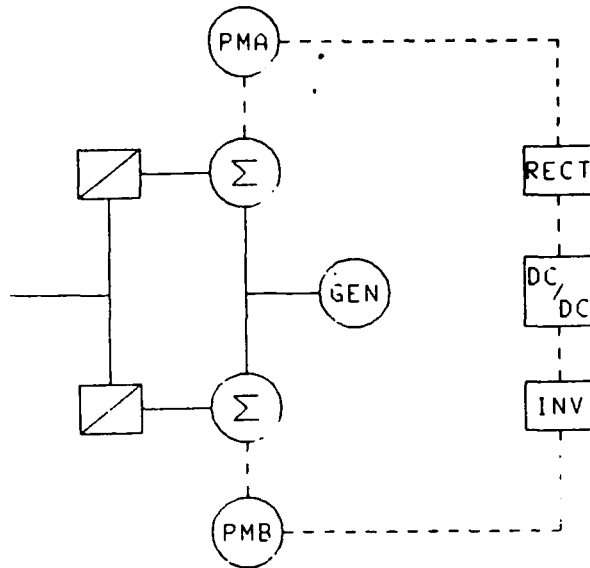


Figure 2.9. Parallel Differential

Use of parallel differentials improves efficiency by reducing power that must be added or subtracted from a single differential. Use of two parallel drive paths which are geared together will split the transferred power between the two differentials with the system operating as a midrange speed option. One differential is geared so that PMA always subtracts speed and removes power. The second differential is geared so that PMB unit always adds speed and power. Therefore PMA is always a generator and PMB is always a motor. The power splits in the parallel path minimizing power transfer thus providing a means of reducing losses and improving efficiency.

The parallel differential as an option was not pursued because of the added mechanical complexity of the arrangement and total absence of standard parts for the required differentials.

2.1.5 PM Motor/Generator

The purpose of the permanent magnet motor/generator is to provide electrical compensation of the differential and maintain a constant output speed from a variable input shaft speed. Permanent magnet (PM) machines have no rotating windings resulting in a highly reliable design for high speed applications. Use of high operating speed minimizes the electromagnetic weight. PM machines also result in less severe rotor cooling problems, since there are no field losses in the PM rotors.

Two PM machines are necessary in either of the system configurations: Input Differential or Output Differential. Their size is determined by the electrical requirements for the system. Their electrical rating is directly related to the speed options within each configuration.

An electromagnetic trade study was completed to determine the most viable speed options. Preliminary designs allowed establishment of required machine performance and their physical dimensions.

For the midrange option, the PM machines function interchangeably as motor and generator, depending on whether input speed is above or below the straight through operating point.

For the always above and always below options, the PM machines have a fixed mode of operation being either a generator or motor. These operating modes result in the largest PM machines, a result of the power which must be transferred to maintain constant speed.

2.1.5.1 System Speed

The input speed of the system is variable. For the purpose of this study, the input speed variation is constrained by:

$$(\text{MAX INPUT SPEED}) = 1.8 (\text{MIN INPUT SPEED})$$

Output shaft speed is maintained at 12,000 RPM.

The condition referred to as straight through is the point where the input shaft speed is such that no speed need be added or subtracted at the differential to produce 12,000 rpm at the output shaft. An inherent characteristic of the differential is that the input speed is multiplied by two. Therefore, straight through occurs at an input shaft speed of 6,000 rpm. If the input speed is above or below 6,000 rpm, then speed must be respectively subtracted or added at the differential according to the equation:

$$(\text{SPEED TO BE ADDED}) = 12,000 - (\text{INPUT SPEED} \times 2)$$

Figure 2.10 illustrates this relationship.

The speed of the PM machine attached to the differential is governed by the amount of speed to be added or subtracted and the gear ratio through which this PM machine is fixed to the differential.

For the output differential system in Figure 2.6 PMA is attached to the input shaft. Thus, the speed of this PM machine is proportional to the speed of the input shaft.

For the input differential system in Figure 2.6 PMB is attached to the output shaft of the electric drive. Thus, this machine runs at constant speed.

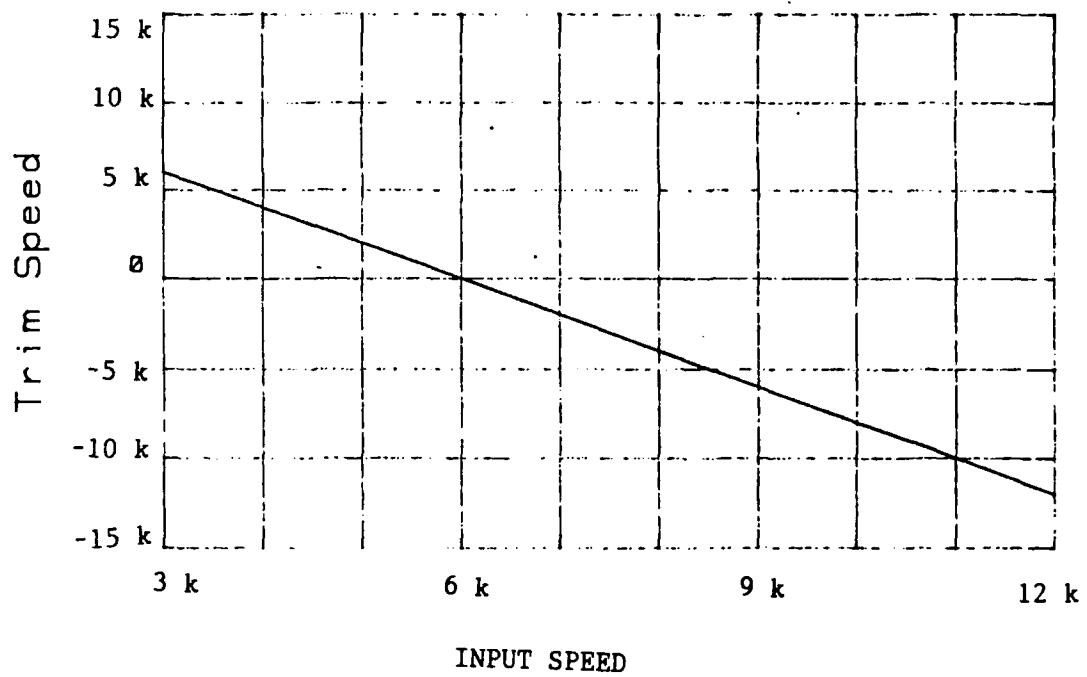


Figure 2.10. Differential Makeup Speed Characteristic

2.1.5.2 PM Motor Torque Requirements

A characteristic of the differential is that the same torque is required at each of the differential input/output points.

For the output differential option, torque is determined by output shaft load. In this option output shaft speed is constant. Thus, for a given load, torque is constant regardless of input speed.

For input differential systems, torque varies with input speed. These torque variations for the 2.0 P.U. load condition are given in Figure 2.11. Trim power required from the differential drive PMG is given in Figure 2.12.

In the systems using an output differential Figure 2.6, where PMA is attached to the input shaft and input shaft speed varies, PMA torque is determined by the power flow through PMA. Figures 2.13 and 2.14 give the relationship of PMA torque and trim power required for a fixed output power.

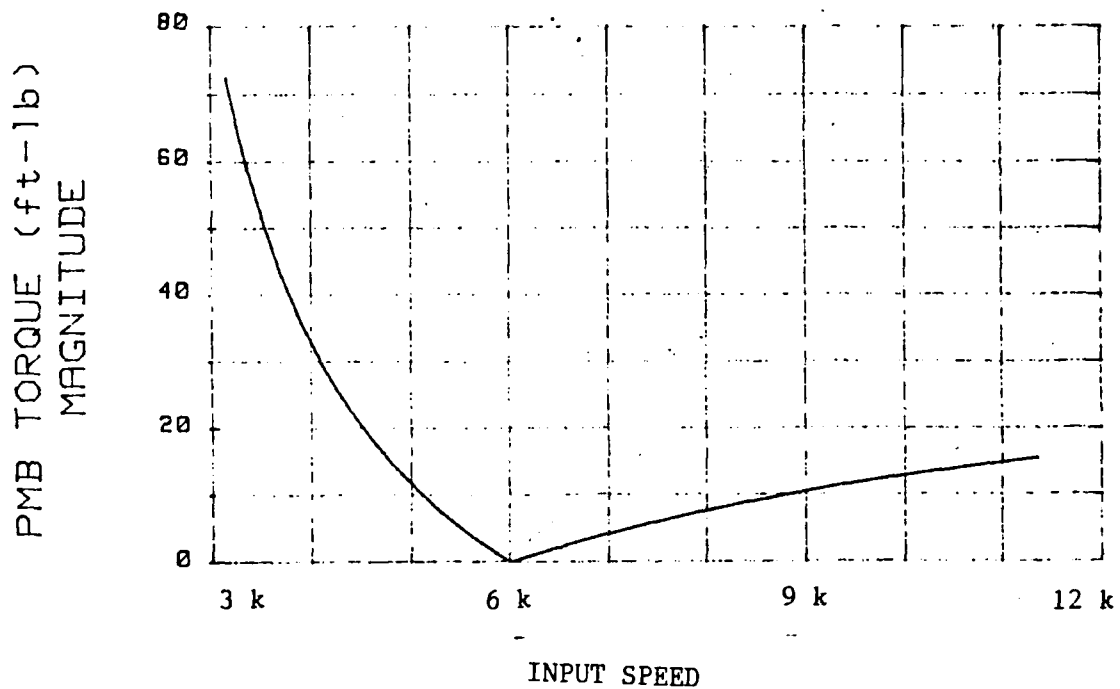


Figure 2.11. PMB Torque vs Input Speed
Input Differential, 2.0 PU Load

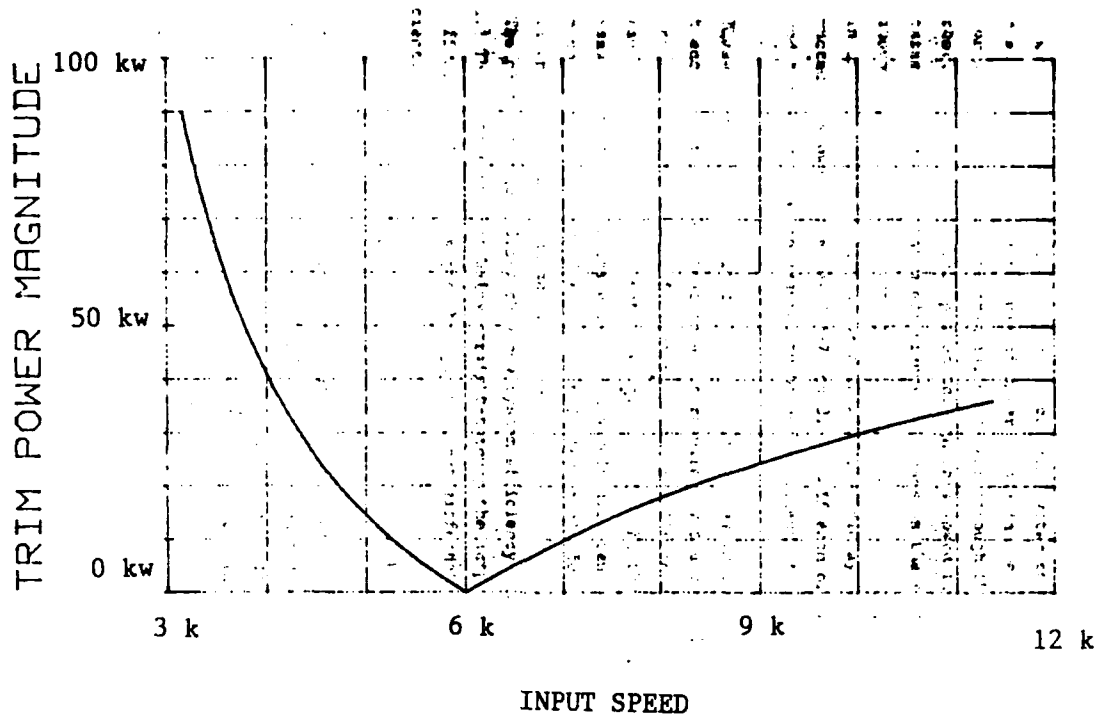


Figure 2.12. Trim Power vs Input Speed Input Differential, 2.0 PU Load

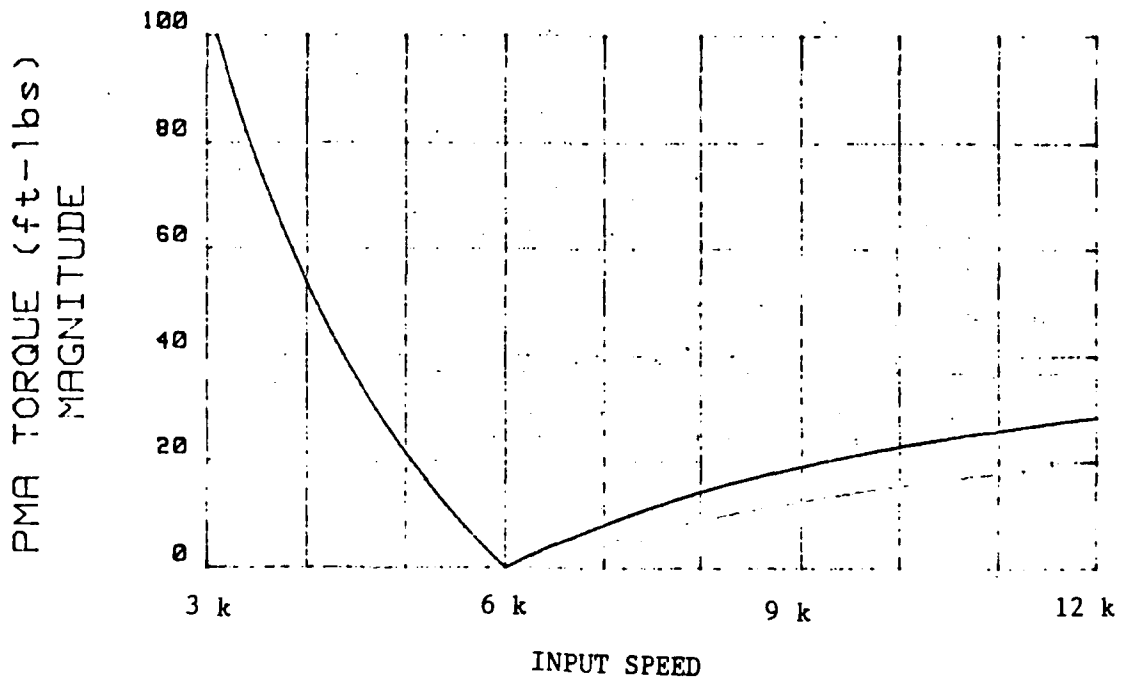


Figure 2.13. PMA Torque vs Input Speed Output Differential, 2.0 PU Load

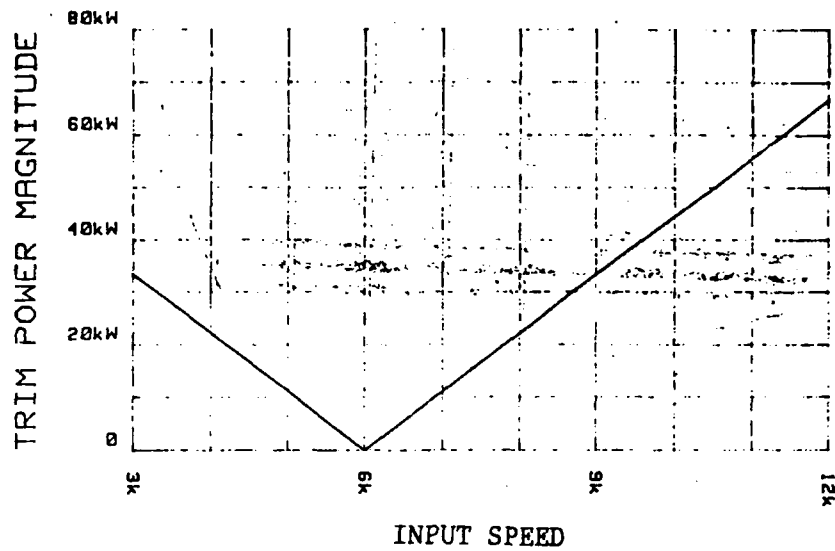


Figure 2.14. Trim Power vs Input Speed
Output Differential, 2.0 PU Load

2.1.6 System Trade Study

In the system trades it was necessary to establish relative efficiencies. The majority of power loss in a system occurs in the parts of the system which must transfer the compensation power. These losses are thus located in PMA, PMB and the controller.

A comparison basis was established by using simple models as illustrated in Figures 2.15 and 2.16. These simple models neglected gearing loss and the power loss required to develop torque where little or no compensation speed is required.

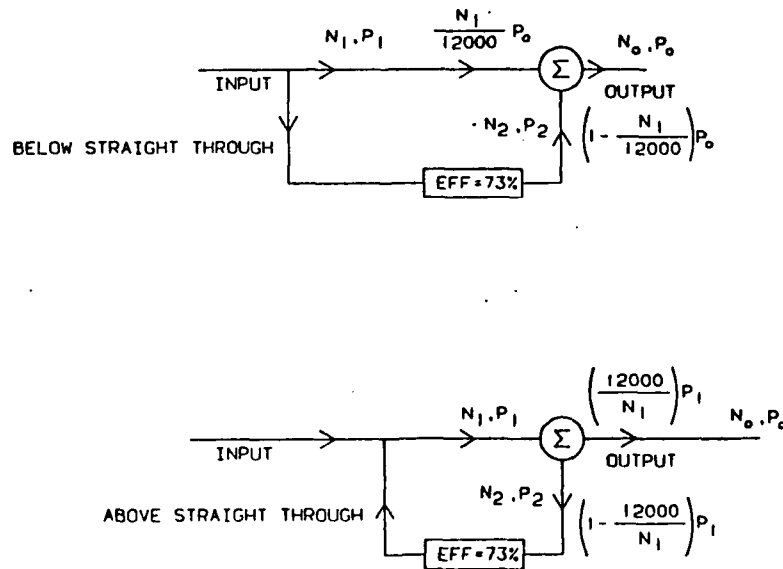


Figure 2.15. Output Differential Simplified Model
For Efficiency Calculations

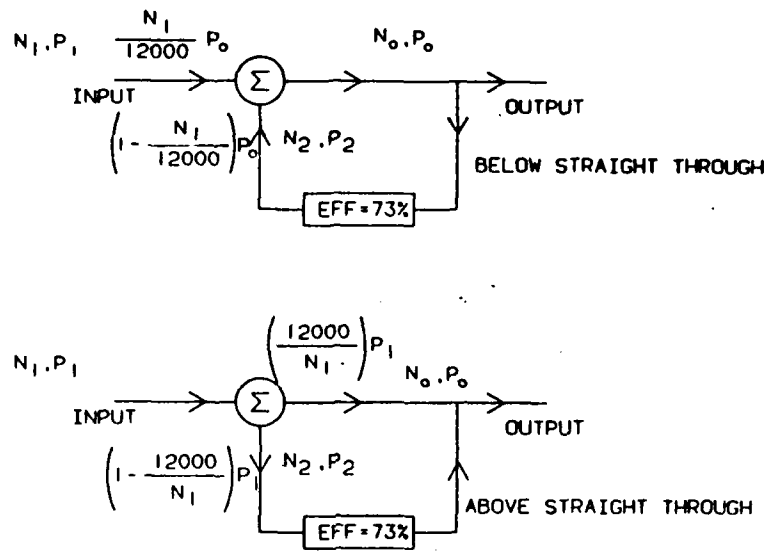


Figure 2.16. Input Differential Simplified Model For Efficiency Calculations

The losses for the condition where no compensation speed is required will not vary greatly and are assumed to be constant from system to system. Controller and motor losses for the options being considered are given in Figures 2.17 and 2.18.

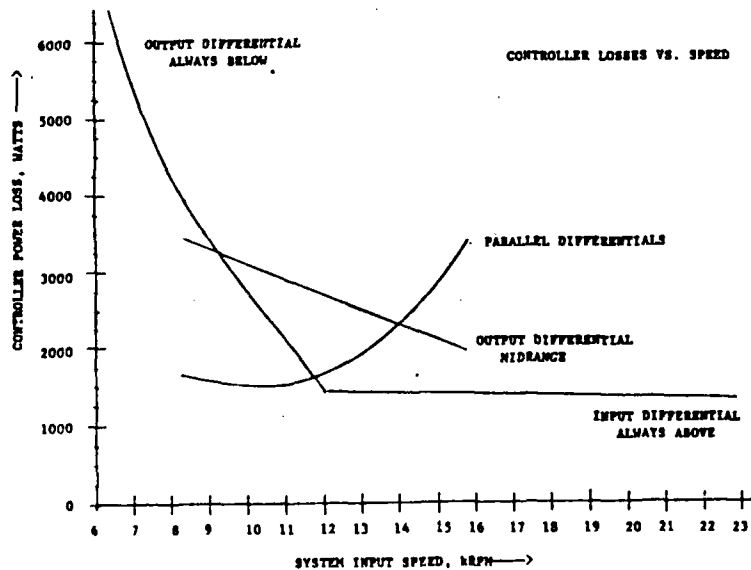


Figure 2.17. Controller Losses

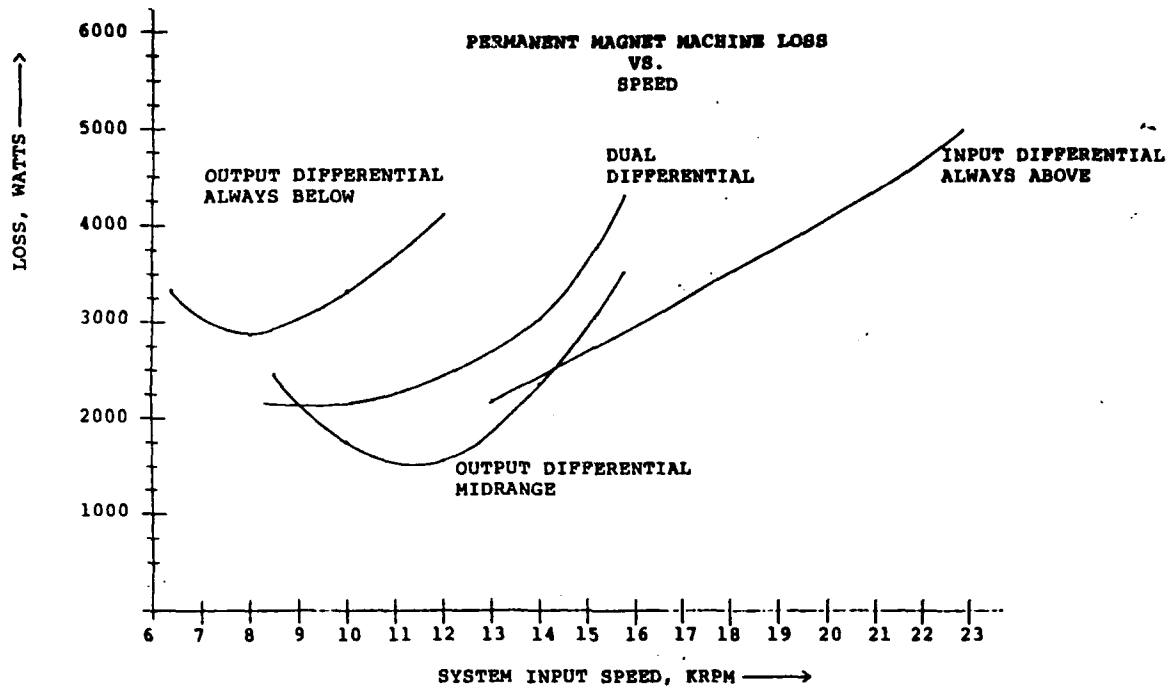


Figure 2.18. Motor Losses

Resulting preliminary trade efficiencies are given in Figure 2.19.

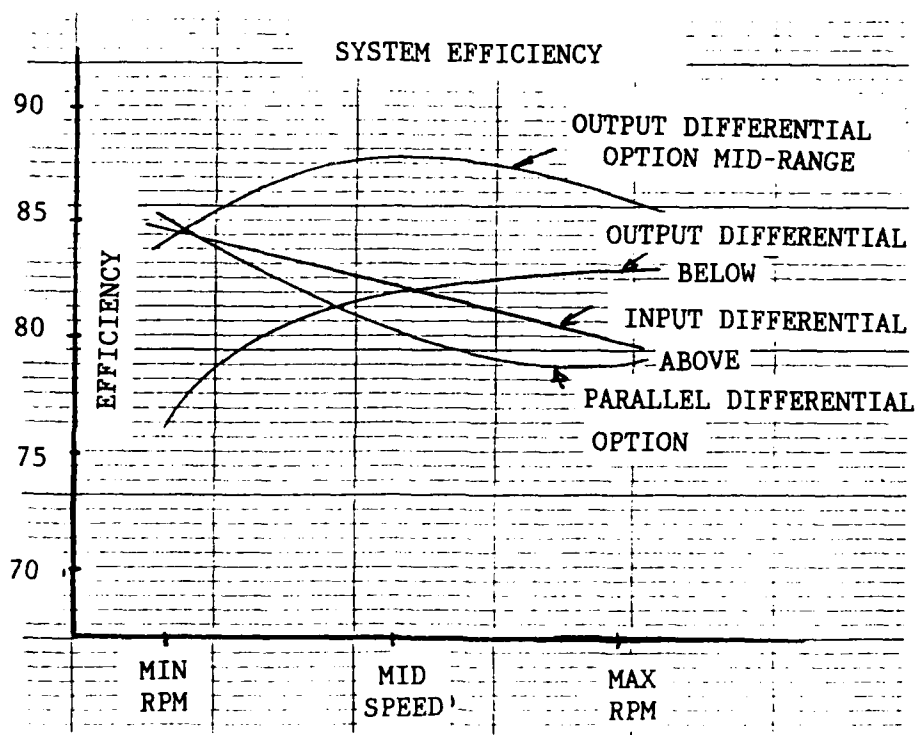


Figure 2.19. System Efficiency

2.1.6.1 Trade Analysis

Preliminary trades in selecting the system to be designed were supported by detail dynamic models, simulation, and system analysis for each concept.

Each element of the ECCSD system is modeled in such a way as to take into account power flow considerations so the performance and efficiency of each component, as well as the system as a whole, can be optimized. This modular structure is illustrated in the model schematic of Figure 2.20, which deals specifically with the output differential case. Figure 2.21 illustrates the hardware used for the realtime system simulation.

The two permanent magnet machines (motor/generators) have been modelled using the Direct and Quadrature axis representation of a brushless DC motor, and these have been incorporated into the overall system model so that they each may act either as a motor or a generator, thereby enabling full analysis and emulation of through midrange conditions as well as options involving either all-above or all-below midrange operation.

The converter has been represented by a simple RC network, enabling bidirectional operation and duty-cycle inputs from the controller.

A simple speed summer is used to model the output differential, and compliance effects currently being neglected. Torque levels remain invariant through the differential. A representative inertia is used to model the 400-Hz generator. Load torque is computed assuming a constant generator power for speed changes about 12,000 RPM.

The model overall is configured so that the input shaft speed range is 1.8 to 1. Maximum rotor speeds of 50,000 RPM are assumed for PM machine operation. The dynamic effects of shaft compliances have been assumed negligible throughout the system, and the inertia of motor/generator unit "A" has also been neglected in comparison with the driving inertia.

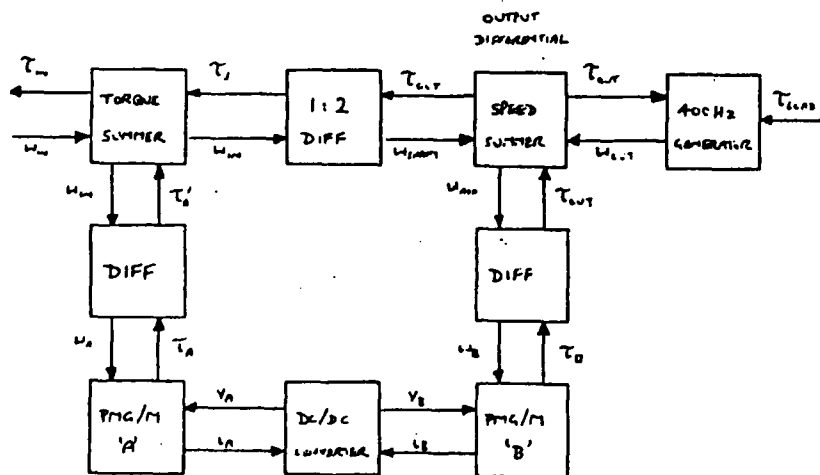


Figure 2.20. Modular System Structural Schematic

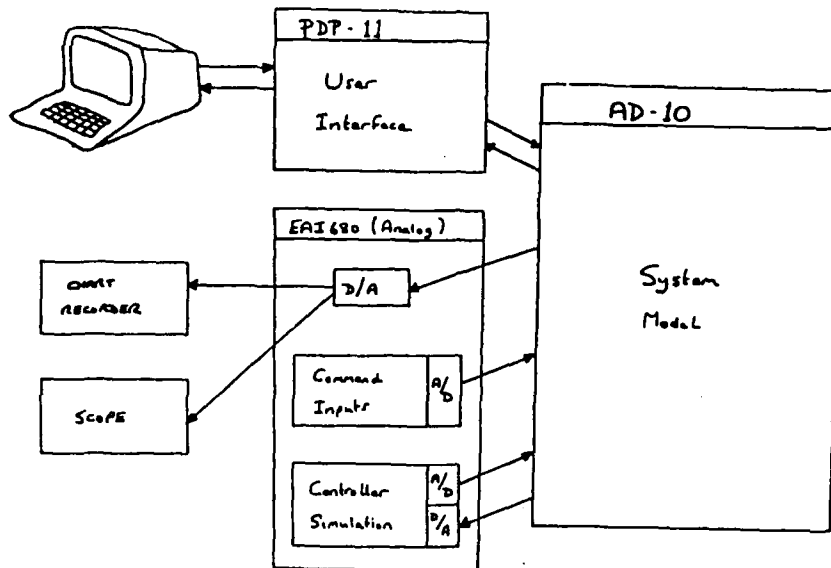


Figure 2.21. Real Time Simulation Hardware

2.1.6.2 Controller

The performance of the system is determined solely by the speed and power which are provided to the differential in response to changes in input speed and output power of the system. The performance requirements of the controller are derived entirely from knowing the speed and power which must be added or subtracted at the differential.

The controller trades used designs to meet the performance requirements, but are subject to a set of design constraints. These are summarized as follows:

Output Differential Performance Requirement

Speed to be added at the differential:

$$N_2 = N_0 - N_1 = 12,000 - N_1 \text{ RPM}$$

Power to be added at the differential:

$$P_2 = \frac{N_2 P_0}{N_0} = \frac{(12,000 - N_1) P_0}{12,000} \text{ Watts}$$

Torque required at the differential:

$$\tau = \frac{7.04 (P_0)}{12,000} \text{ lb ft}$$

Where:

N_0 = Output speed of the differential. Normally 12,000 RPM.

P_0 = Output power of the differential. Determined by the load on the 400-Hz generator, and generator efficiency.

Input Differential Performance Requirement

Speed to be added at the differential:

$$N_2 = N_o - N_1 = 12,000 - N_1 \text{ RPM}$$

Power to be added at the differential:

$$P_2 = \frac{(12,000 - N_1) P_1}{N_1} \text{ Watts}$$

Torque required at the differential:

$$\tau = \frac{7.04 (P_1)}{N_1} \text{ lb ft}$$

Where:

N_o = Output speed of the differential. Normally 12,000 RPM.

P_1 = Input power of the differential. Determined by the load on the 400-Hz generator and system efficiency.

2.1.6.3 PM Machines

PM machine configurations were determined based on the requirements for each of the speed options for each system configuration. The constraints which were used are given in Appendix A.

2.1.7 System Selection

Study weight estimates required a conceptual package arrangement of PM's and differential that could be used for aircraft application. The necessary hardware arrangements of the system considered in the final trade are given in Figures 2.22, 2.23, 2.24, and 2.25. Using these hardware arrangements, the relative weight estimates of Figure 2.26 were derived, along with reliability values of Figure 2.27. Reliability data is based on MIL 217-D guidelines. Relative efficiency values, as illustrated in Figure 2.19, are used in the final selection process.

2.1.7.1 Selection Considerations

All possible options have not been carried through a detailed analysis. Based on efficiency as illustrated in Figure 2.19, only midrange and always below options were selected for further comparison.

Except from a reliability stand point, the midrange options are better considering efficiency and weight. These options, however, carry a high technical risk primarily because of the topology which requires power transfer at the straight through operating point of the differential. The need to develop a bidirectional converter capable of using the voltages available, and producing the voltages required, is not possible within the time frame of this feasibility study. Therefore, the midrange options are dropped.

The always below straight through option results in a less complex controller and does not require motor operation at zero speed and full torques. For this option, a system using a wound field machine would be the lightest however the complexity and reliability of the wound field machine negates its use. The forced commutation and transistorized controller version indicated higher weights. The forced commutated approach also resulted in a highly complex controller.

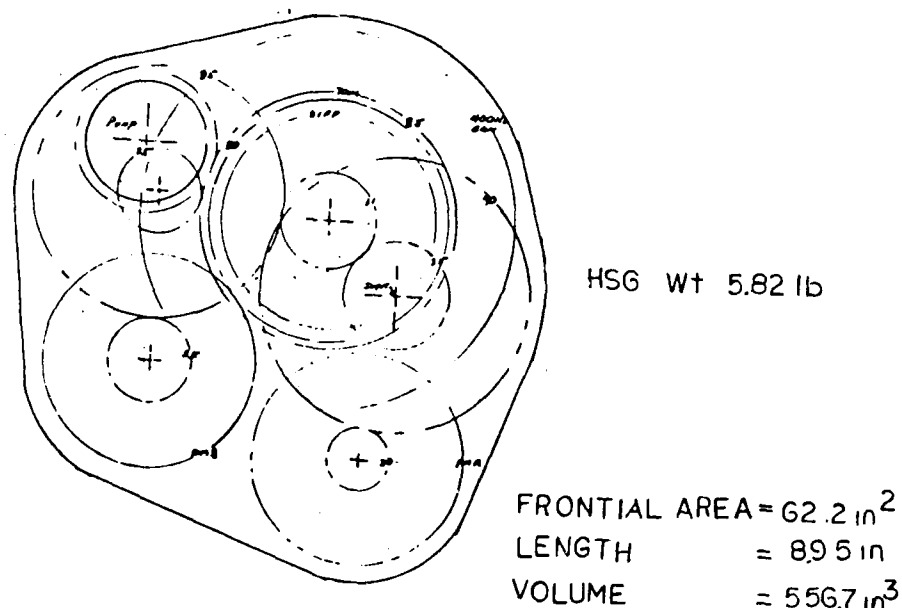


Figure 2.22. Output Differential Mid Range

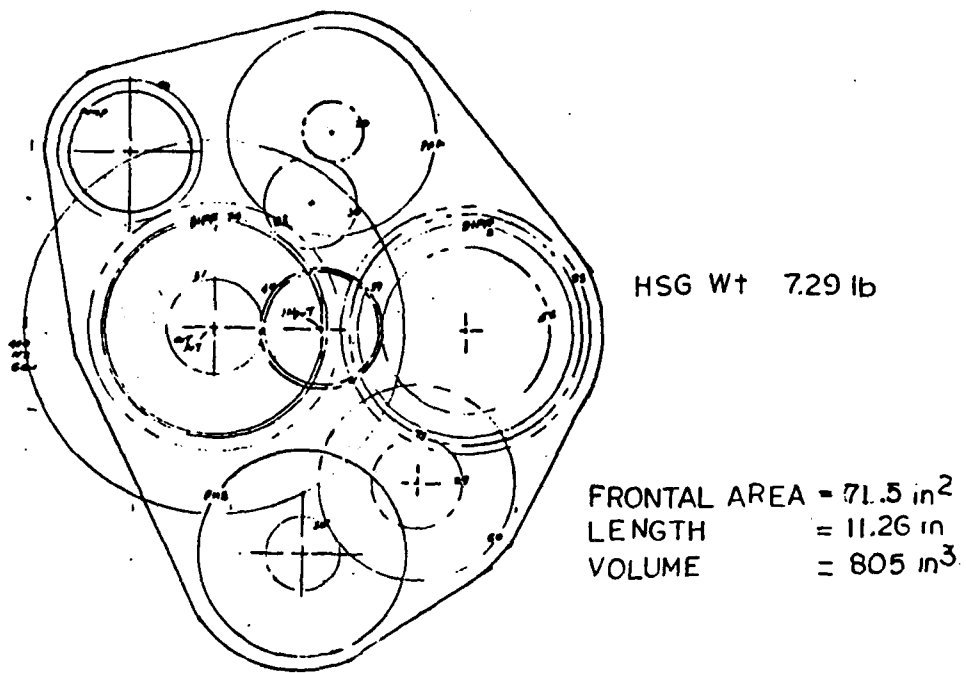


Figure 2.24. Parallel Differential

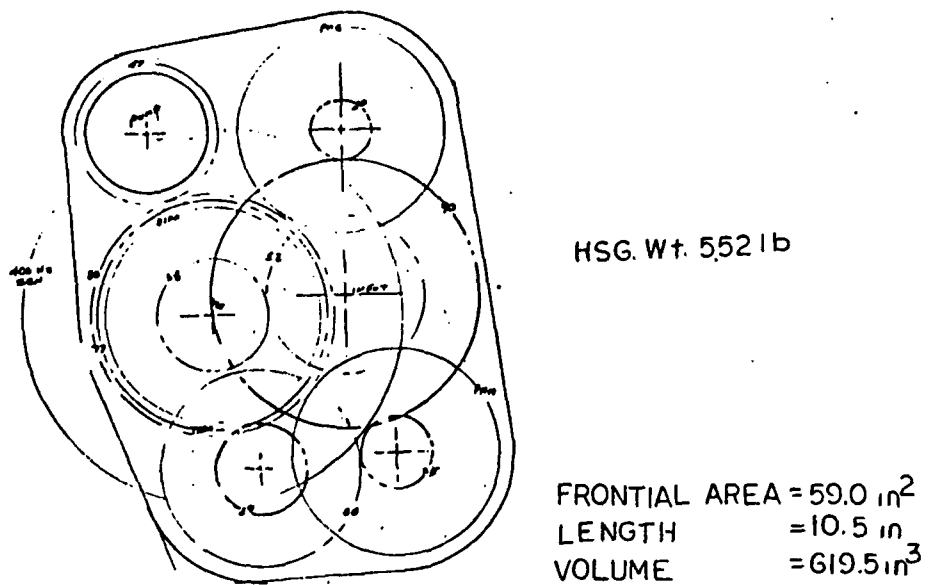


Figure 2.25. Output Differential Always Below

CSD

PMA (INC 1.5# FOR GEAR
BRG + POSITION SENSOR).

PMB (INC 1.5# FOR GEAR
BRG + POSITION SENSOR).

CSD TOTAL

CONTROLLER TOTAL

GENERATOR

TOTAL *(POUNDS)

DELTA

MIDRANGE			ALWAYS BELOW STRAIGHT THROUGH			
PMG SCR VERSION	PMG TRANSISTORIZED VERSION	PMG FORCE COMMUTATED CYCLOCON- VERTER	WOUND FIELD & PMG	PMG SCR VERSION	PMG TRANSISTORIZED VERSION	PMG FORCE COMMUTATED CYCLOCON- CONVERTER
13.5	13.5	13.5	25.2	25.0	22.0	26.2
13.5	13.5	15.7	12.0	12.0	12.0	14.3
(59.1)	(59.1)	(62.6)	(63.7)	(70.8)	(70.8)	(73.5)
30.8	32.8	(28.5)	20.0	28.0	40.9	29.9
(38.2)	(38.2)	(38.2)	(38.2)	(38.2)	(38.2)	(38.2)
(128.1)	(130.1)	(129.3)	(121.9)	137.0	(149.9)	(141.6)
6.1	6.2	7.4	0.0	15.1	28.0	19.7

* TOTAL WEIGHT FOR COMPARISON
PURPOSES ONLY

Figure 2.26. System Weight Trades

Failures Per Million Flight Hours				
Sub Assembly	Input Differential Above	Output Differential Midrange	Output Differential Below	Parallel Differential
Differential	2.5	2.5	2.5	5.0
Gen 400 Hz	29.0	29.0	29.0	29.0
Input Unit	15.0	15.0	15.0	15.0
Disconnect	0.6	0.6	0.6	0.6
Accessory	4.0	4.0	4.0	4.0
Idler Gears	1.5	1.0	1.0	2.0
HSG	0.5	0.5	0.5	0.5
PMG/PMM	2.5	2.5	2.5	2.5
Miscellaneous	5.0	5.0	5.0	5.0
Subtotal	60.6	60.1	60.1	63.6
MTBF	16,500	16,640	16,640	15,720
Electronic MTBF	8,000	2,500	5,000	6,000

Figure 2.27. Reliability

The topology, given in Figure 2.28, which functions with a system using an output differential and operating below the straight through speed is selected for proof of principle design, build, and test.

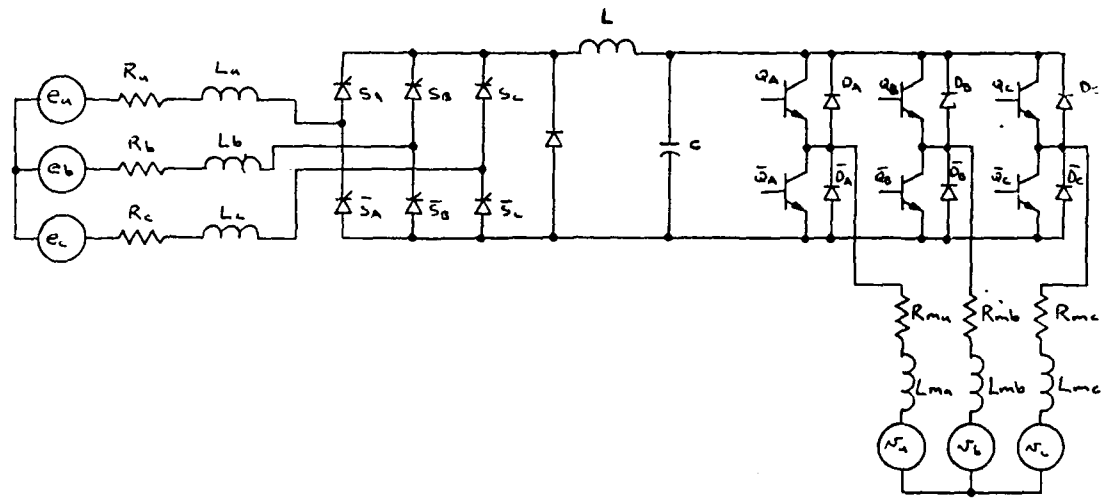


Figure 2.28. Selected Topology

2.2 DESCRIPTION OF SELECTED SYSTEM CONFIGURATION

2.2.1 Speed Range and System Gearing

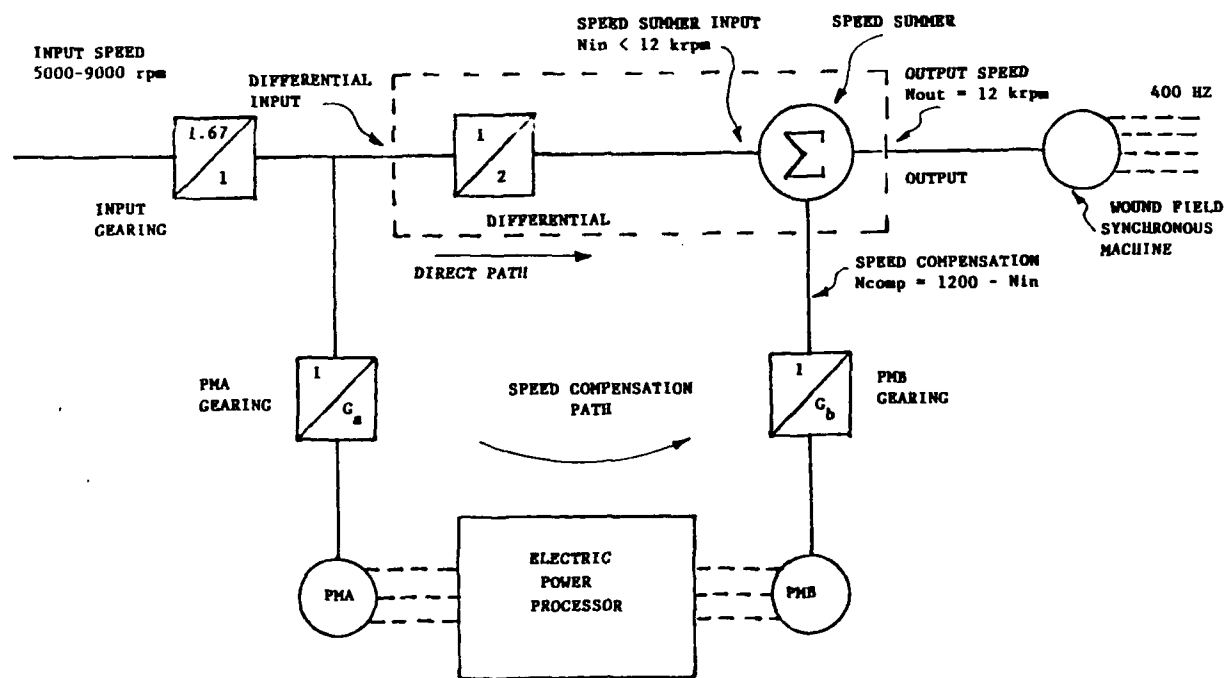
The input speed ratio,

$$\frac{N_{in}(\max)}{N_{in}(\min)} = 1.8,$$

for the system is fixed. System output speed and output power are also fixed. The only remaining variable at the system level is the system gearing. Figure 2.29 shows important gear ratios in the system. For simplicity of explanation the differential is represented by a gear ratio that is fixed at 2:1 and a speed summer. Choice of the input gear ratio determines how closely the speed summer input approaches 12,000 rpm. This affects the speed ratio,

$$\frac{N_{comp}(\max)}{N_{comp}(\min)},$$

and speed compensation power of the system. These parameters influence efficiency, weight, and size of the system.



OUTPUT DIFFERENTIAL ALWAYS BELOW STRAIGHT THROUGH CONFIGURATION

Figure 2.29. System Block Diagram

One of the reasons for selecting the always below straight through option is to avoid the straight through condition where $N_{in} = 12,000$ rpm. For input speeds approaching straight through the machine PMB must be controlled at or near zero speed and control of this motor becomes more complex. On the other hand as N_{in} decreases more power flows through the speed compensation path. Therefore, a compromise is desired that will not impose an extreme operating range on the Electric Power Processor driving PMB or cause the power in the speed compensation path to be unacceptably high. The Table 2.1 shows some examples.

Table 2.1 Compensation Speed Ratios

<u>Ncomp Speed Ratio</u>	<u>N_{in} (max)</u>	<u>Ncomp (max)</u>	<u>Compensation Power % of Output Power</u>
*			
∞	12,000	5,333	44%
10:1	11,435	5,647	47%
5:1	10,800	6,000	50%
3:1	9,818	6,546	55%

* Ncomp (min) = 0

The case where the compensation speed ratio is 5:1 is chosen for the ECCSD system described in this report. This fixes the maximum input speed to the speed summer at 10,800 rpm. Thus, the input gear ratio should be 1.67 as shown in Figure 2.29. The gear ratios G_a and G_b for PMA and PMB, respectively, are chosen so that PMA and PMB will operate up to but not beyond their maximum designed speed rating. Making G_a and G_b as high as possible minimizes the torque and thus size of the two machines PMA and PMB.

2.2.2 System Power Rating

The speed summer as shown in Figure 2.29 exhibits constant torque operation. That is, all the input and outputs of the speed summer experience the same torque. Because the output speed of the speed summer is constant, the torque on the speed summer is determined by the load placed on the output shaft by the 400Hz generator.

Knowing the speeds and torques within the system makes it possible to determine power flow (rating) at various points in the system as illustrated by the following equations:

$$P_{out} = \frac{P_{gen} \text{ (kW)}}{\eta_{gen}}$$

$$P_{in} = \frac{N_{in} P_{out} \text{ (kW)}}{12000 \eta_{diff}}$$

$$P_{comp} = \frac{N_{comp}}{12000} \cdot \frac{P_{out} (kW)}{\eta_{diff}}$$

$$T_b = \frac{P_{comp} (ft.lb)}{N_{comp} (7.04) \eta_{gb} G_b}$$

$$P_a = \frac{P_b (kW)}{\eta_b \eta_{epp}}$$

Where

P_{out} = drive output power
 P_{in} = differential input power
 P_{comp} = differential compensation power
 P_{gen} = generator output power
 η_{gen} = generator efficiency
 η_{diff} = 0.96 = differential efficiency
 η_{ga} = 0.99 = PMA gearing efficiency
 η_{gb} = 0.98 = PMB gearing efficiency
 η_{epp} = electric power processor efficiency
 T_a = PMA shaft torque
 T_b = PMB shaft torque
 P_a = PMA terminal power
 P_b = PMB terminal power

Steady state power flow in the system can now be determined at various operating points. The Table 2.2 summarizes steady state power flow in the system. As we see from the table, power flow in the speed compensation path is greatest at low input speeds. Thus, the design points for PMA, PMB, and the Electric Power Processor occur at minimum input speed. Because the torque of the differential changes with load, not speed, the currents flowing in PMA, PMB and Power Processor do not change significantly with speed. This is evidenced by the drop in efficiency of PMB (η_b) at 5400 rpm input speed.

Table 2.2. Steady State Power Flow

<u>N_{in}</u>	<u>P_{gen} (kw)</u>	<u>η_{gen}</u>	<u>P_{out} (kw)</u>	<u>P_{in} (kw)</u>	<u>P_{comp} (kw)</u>	<u>η_b</u>	<u>η_{epp}</u>	<u>P_a (kw)</u>
3000	40	.875	45.7	23.8	23.8	*	*	*
3000	60(1pu)	.880	68.2	35.5	35.5	.92	.90	42.9
3000	80(2pu)	.862	92.8	48.3	48.3	.94	.90	57.1
3000	95(shock load)	.845	112.4	58.5	58.5	.94	.90	68.9
5400	40	.875	45.7	42.8	4.76	*	*	*
5400	60(1pu)	.880	68.2	63.9	7.10	.90	.90	8.77
5400	80(2pu)	.862	92.8	87.0	9.67	.84	.90	12.80
5400	95(shock load)	.845	112.4	105.4	11.70	.84	.90	15.50

One advantage of the differential based constant speed drive is that some portion of the system power travels directly through low order gearing to the output. This is desirable because the gears are highly efficient. The remaining portion of the system power travels via the speed compensation path which is less efficient. It follows that when most of the power is flowing directly to the differential the system will be more efficient. As the proportion of power flowing via the compensation path increases, the system efficiency will decrease. For the always below straight through option described herein the compensation path power decreases as system input speed increases. Thus, the system will be most efficient at high input speeds.

By using some estimates for the efficiencies of various parts of the system a rough estimate of efficiency can be made to illustrate how system efficiency changes with speed.

$$P_{in \text{ total}} \approx \frac{1}{0.99} \left(P_{in \text{ differential}} + \frac{P_{comp}}{\eta_{gb} \eta_b \eta_{epp} \eta_a \eta_{ga}} \right)$$

↑
input gear mesh

@ 3000 rpm, $P_{out} = 68.2 \text{ kW}$

$$P_{in \text{ total}} = \frac{1}{0.99} \left(35.5 + \frac{35.5}{(0.98)(0.92)(0.90)(0.93)(0.99)} \right)$$

$$= 83.9 \text{ kW}$$

$$\eta_{total} = \frac{68.2}{83.9} = 0.81$$

@ 5400 rpm, $P_{out} = 68.2 \text{ kW}$

$$P_{in \text{ total}} = \frac{1}{0.99} \left(63.9 + \frac{7.1}{(0.98)(0.90)(0.90)(0.65)(0.99)} \right)$$

$$= 77.8 \text{ kW}$$

$$\eta_{total} = \frac{68.2}{77.8} = 0.88$$

2.2.3 Electric Power Processor (Controller)

The machines PMA and PMB have permanent magnet rotors. The back emf magnitude of these machines varies directly with their speed. The speed of PMB decreases with increasing input speed. The output voltage of PMA is the lowest at the point where the voltage applied to PMB must be the highest. This situation must be accommodated by the power processor.

The system can be designed for PMA to have an output voltage that is higher than PMB voltage at all operating points. Otherwise, the system can be designed to boost the output voltage from PMA so that enough voltage is available to drive PMB. In the interest of having a low risk approach the topology shown in Figure 2.30 was chosen for the Electric Power Processor.

This topology is a straightforward approach without the added complexity that would result if a boost stage were necessary. By using SCR's in a phase controlled rectifier bridge arrangement the output voltage from PMA can be allowed to go very high without subjecting the PMB inverter drive transistors to high voltage. This arrangement is illustrated in Figure 2.30.

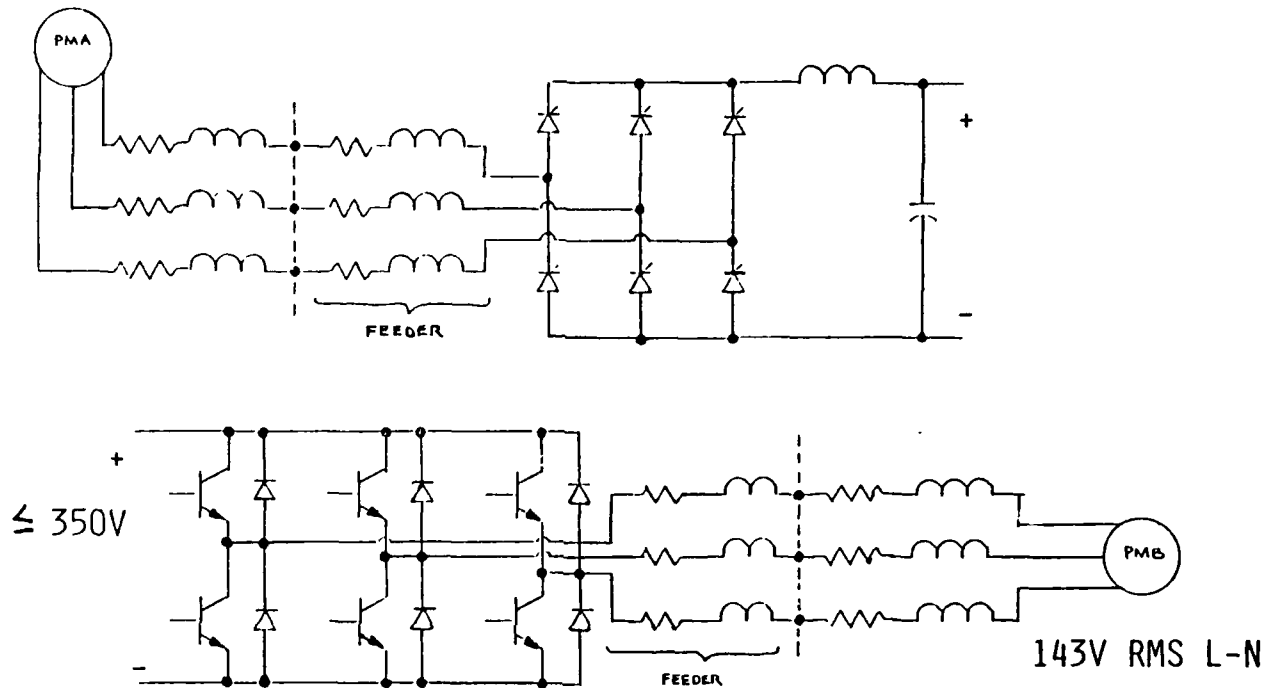


Figure 2.30. Electric Power Processor Topology

The output voltage of the SCR bridge is used to control the magnitude of voltage applied to PMB. The normal operating speed range for PMB varies 5:1, and the output voltage of the SCR bridge will also vary as such. As the output voltage of the SCR bridge decreases, however, the input voltage to the bridge is increasing. Thus, the effective control range for the SCR bridge is $(5)(1.8):1 = 9:1$. The input frequency to the SCR bridge will be 2.5 kHz at maximum input speed.

The inverter used to drive PMB operates PMB as a brushless motor where the inverter commutates the motor windings in accordance with the position of PMB's rotor. This scheme requires a position sensor on the shaft of PMB. The voltage applied to PMB is determined by the inverter bus voltage.

The torque output of PMB is controlled by varying the commutation of the inverter with respect to motor (PMB) position.

2.2.4 Controls and Simulation

The basic function of the controller is to control motor operation adding speed and power at the differential to maintain output shaft speed of the electric drive constant. The controller must respond to the following operational conditions:

- (1) Changes in input (engine) speed to the system
- (2) Changes in load on the output shaft

Basically, the controller will be driven by a speed error signal. The speed error signal is derived by comparing a signal representing speed of the output shaft to a reference.

Depending upon the polarity of this error signal, the controller will have to increase or decrease the amount of speed being added by the machine attached to the differential. The other PM machine is attached to the input shaft of the system. The speed of this machine is fixed by the shaft to which it is attached.

Two controllers are required: The first one requires the input shaft speed and the link voltage error signals for the PMA/SCR bridge firing angle, and the second one requires only the output speed error signal for PMB/Inverter commutation angle. On negative speed error signal and minimum commutation angle the controller will cause the PMB to operate in the braking mode. The braking mode occurs when the engine is accelerating and/or load off on the 400 Hz synchronous generator occurs.

The simulation tool is EASY 5 by Boeing Computer Services. The system model schematic is shown in Figure 2.31. Machine design parameters based on the tangential design (see Figure 2.32) were used in the simulation.

2.2.4.1 Model Descriptions

Differentials/Gears:

The model neglects the gear train compliance. No speed or power loss is assumed in the differential model.

PMA/SCR Bridge:

The complete PMA/SCR bridge circuit was analyzed using SPICE to obtain the output characteristics to represent a Thevenin's equivalent by assuming the input speed to PMA is constant. Figure 2.33 shows the PMA/SCR bridge circuit as modelled using SPICE, and the derived equivalent circuit for EASY 5 modeling. The model output resistance R_0 and terminal voltage V_{d_0} are functions of the PMA input speed and the firing angle, as shown in Figure 2.34. This simplification technique is valid for firing angles not greater than 100° . This Thevenin's equivalent circuit does not have voltage

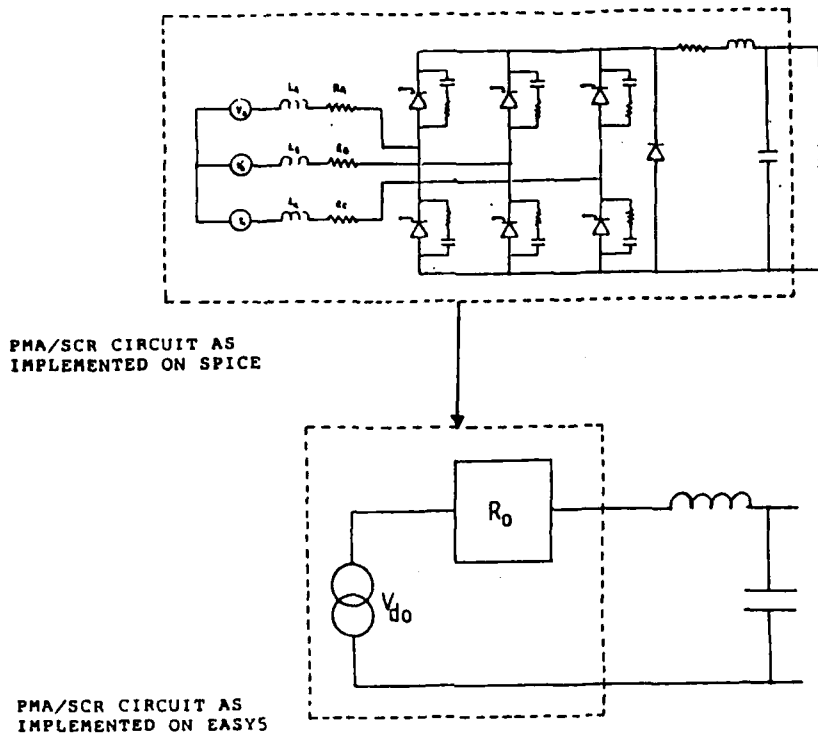


Figure 2.33. Spice Model for SCR Bridge

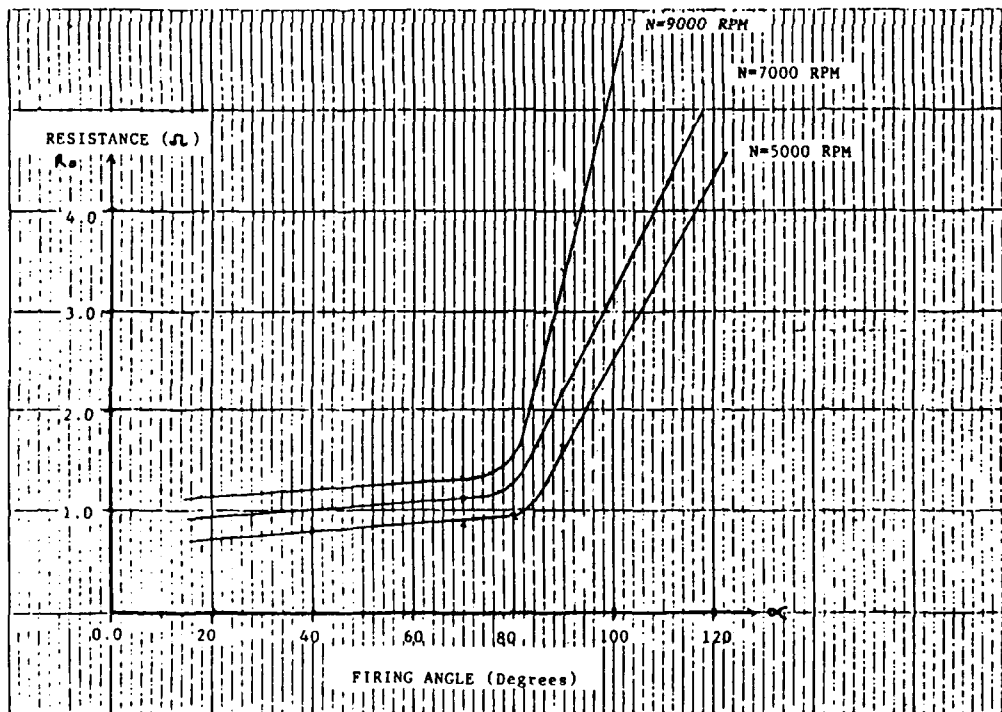


Figure 2.34. SCR Bridge Output Characteristics

and current dynamics, because these dynamics are assumed fast as compared to the system inertial dynamics.

PMB/Inverter:

The inverter is represented as an equivalent model. The PMB is based on the D-Q equivalent model by assuming the flux distribution is sinusoidal in the air gap. Figure 2.35 illustrates the PMB/Inverter model on. The inertial dynamics of PMB are also accounted for in the system model.

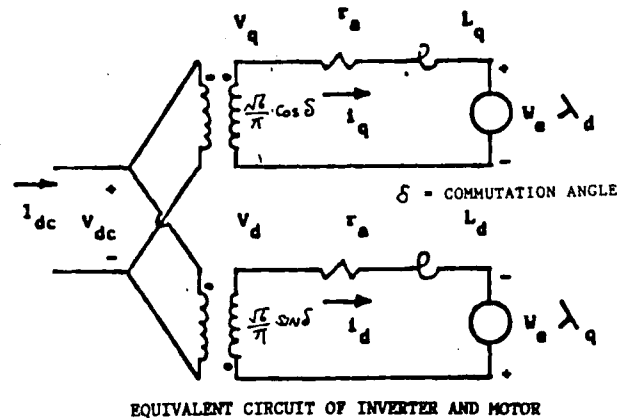


Figure 2.35. EASY 5 Inverter Model

2.2.4.2 Controller Objectives

The controller objectives are to maintain the main generator output frequency within the specifications and to operate PMB at maximum efficiency. The desired transient response of the system is shown in Figure 2.36.

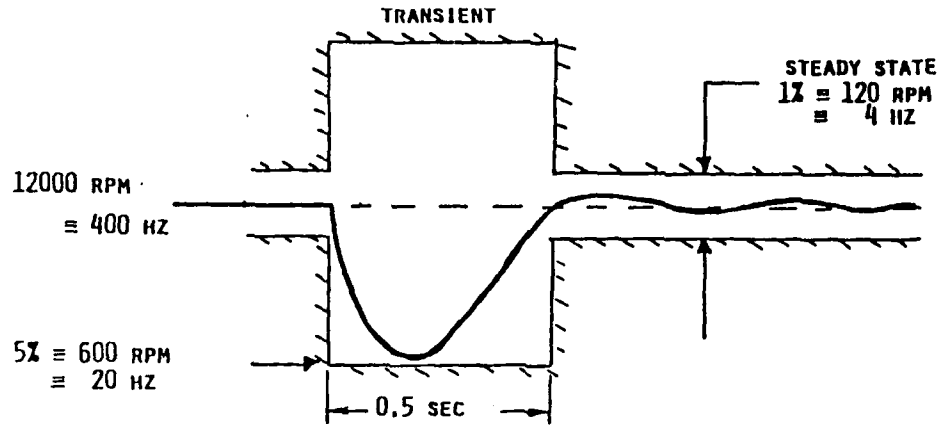


Figure 2.36. Desired Transient Response of System

2.2.4.3 Controller for PMA/SCR

To operate PMB at its maximum efficiency, the link voltage has to be controlled, and Figure 2.37 shows the optimum link voltage for various load conditions. By using the average link voltage command, near maximum efficiency can be achieved. Taking the firing angle as input and the link voltage error as output for the transfer function analysis, an integral controller is adequate to provide the required bandwidth and stability margin for PMA/SCR bridge.

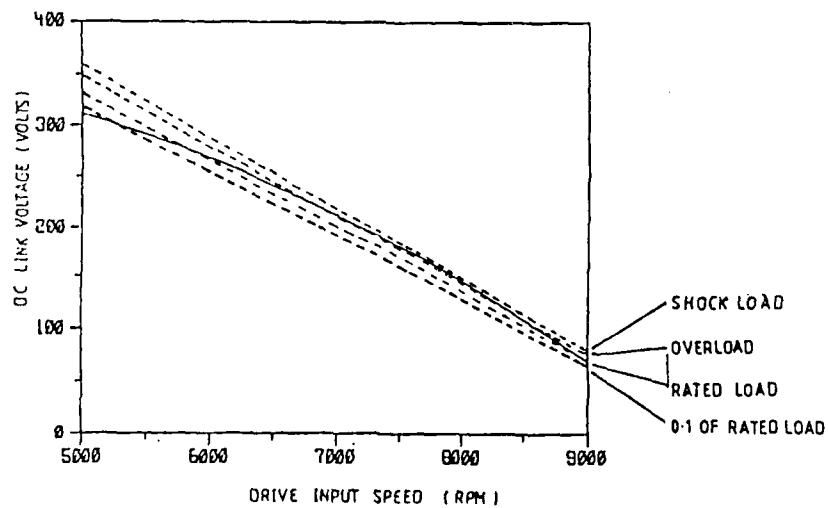


Figure 2.37. DC Link Voltage

2.2.4.4 Controller for PMB/Inverter

The link voltage is set by the engine input shaft speed through the PMA/SCR bridge control, and the output speed of the PMB is therefore defined by this link voltage. The inverter's commutation angle controls the PMB output torque. A transfer function analysis between the commutation angle and the main generator frequency error establishes that a proportional integral (PI) controller provides the necessary bandwidth and stability margin for the PMB/Inverter combination. A negative commutation angle is an indicator for braking when the minimum commutation angle is reached. The braking occurs during load-off transient in the main generator and/or during engine acceleration.

When the braking mode is activated, the current dumping circuit in the link is duty cycled. The current dumping circuit consists of a transistor switch in series with a 10.0 Ω resistor connected across the bus. The switch is controlled so the link voltage does not exceed 350 V. This limit is imposed by the inverter's transistor voltage rating.

2.2.4.5 Simulation Results

The results of the system simulation are summarized in Table 2.3 and Table 2.4. Conditions of shock-load application and removal at maximum and minimum system input speed were simulated. Input acceleration and deceleration were also simulated for the cases of no-load and overload, respectively. The waveforms of Figure 2.38 are examples of simulation results for shock-load application at 5000 rpm input speed. Some examples of simulation results for input deceleration with overload are shown in Figures 2.39 and 2.40.

The simulations were necessary to insure that system transient performance requirements could be met. Also, transient power requirements for the Electric Power Processor and permanent magnet machines were determined. This information was then used to finalize the design of the various system components.

Table 2.3. Simulation Results

Tabulation of Acceleration/Deceleration Simulation Results

Load on simulation represents a transition of 0.1 rated load (6.8 kw) to shock load (112 kw).

Load off simulation represents a transition of shock load to 0.1 rated load.

	Engine Input Speed = 5000 RPM						Engine Input Speed = 9000 RPM					
	Load On Transient			Load Off Transient			Load On Transient			Load Off Transient		
	Peak Value	Steady State	Response Time(s)	Peak Value	Steady State	Response Time(s)	Peak Value	Steady State	Response Time(s)	Peak Value	Steady State	Response Time(s)
DC Link Voltage (Volts)	309	308	-	325	308	-	51	70	-	215	70	-
DC Link Current (amperes)	250	205	-	205	20	-	245	205	-	185	15	-
PMB Torque (in-lb)	122	100	-	100/-20	5	-	125	100	-	100	5	-
Gen. Frequency (Hz)	394.5	400	0.35	405.5	400	0.3	394.5	400	0.3	401.6	400	0.3

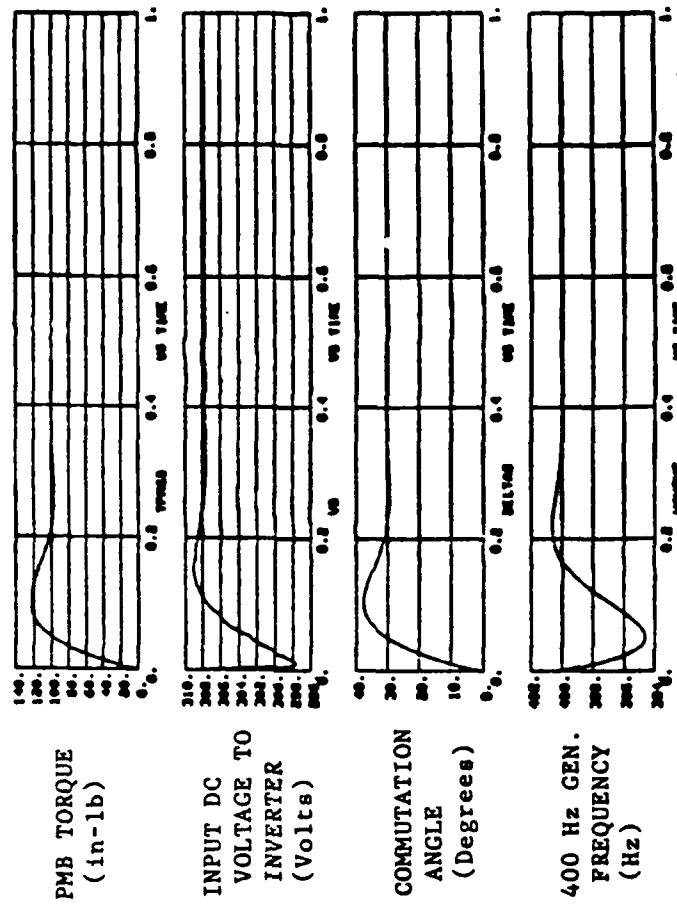
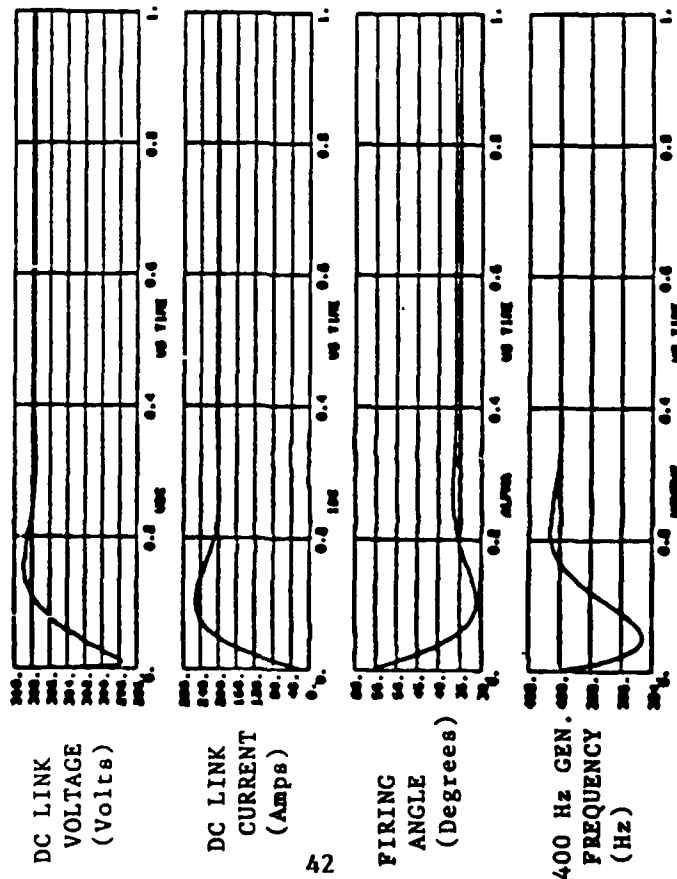
Table 2.4. Simulation Results

Tabulation of Acceleration/Deceleration Simulation Results

Acceleration with no load represents 1000 RPM/sec starting from 5000 RPM.

Deceleration with overload (92 kw) represents 1000 RPM/sec starting from 9000 RPM.

	Engine Input Acceleration			Engine Input Deceleration		
	5000 RPM to 5500 RPM			9000 RPM to 8500 RPM		
	Initial Value	Peak Value	Final Value	Initial Value	Peak Value	Final Value
DC Link Voltage (Volts)	308	-	292	70	-	105
DC Link Current (amperes)	10	-	-8	160	198	180
PMB Torque (in-lb)	0	35	-	80	98	93
Gen. Frequency (Hz)	400	400.5	400	400	399.1	400.1



(LOAD TRANSIENT - 0.1 RATED LOAD TO SHOCK LOAD)

Figure 2.38. 5000 RPM Load-on

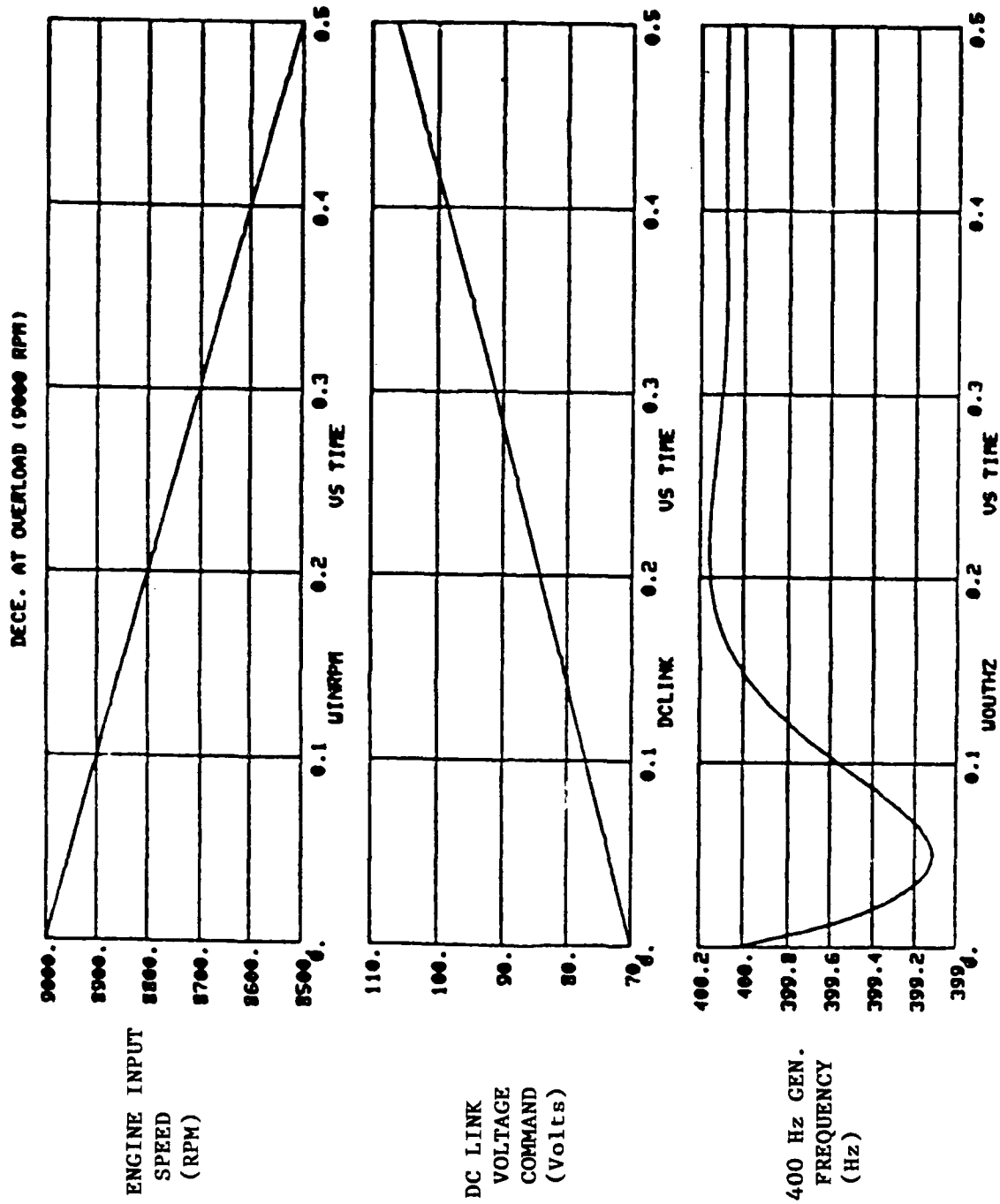


Figure 2.39. 9000 RPM Decel w/Overload

DECE. AT OVERLOAD (9000 RPM)

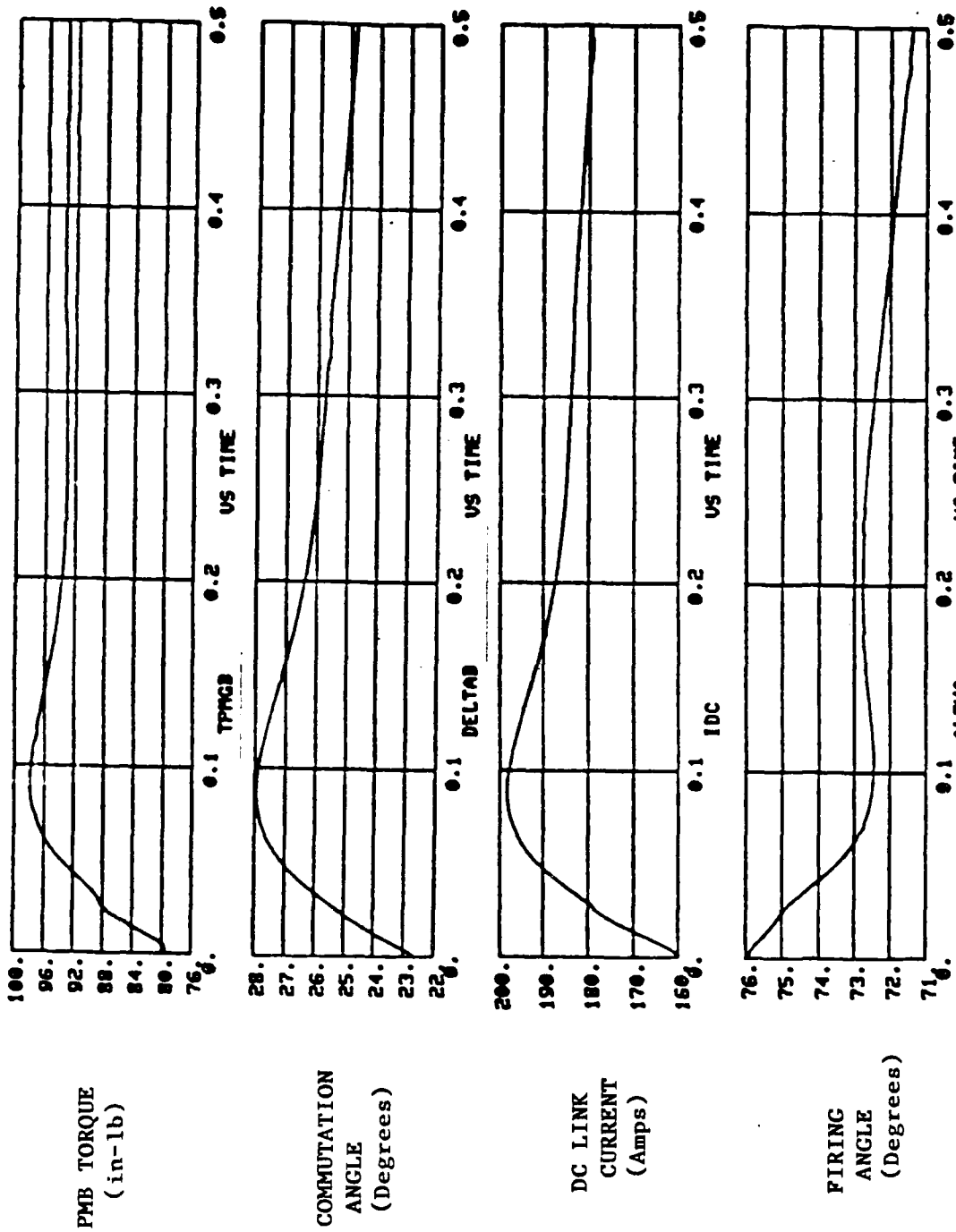


Figure 2.40. 9000 RPM Decel w/Overload

3.0 POWER ELECTRONICS

3.1 AC/DC CONVERTER

The power converter changes the variable power from the permanent magnet machine (PMA) to a controllable voltage source for the PMB/inverter drive. The block diagram of this power converter is shown in Figure 3.1. The permanent magnet machine (PMA) generates variable frequency power. The variable power from the generator is rectified and regulated by the 3 phase, 6 pulse phase controlled rectifiers.

Operating range:

Input Voltage	219 - 393 phase voltage
Input Frequency	1380 - 2500 Hz
Output Voltage	35 - 315 V
Current Rating	150 A continuous

The control of the phase-controlled rectifier relies on the phase information derived from the PMA terminal voltage waveform. Control functions include voltage regulation, unbalance and overcurrent protections of the PMA and SCR bridge.

This converter has an improved control circuit for converting a three phase variable frequency voltage, having a high degree of distortion and noise, into regulated output power.

INPUT VOLTAGE: 219 - 393 PHASE VOLTAGE
FREQUENCY: 1.38 - 2.5 kHz

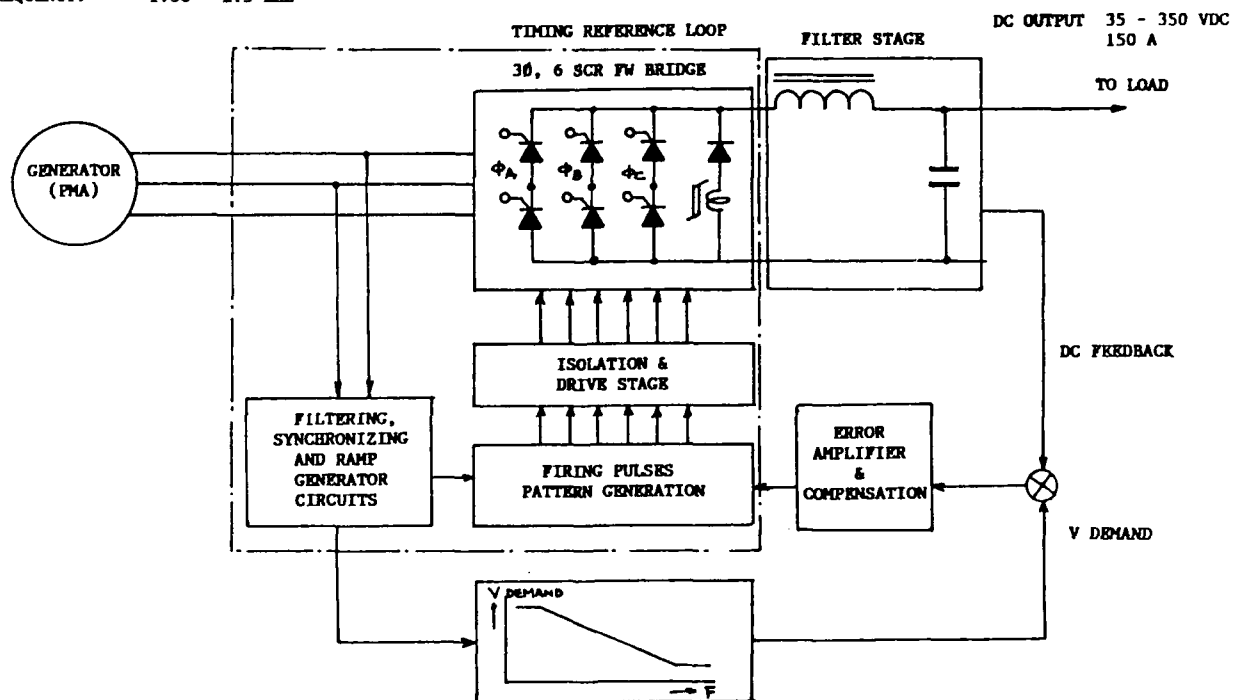


Figure 3.1. Block Schematic of 3Ø Six SCR FW Bridge Regulator

A single stage LC filter attenuates the voltage ripple of the bridge to the required level.

3.1.1 Detailed Description

3.1.1.1 Power Module Assembly

Power circuit is shown in Figure 3.2. The photograph in Figure 3.3 shows the assembly of the controlled rectifier bridge with output filter.

The controlled rectifiers used in the power circuit are rated 135 A and 65 A average at 85°C and 125°C case temperature respectively. The selected devices are inverter grade SCRs with turn-off time of 30 μ s which have a blocking and reverse voltage rating of 1600 V. In this application, the maximum reverse voltage experienced by each thyristor is 970 V at PMA top speed. This degree of voltage derating enhances the operational reliability of the thyristors.

Stud mount thyristors were chosen for this application. They are mounted onto the chassis of two 1/4 in. thick, 5 in. x 13 in. extruded aluminum U channels. Each channel is fitted with a 3/8 in. diameter copper tube for single sided liquid cooling. One cool plate accommodates three thyristors and the free wheeling diode to form the positive half bridge; the remaining three thyristors and cool plate assembly forms the negative half bridge. All the thyristors and diode are electrically insulated from the cool plate using COTHERM which is a very efficient thermal conducting and electrical insulating material.

Snubber resistors with aluminum housings are mounted on the cool plate chassis to utilize heat sink effect.

Cooling tubes of the cool plates were connected in series and hooked up to a closed circuit water cooling system. Inlet water cooling temperature was maintained between 20 to 25°C.

3.1.1.2 Snubber Circuit

R-C non-polarized snubbers were used to limit induced voltage spikes produced during reverse recovery of the thyristor storage charge. The snubbers also served to limit the forward voltage rate of rise applied to the thyristor after recovery from turn-off. At large delay angles, the slope of this forward blocking voltage could be very steep and the thyristor could inadvertently be turned on.

The data required for snubber design are maximum peak reverse voltage across the thyristor, maximum allowable thyristor dv/dt rating and the estimated value of the commutation reactance in the power circuit. The discontinuities of the voltage across the thyristor (worst transient

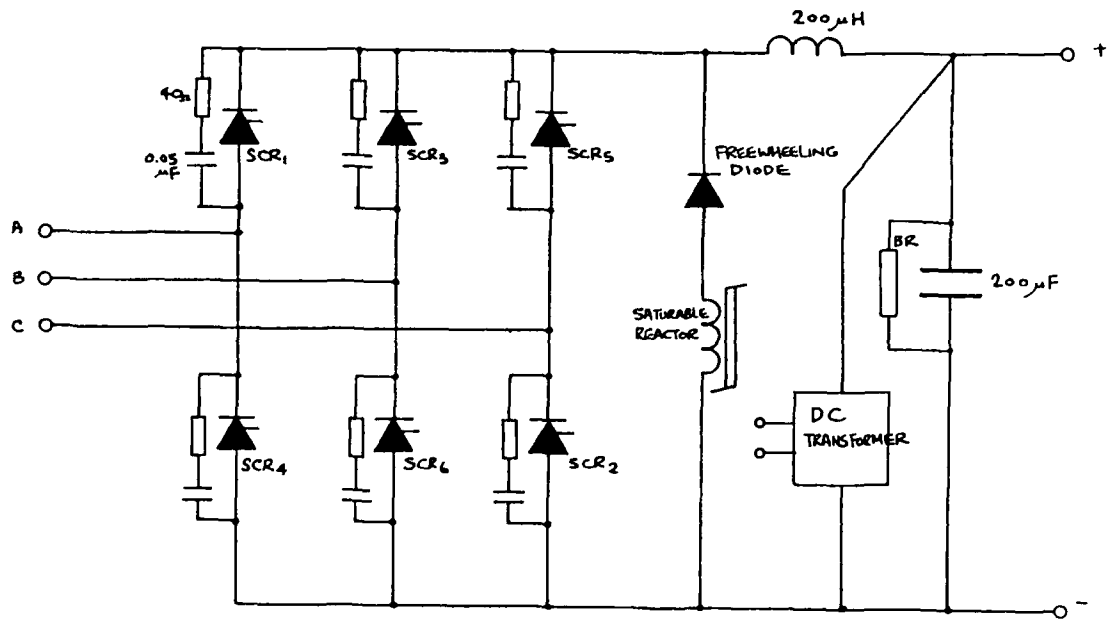


Figure 3.2. Power Circuit



Figure 3.3. Power Module Assembly

voltage) are at a maximum when the delay angle is 90° . The final values of R and C used in the circuit are 40Ω and $0.05 \mu\text{F}$ respectively.

3.1.1.3 LC Filter

If there are no constraints on the weights and sizes of components, the criteria for the selection of the LC filter can be formulated as follows:

- (a) The filter input current should not be discontinuous, and its peak to peak ripple current should be less than a specified value.
- (b) The peak to peak ripple value of the capacitor voltage should be less than a certain specified value.
- (c) The resonance frequency of the L-C circuit must be below the minimum operating frequency of the inverter drive.
- (d) The losses in the DC link should be kept to a minimum value.
- (e) The DC link filter component values should not affect the stability of the overall system.

To arrive at reasonable values in the selection of filter components, the following assumptions are made:

- (1) The voltage at the input of the filter is ideal.
- (2) The inductor is so large that the current ripple is negligibly small.
- (3) The inverter current waveform is not significantly affected by the ripple voltage at its input terminals due to the finite value of the capacitor.
- (4) The resistance of the inductor is negligible.

Using the above assumptions, which are considered permissible from a practical point of view, procedures for the choice of filter components are based on (a) limiting the voltage and current ripples to a specified value, (b) component sizes and weights considerations, and (c) resonant frequency considerations. The values of L and C used in the circuit are $200 \mu\text{H}$ and $200 \mu\text{F}$ respectively.

DC Choke Data

Inductance	195 μH
Resistance	0.00782 Ω
Rating	150 DC continuous
Ripple Current	15 A peak to peak
Ripple Frequency	8 kHz - 15 kHz

DC Choke Data (continued)

Material	12 mil Nickel iron cut core
Cooling	Air
Weight	7 lb.

Filter Capacitor

Capacitance	200 μ F +/- 10%
Rating	600 V
Ripple Frequency	6 kHz - 15 kHz
Material	Paper dielectric; oil impregnated

Multilayer ceramic capacitors had been used during the development but they were found to run hot with low ripple current. Thermal stress of these capacitors was a concern because of the high frequency pulse current drawn by the inverter at rated load. Eventually they were replaced by paper dielectric, oil filled capacitors in subsequent tests.

3.1.1.4 Phase Delay Controls

Figure 3.4 is the block diagram of the controlled-rectifiers system with voltage feedback loop. Figure 3.5 is the timing diagram of the relevant signals described in the following section.

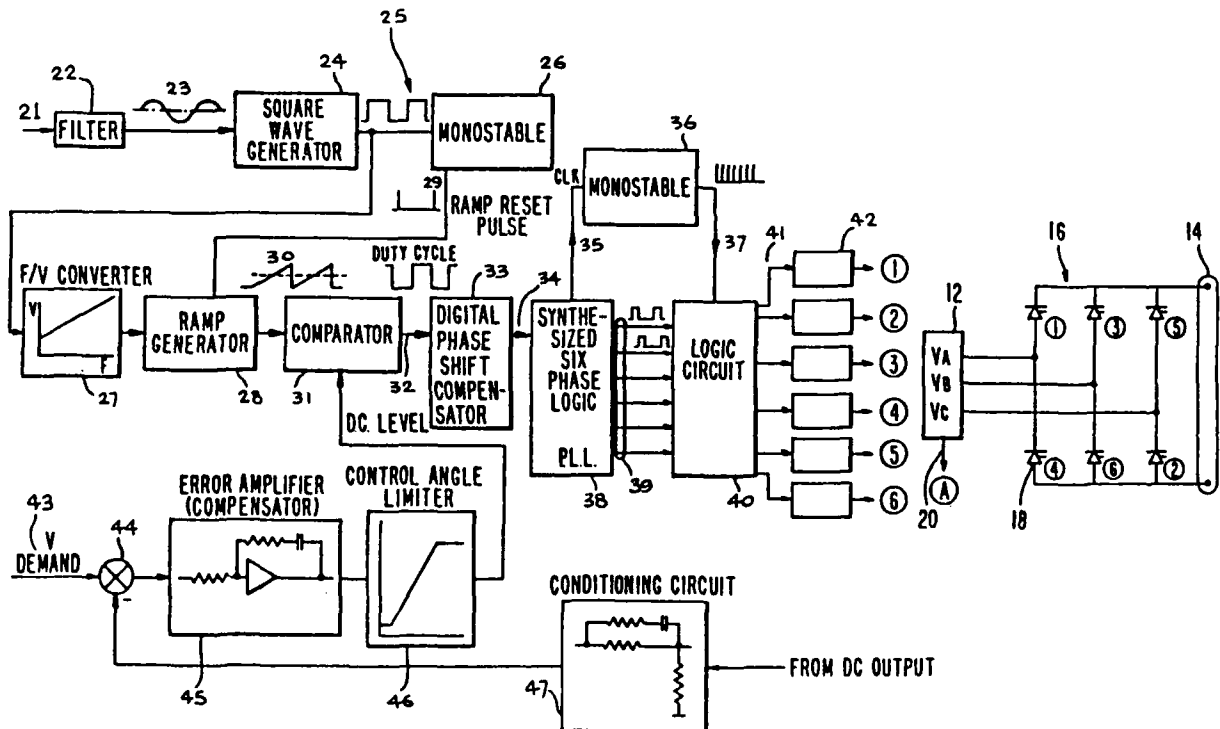


Figure 3.4. Block Diagram of Phase Delay Control

The traditional approach to generating an ensemble of firing pulses requires a timing reference which occurs at the same point in each cycle of the reference voltage waveform. The timing signals for triggering the SCRs are generated at the end of some controllable delay which begins at the timing reference; this delay may be either a time delay or a phase delay, depending on implementation. Converter output is adjusted by varying the delay with a DC signal.

A single phase reference signal is derived from zero crossing detection of the filtered generator line voltage. A signal transformer is used to provide isolation and matching of the low voltage electronic circuit to the high generator output voltage. The timing reference signal 24 is a square wave and is applied to a frequency to voltage converter 27 which produces an output voltage directly proportional to the input frequency.

The output signal from the F/V converter 27 is taken to a ramp generator 28 which produces a sawtooth waveform 30 with a slope proportional to the input signal. The output of the ramp generator 28 is reset to zero for 3 μ s by a reset pulse from the monostable 26 at the start of each cycle. The time base of this sawtooth signal 30 is, therefore, synchronized to the first zero crossing point of the input signal 23.

A variable duty cycle square wave 32 is generated from the comparator 31 when the ramp 30 is above the level applied to the comparator. Since this variable duty cycle square wave is synchronized to the terminal voltage signal 21, phase delay is a measure of the off time period of this variable duty cycle signal from the comparator.

The output of the phase logic circuit in 38 tracks the leading edge of the variable duty cycle signal 32 and synthesizes a series of 60° wide output pulses 39 each with 60° phase shift. The synthesized six phase logic circuit 38, including a PLL chip and a divide by six counter, contains an oscillator running at six times the variable input frequency. The signal produced by the VCO is applied to a one shot multivibrator 36 which produces a train of 25 μ s pulses 37 spaced 60° apart.

The synthesized six phase logic signals 39 and the pulse train 37 are mixed by using AND/OR gates to produce a 25 μ s wide, 60° apart double pulse gating signals 41 for thyristor switching.

The signal 21, used as a reference for phase delay control, is derived from the PMA output using a step down transformer; this signal is a replica of the generator terminal voltage waveform which is distorted and superimposed with notches along the envelope. Distortion of the terminal voltage is due to

- (a) harmonic currents, produced by the converter, flowing into the source,

The traditional approach to generating an ensemble of firing pulses requires a timing reference which occurs at the same point in each cycle of the reference voltage waveform. The timing signals for triggering the SCRs are generated at the end of some controllable delay which begins at the timing reference; this delay may be either a time delay or a phase delay, depending on implementation. Converter output is adjusted by varying the delay with a DC signal.

A single phase reference signal is derived from zero crossing detection of the filtered generator line voltage. A signal transformer is used to provide isolation and matching of the low voltage electronic circuit to the high generator output voltage. The timing reference signal 24 is a square wave and is applied to a frequency to voltage converter 27 which produces an output DC voltage directly proportional to the input frequency.

The DC output signal from the F/V converter 27 is taken to a ramp generator 28 which produces a sawtooth waveform 30 with a slope proportional to the DC input signal. The output of the ramp generator 28 is reset to zero for 3 microseconds by a reset pulse from the monostable 26 at the start of each cycle. The time base of this sawtooth signal 28 is, therefore, synchronized to the first zero crossing point of the input signal 23.

A variable duty cycle square wave 32 is generated from the comparator 31 when the ramp 28 is above the DC level applied to the comparator. Since this variable duty cycle square wave is synchronized to the terminal voltage signal 21, phase delay is a measure of the off time period of this variable duty cycle signal from the comparator.

The output of the phase lock circuit in 37 tracks the leading edge of the variable duty cycle signal 32 and synthesizes a series of 60 degrees wide output pulses 36 each with 60 degree phase shift. The synthesized six phase logic circuit 37, including a PLL chip and a divide by six counter, contains an oscillator running at six times the variable input frequency. The signal produced by the VCO is applied to a one shot multivibrator 36 which produces a train of 25 microseconds pulse 37 spaced 60 degrees apart.

The synthesized six phase logic signals 39 and the pulse train 37 are mixed by using AND/OR gates to produce a 25 microseconds wide, 60 degree apart double pulse gating signals 41 for thyristor switching.

The signal 21, used as a reference for phase delay control, is derived from the PMA output using a step down transformer; this signal is a replica of the generator terminal voltage waveform which is distorted and superimposed with notches along the envelope. Distortion of the terminal voltage is due to:

- a) harmonic currents, produced by the converter, flowing into the source.

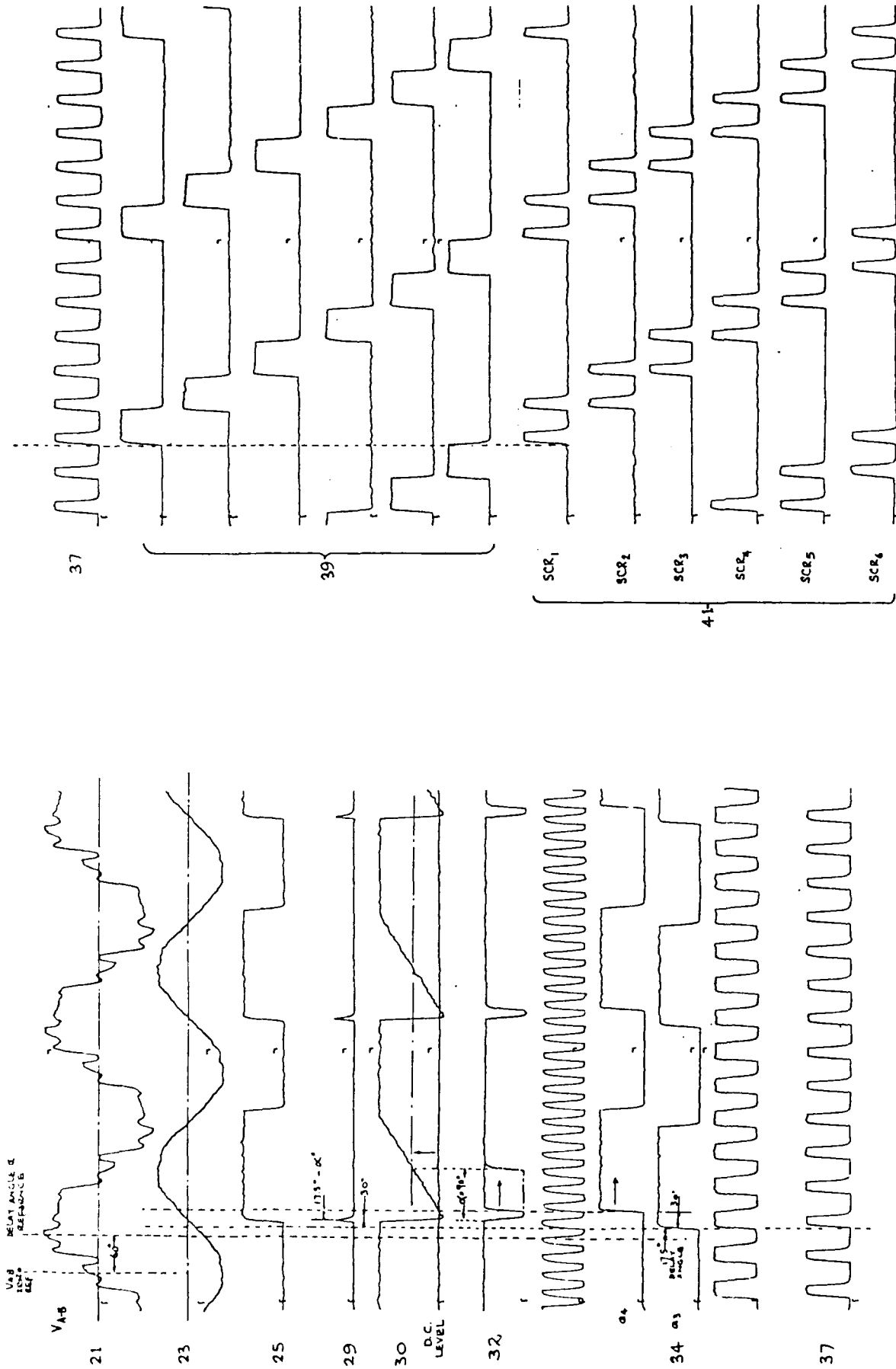


Figure 3.5. Timing Diagram of Phase Delay Control Circuit

- (b) commutation spikes and notches caused by thyristor switching, and
- (c) the source voltage is not stiff. Converter rating is close to the system fault level, which is commonplace in aerospace applications.

The zero crossing detection is the simplest method of obtaining a reference point in a sinusoidal signal. As a result of waveform distortions, there are multiple zero crossings for each cycle of the phase reference signal 21. This signal is applied to an integrator 22 which produces a clean and near sinusoidal waveform. The phase shift introduced by the filter is made independent of input frequency.

The phase shift introduced by the integrator is compensated for by using a digital phase shift circuit 33 as shown in Figure 3.6. Also included are a PLL chip 52 and a six stage shift register 53. Each stage is connected in cascade and operated as a ring counter with a clock signal fed from the VCO of the PLL chip 52. For example, the output Q4 from one of the registers is connected to the input of the phase error detector to form a phase lock feedback loop. The output state of each register (Q1 - Q6) is delayed from its preceding stage by one 30° clock pulse; the incoming signal 51 is rippled through and appears at the output of each register.

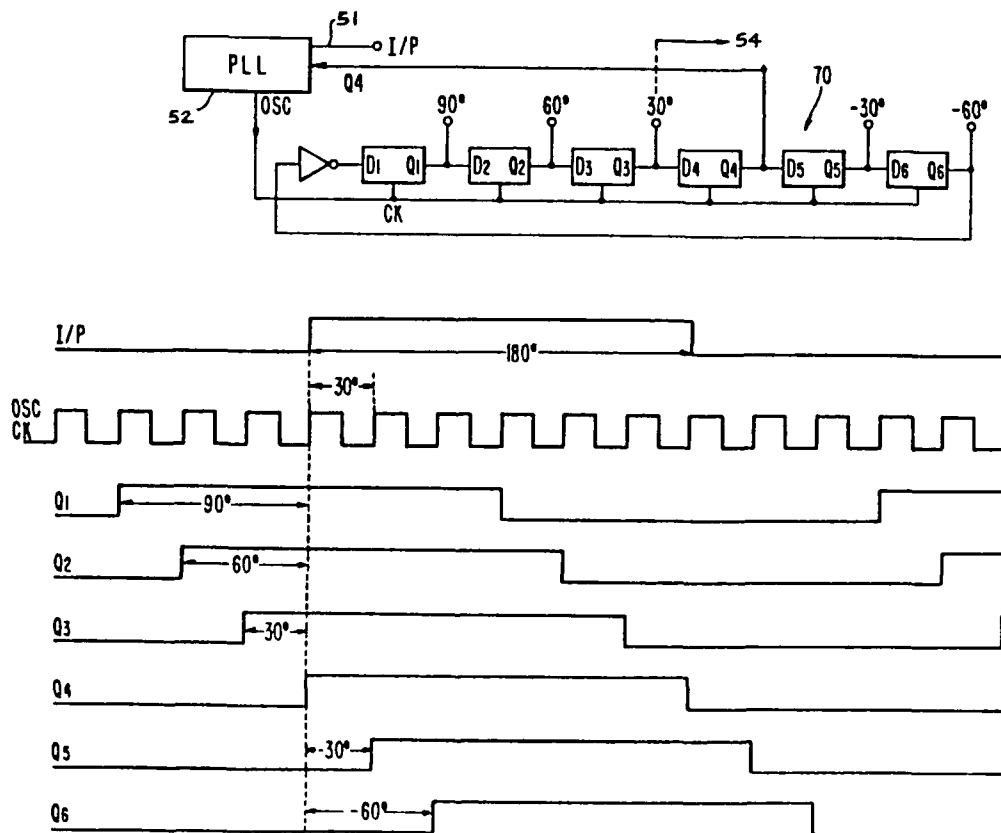


Figure 3.6. Phase Shift Circuit

Because of phase lock action Q4 is in phase with the incoming signal 51 under phase lock action, the preceding and the following registers of Q4 synthesize the leading and lagging waveforms of 51. A phase shift range of 150° ($+90^{\circ}$ to -60°) is provided by a six stage register.

3.1.1.5 Control Electronics

The converter output voltage is regulated by sensing the voltage across the link filter capacitor for closed loop control. The link voltage 14 is interfaced to the low-voltage level electronic circuit using a isolation transformer 47 with ratio 1:0.0328. This gives an output voltage signal of 10.3 V to the voltage error amplifier 45 with 315 V from the bridge. The duty cycle output of the comparator varies with the signal from the error amplifier which, in turn, sets the triggering delay time for the thyristors. The converter output is therefore controlled and regulated to the command signal of the feedback loop.

The output voltage of the SCR bridge is programmed to decrease linearly with an increase of PMA speed. This is implemented by using a summing amplifier with constant gain M and a bias B to produce an output function of $Y = -Mx + B$. The DC signal from the F/V converter is applied to the summing amplifier input x.

3.1.1.6 Gate Drivers

The isolation of thyristor gate drive from control electronics is provided by using a pulse transformer. The pulse transformer has a 1:1 turns ratio with low leakage inductance. The gate drive circuit 42 is designed to deliver a current pulse with di/dt of 3 A/ μ S and a peak current of 4 A into the gate cathode junction of the thyristors. The peak current is significantly higher than the manufacturer's specification to ensure a reliable triggering. An RC speed up circuit is used to provide a two stage gate current waveform, as shown in Figure 3.7A for fast turn-on and latching of the thyristors.

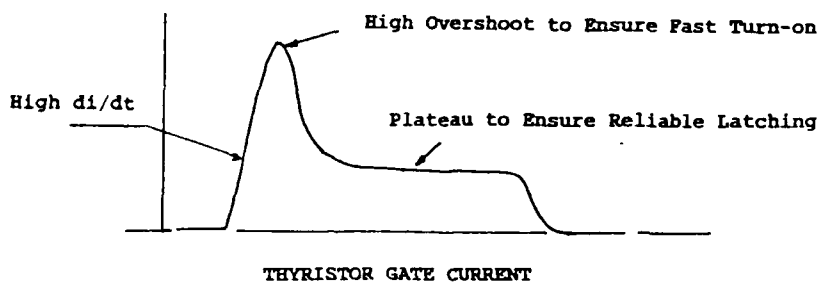


Figure 3.7A. Thyristor Gate Current Waveform

3.1.2 Performance Verification of the Thyristor Converter

3.1.2.1 Open Loop Test

A heat run of the SCR bridge was performed with PMA running at 27780 rpm and 45000 rpm and the converter loaded to 100 A using a water cooled resistive load bank. The thyristor case temperatures were measured after a 1/2 hour heat run; they were between 50 to 74°C.

The following photographs are examples extracted from test data of the power circuit tests.

Figure 3.7B is a typical thyristor triggering pulse. The upper traces are thyristor gate voltage and current waveforms. The lower traces are the same waveforms but with expanded time scale to show rising edges.

Figure 3.8A is the example of the PMA terminal voltage waveform, filtered timing reference signal and bridge input current with PMA running at 27780 rpm (1.38 kHz).

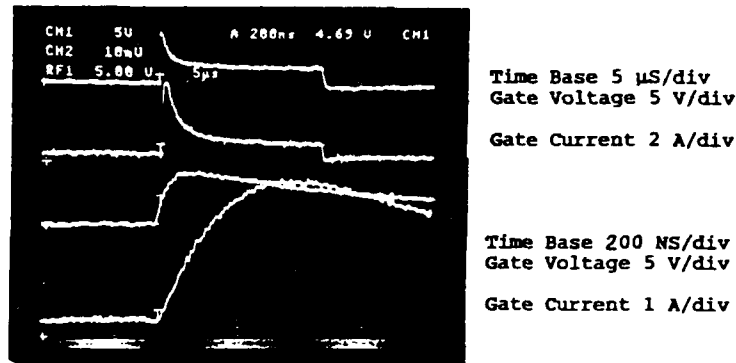
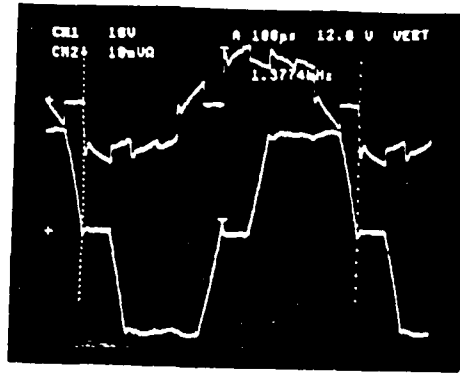


Figure 3.7B. Thyristor Gate Voltage and Current Waveforms

Figure 3.8B shows the same voltage but with PMA running at 45000 rpm (2.37 kHz).

3.1.2.2 Diode Reverse Recovery

The converter would occasionally trip on overcurrent at light load with

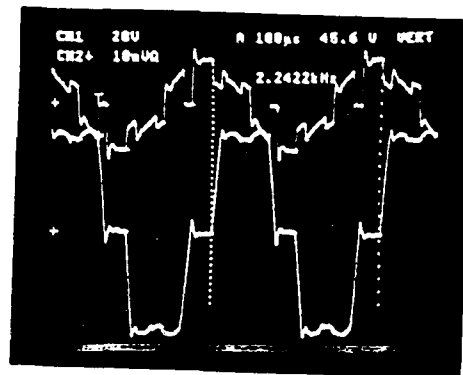


V_{A-B} 187 V RMS

I_A 100 A RMS

PMA AT 27780 RPM
SCR BRIDGE OUTPUT VOLTAGE = 350 VDC

A) PMA Terminal Voltage



V_{A-B} 267 V RMS

I_A 100 A RMS

PMA AT 45000 RPM
SCR BRIDGE OUTPUT VOLTAGE = 350 VDC

B) PMA Terminal Voltage

Figure 3.8. Bridge Input Voltage and Current

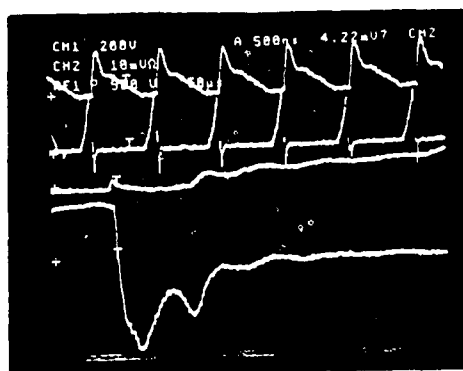
PMA running at higher speeds. The occurrence increased with PMA operating speed. It was found that noise and voltage spikes were induced in the electronic circuit resulting from rapid switching of the free wheeling diode following recovery. These spikes and noise caused thyristor timing circuit to malfunction and thyristors were misfired. The diode provides a freewheel path for the discontinuous current occurring at light load with large delay angles.

When a diode is suddenly reverse polarized from forward current conduction, reverse current flows for a time until the carriers accumulated

in the PN junction disappear. When the diode carriers disappear, the reverse recovery current rapidly decreases creating a large current change (di/dt). This large current change is induced in the surrounding conductors via diode connections resulting in generated noise and spikes.

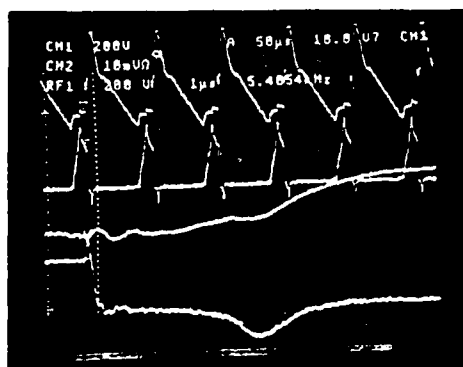
To reduce the voltage spikes, a saturable reactor is used to absorb the diode reverse recovery energy. The diode reverse current is limited by the impedance of the saturable reactor. This impedance is relatively high during the diode recovery interval where the reactor is not saturated. The recovery is then softened by the reactor's moderate transition into its saturated region.

The reactor is made from a stack of eight tape wound cores using 4 mil supermalloy magnetic material; the stack is wound with five electrical turns. The reactor is required to withstand the volt-seconds product developed across its winding by the diode reverse current which causes a change in flux. This saturable reactor is connected in series with the free wheeling diode. Figure 3.9 shows the diode recovery current with and without the saturable reactor.



Time Base 50 US/div
 - Diode Voltage 500 V/div
 - Diode Current 10 A/div
 - Diode Voltage 200 V/div
 - Diode Current 5 A/div
 Lower Two Traces
 Time Base 500 NS/div

A) WITHOUT SATURABLE REACTOR



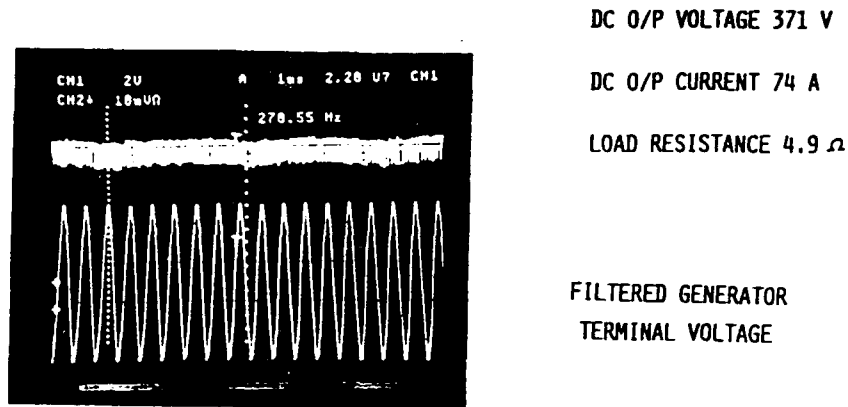
Time Base 50 US/div
 - Diode Voltage 200 V/div
 - Diode Current 10 A/div
 - Diode Voltage 200 V/div
 - Diode Current 5 A/div
 Lower Two Traces
 Time Base 1 μ S/div

B) WITH SATURABLE REACTOR

Figure 3.9. Diode Reverse Recovery

3.1.2.3 Harmonic Instability Between Converter and Source

During load test of the thyristor converter with the permanent magnet generator (PMA), a low frequency modulation of the DC output voltage was observed with the converter operating in open loop voltage control. The magnitude of this low frequency modulation increases not only with the increase of load current but with the decrease of load impedance at constant current. (See Figure 3.10 with filter capacitor removed to eliminate secondary effects.)



PMA RUNNING AT 35000 RPM (1.745 KHZ)
SCR BRIDGE FILTER CAPACITOR REMOVED

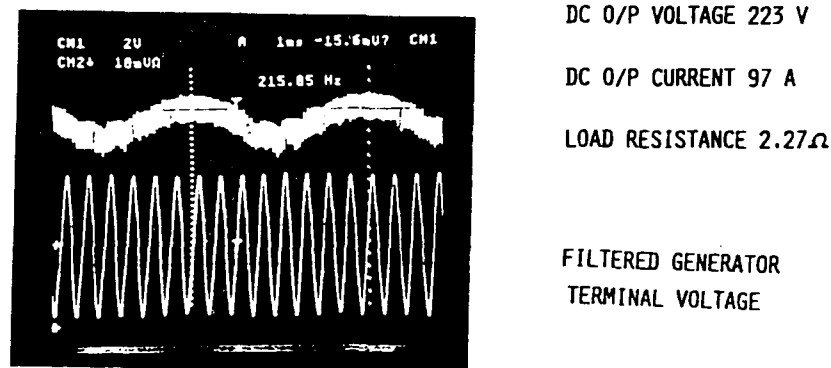


Figure 3.10. Effects of Load Current and Impedance on Harmonic Instability

Power spectral analysis of the filtered timing reference signal (B) is shown in Figure 3.11. The spectrum of this waveform has four major components:

- A carrier frequency of 1.38 kHz which is the PMA fundamental frequency of PMA running at 27780 rpm.
- Side band frequencies of 1.18 kHz and 1.6 kHz above and below carrier frequency.
- A low frequency offset component at 212 Hz.

The filtered timing reference signal can be described by the following equation:

$$Y = \underbrace{A \sin(W_c t)}_{\text{AM modulation}} [1 + m \sin(W_m t)] + \underbrace{K \sin(W_m t)}_{\text{Low frequency offset}}$$

W_c = PMA fundamental frequency

W_m = Modulated frequency

m = Modulation index

The above low frequency offset component superimposed on the carrier causes the zero crossing detection circuit to generate a frequency modulated square wave. The correct timing reference for thyristor triggering is perturbed in a manner to produce a cyclic variation of output voltage. This cyclic varying voltage will draw a corresponding current from the generator, the interaction of this current and the source impedance may exaggerate the original distortion and aggravate the degree of modulation.

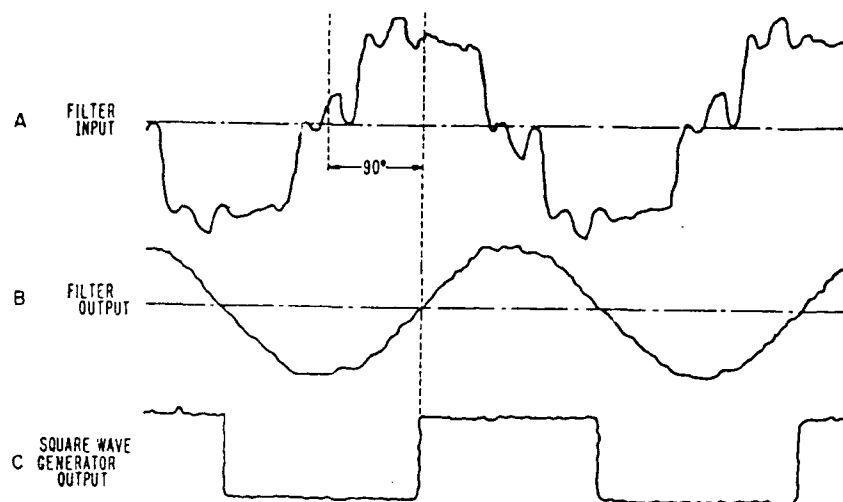
The fundamental frequency of PMA running at 27780 rpm is 1.38 kHz. The envelope of the PMA terminal voltage was modulated at a frequency of 21 Hz. (See Figure 3.12 for filtered PMA terminal voltage.)

Power spectrum analysis of this filtered signal indicates that there is a beat frequency of 212 Hz in addition to the fundamental frequency of PMA at 1.38 kHz.

The above phenomena is due to a form of harmonic magnification or instability between converter and source. This interaction is caused by a positive feedback loop via the thyristor pulse timing circuit (Figure 3.1); in which distortion of line voltage reaching the control systems disturbs the timing signals for thyristor triggering.

In steady state operation, these firing pulses must occur at a fixed, stable time with reference to the fundamental frequency of the input waveform of a given phase.

Harmonic distortion and noise are present in the reference voltage waveform derived from the generator terminal. This can perturb the timing reference for the generation of the pulse pattern. The effect is to cause the timing reference to shift relative to the fundamental component of the source voltage and can be manifested in a positive feedback manner via the synchronizing circuit to produce a cyclic variation of the output voltage.



X=1.18KHz
 Y=-31.26 dBVrms
 POWER SPEC1 10Avg 0%Ovlb Ftop
 60.0

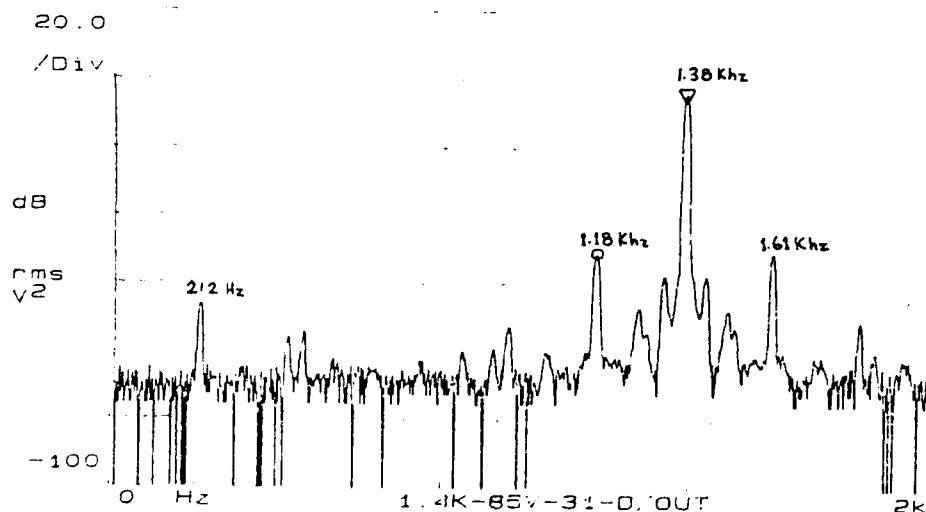
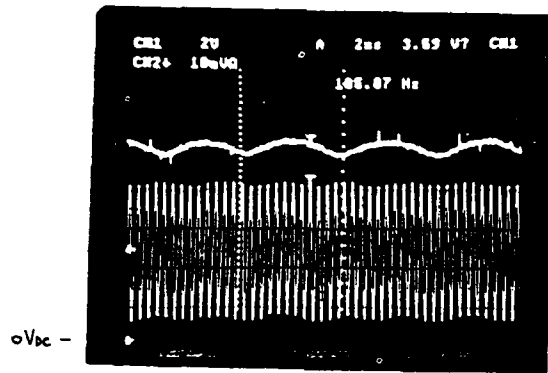


Figure 3.11. Power Spectral Analysis of Filtered Generator Terminal Voltage (B)

The method used to reduce and suppress this undesirable and detrimental modulation was to use a phase locked circuit to provide filtering of the unwanted modulation using the loop dynamics. This was achieved by placing a low pass filter between the phase comparator and the voltage controlled oscillator control input of the phase lock circuit. This filter is a lead lag type and has a bandwidth below the unwanted modulation frequency. The PLL chip also provides a frequency to voltage signal as described in the phase delay control section. The output signal from the F/V conversion is applied to the ramp generator which produces sawtooth signal with slope proportional to PMA frequency. This PLL was connected to the output of the zero crossing detector preceding the pulse timing and pattern generation circuits.

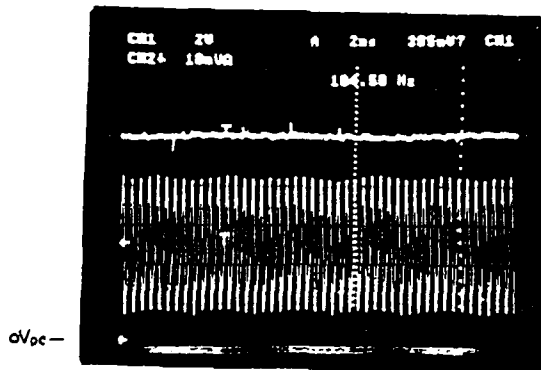
Figure 3.12 shows the reduction in the harmonic instability of the converter operating from a weak power source while employing the above



BRIDGE O/P VOLTAGE 227 VDC
CURRENT 97 ADC

FILTERED GENERATOR
TERMINAL VOLTAGE

PMA FREQUENCY 2.24 KHZ



AS ABOVE BUT WITH
MODULATION
SUPPRESSION CIRCUIT
USING P.L.L.

Figure 3.12. Harmonic Instability Between Converter and Weak AC Source

mentioned modulation filter. Although the cyclic variation of output voltage has been suppressed, modulation of the generator terminal voltage is still present due to the interaction of nonlinear load with a high impedance source.

3.1.2.4 Frequency Response Test

Preliminary tests of the voltage regulator utilized a proportional control system. The control produced an unacceptable voltage drop. A proportional-integral controller was used and tuned at the highest gain point of the PMA/SCR bridge which is at light load and maximum speed.

Frequency response measurement of the converter voltage control loop was performed with PMA delivering 45 A at 27780 rpm to 45000 rpm.

Gain and phase plots of bridge feedback voltage to delay angle control (V_{fb}/V_a) are shown in Figure 3.13.

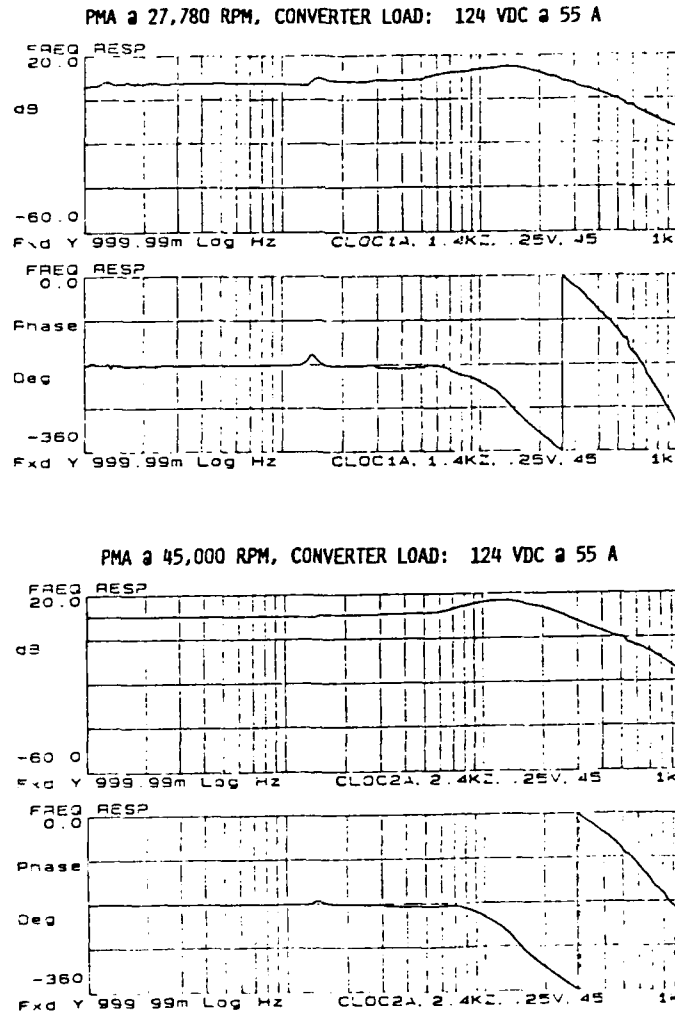


Figure 3.13. Open Loop Frequency Response $\left(\frac{V_{fb}}{V_a}\right)$ Excluding Compensator

Gain and phase plots of the overall voltage control including proportional and integral compensation are shown in Figure 3.14.

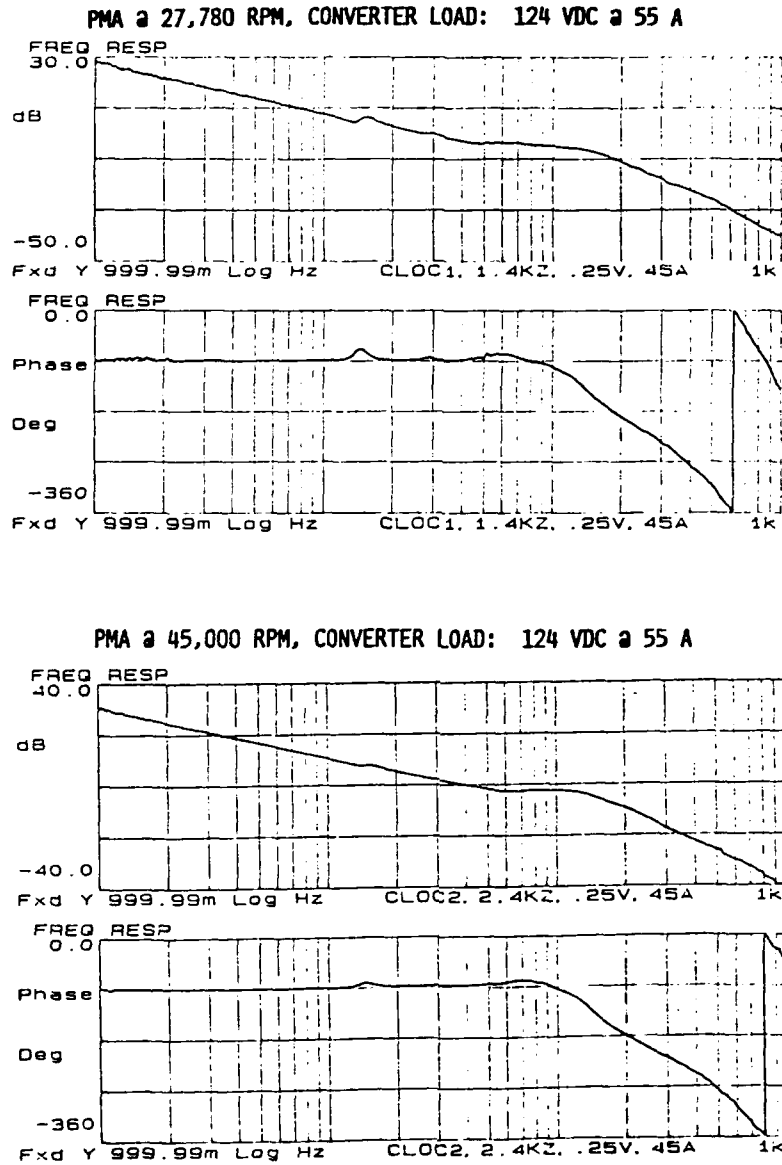


Figure 3.14. Overall Open Loop Frequency Response with P.I. Compensation

To account for the sampler nature of the controlled rectifiers, a transport lag (e^{-st}) was included in the approximate transfer function derived from frequency response measurement. This is justified by the fact that the rectifier cannot be controlled during the interval between two successive cycles of the incoming voltage waveform. Therefore a statistical transport time delay equal to a half period of the input frequency can be postulated. A linearized model based on this assumption is shown in Figure 3.15.

The approximate transfer function (V_o/V_α) indicates that there is a right half plane zero at 670 Hz and a pair of dominant poles at 140 Hz. No practical compensators offer enough phase boost to compensate for R.H.P. zero phenomenon, therefore maximum bandwidth of the converter is restricted

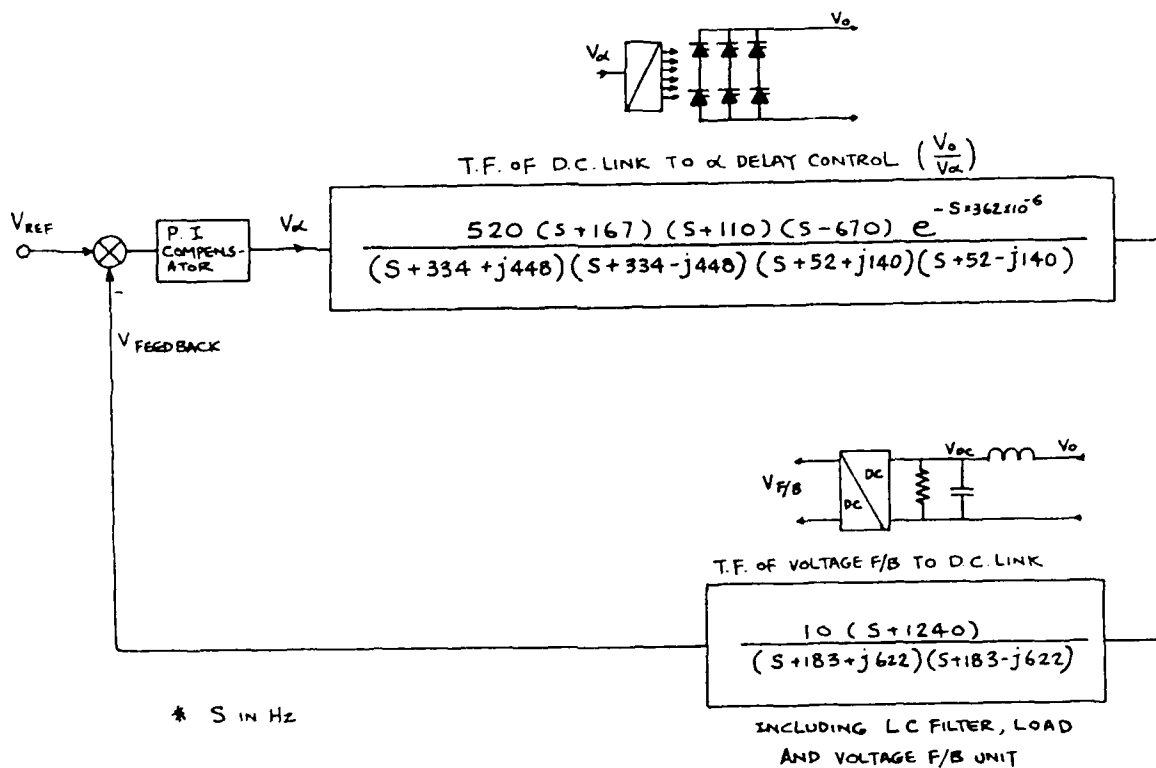


Figure 3.15. Linear Approximation Transfer Function of SCR Bridge

to cross-over frequencies below 670 Hz. The actual converter bandwidth was further reduced to 60 Hz due to the system dominant poles, nonlinearities and noises in the control circuit. However, this bandwidth should be adequate to meet the requirement of the inverter drive dynamics.

3.1.2.5 Step Response Test

Figure 3.16 shows the output voltage response of the converter when subject to a large step change of the input demand. The converter output voltage increase from 125 V to 250 V within 10 ms.

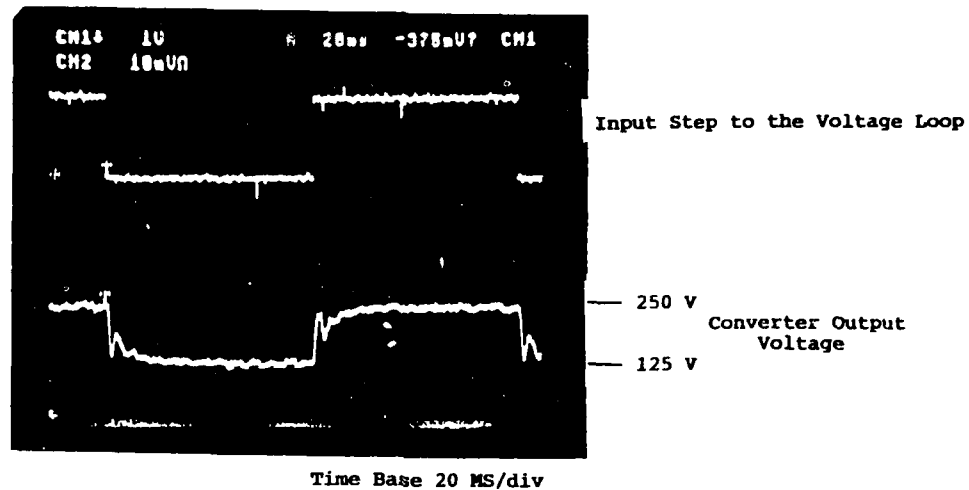


Figure 3.16. Output Response of Converter for a Step Input

There are damped high frequency oscillations superimposed on the normal response. The oscillations are not due to low phase margin but caused by the converter that has loop crossover frequency below the system resonant frequency. Figure 3.13 indicates the gain curve has a peak at 140 Hz which appear as the dominant complex poles in the approximate transfer function.

When the loop crossover frequency is below this corner frequency the feedback loop is not capable of rejecting the ringing appearing during the response to a transient. However this ringing frequency (140 Hz) is well above the inverter drive crossover frequency and much below the inverter switching frequency (3 kHz to 15 kHz), therefore interaction with inverter drive dynamics is negligible.

3.1.2.6 Impact Load Test

Test setup and result are shown in Figure 3.17. The converter was subjected to a 75 percent and switching (30 A - 120 A) with PMA running at 27780 rpm. The variation of link voltage under transient condition was recorded to be less than +/- 9 percent at 350 V.

With no load on the system, there is a minimum power requirement from the converter to supply the windage and frictional losses of PMB and gearbox operating at minimum speed. Since there is always some loading on the converter, a complete load switching test is not required.

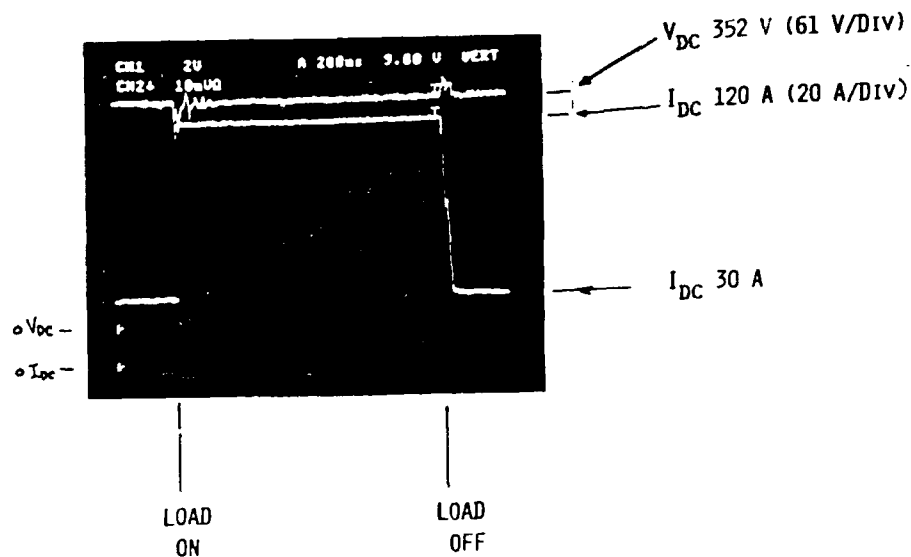
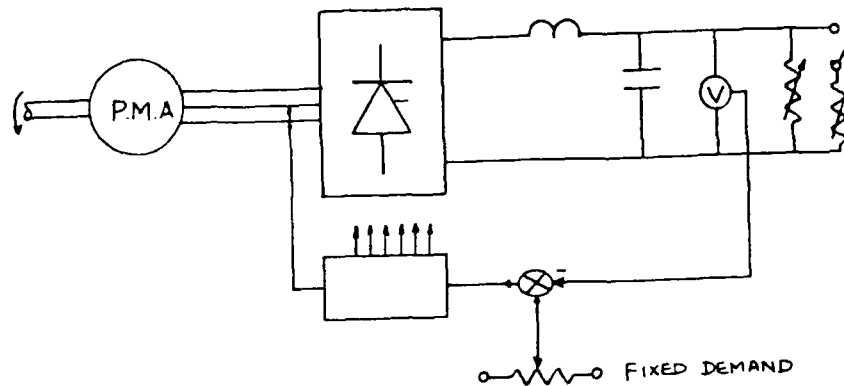


Figure 5.17. Transient Test with Step Load (30 A - 12^o A)

3.2 INVERTER/MOTOR DRIVE

The basic requirement for the inverter is to drive the permanent magnet machine PMB. The inverter uses the bus voltage provided at the output of the SCR bridge to form a three phase set of voltages to operate PMB as a brushless motor. As shown in Figure 3.18 the transistor based inverter commutates the motor windings in response to a set of motor position signals. The inverter control also responds to a system speed error command to increase or decrease PMB output torque as required to maintain constant output speed.

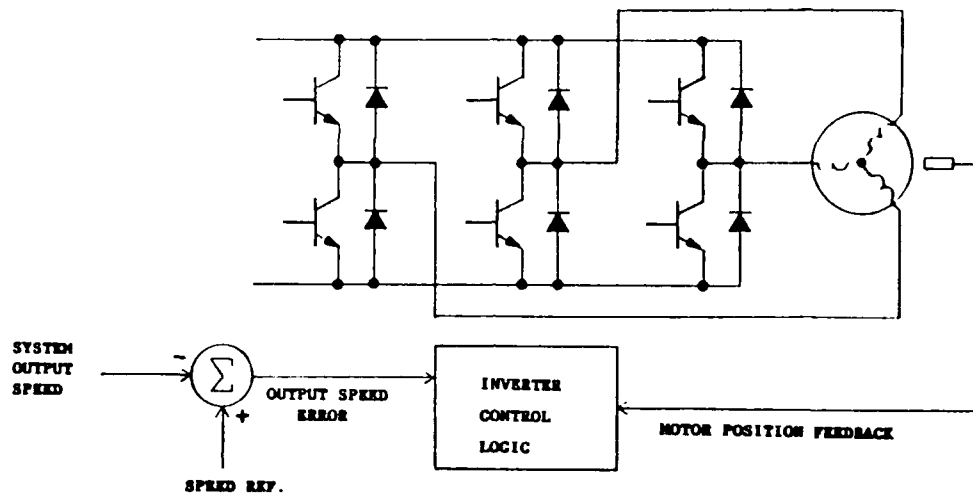


Figure 3.18. Inverter Schematic and Block Diagram

3.2.1 Motor Control Strategy

Two motor control schemes were considered:

- (1) commutation angle control
- (2) hysteresis current control

Option (1), commutation angle control, varies the phase relationship between motor applied voltage and motor back emf in order to control motor torque. Option (2), hysteresis current control, maintains the rotor and stator fluxes in quadrature to operate the motor at maximum torque for a given current magnitude. With option (2) the motor torque is controlled by varying the magnitude of motor current. Figure 3.19 shows the phasor diagrams for both options.

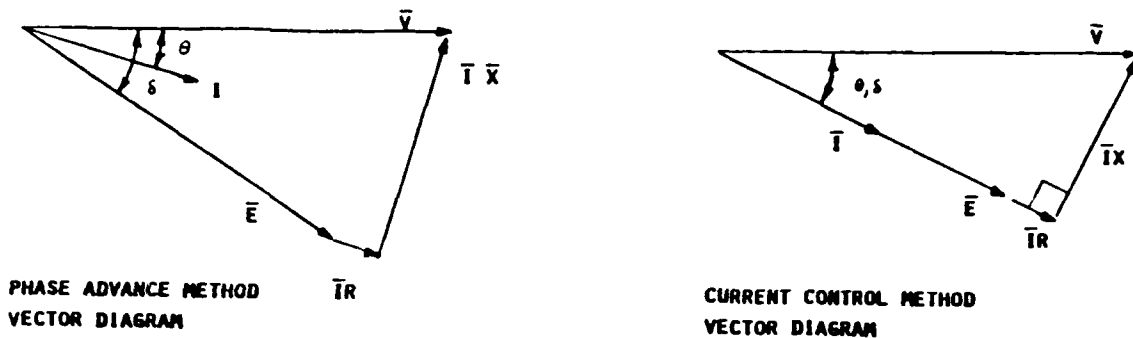


Figure 3.19. Motor Vector Diagrams

Hysteresis current control provides more nearly sinusoidal waveforms to the motor. This greatly reduces losses in the motor, and results in precise control of motor torque. Inverter switching losses, however, are high. Figure 3.20 shows how the motor current waveform is maintained within an error band about a sine wave current reference. An example waveform from the simulation of the motor and inverter combination is shown in Figure 3.21.

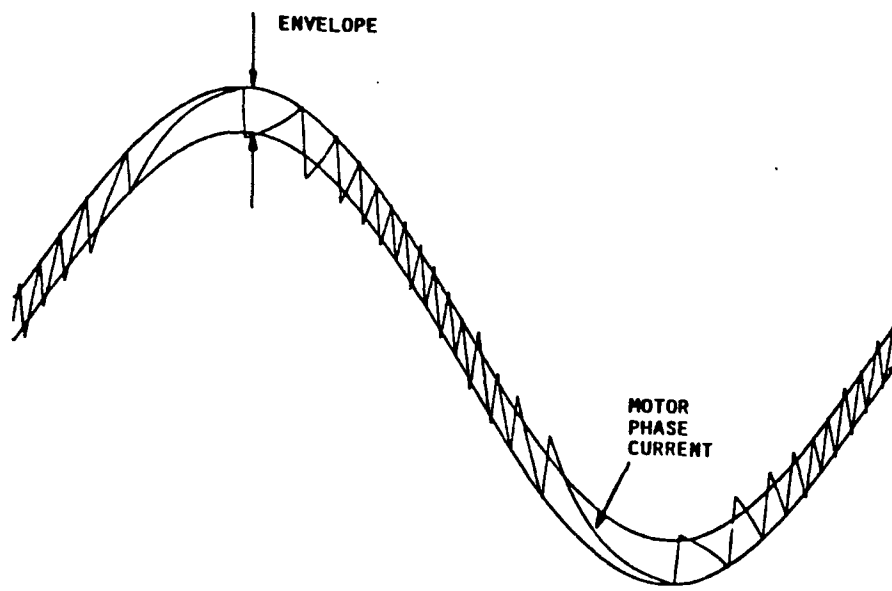


Figure 3.20. Hysteresis Current Control Waveform Generation

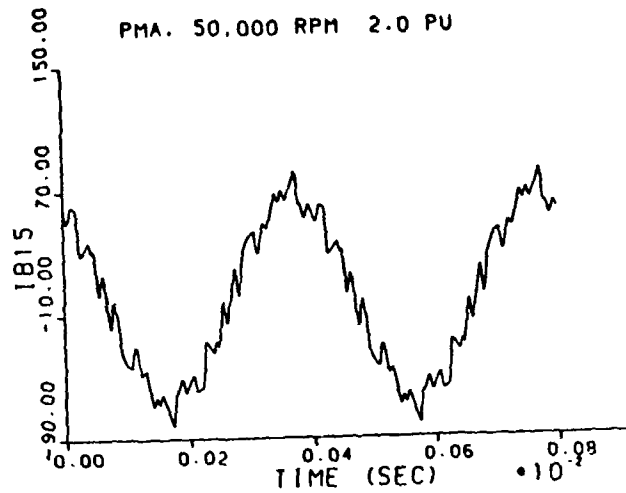


Figure 3.21. Hysteresis Current Control Simulation Result

Commutation angle control allows the inverter to operate with a straightforward six-step sequence. Switching losses in the inverter are minimized, but higher harmonics are present in the motor currents causing higher losses in the motor. The waveform produced by the commutation angle control scheme is shown in Figure 3.22.

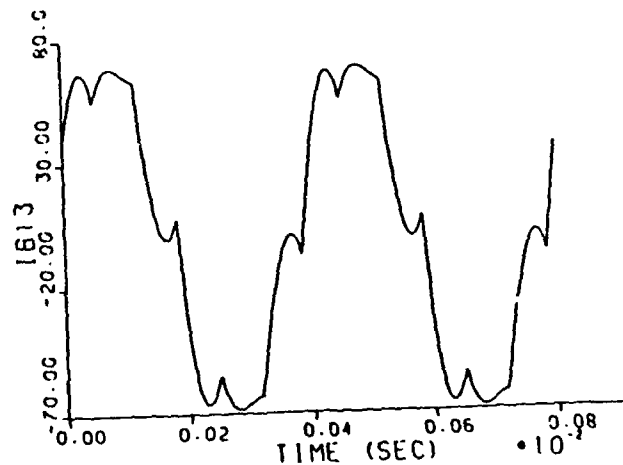


Figure 3.22. Commutation Angle Control Waveform

The motor control scheme was being studied in the early stages of motor design, and motor voltage levels required a bus voltage up to 350 V. For a given motor speed the current control scheme required a higher bus voltage, and thus transistors with a higher voltage rating. The motor voltage could have been lowered at the expense of higher current. In the end the decision was made to apply the commutation angle control scheme due to significantly lower stresses on the inverter transistors.

The block diagram for the motor control scheme is shown in Figure 3.23. The motor control has three modes of operation: run, start, and brake. Start mode uses a different portion of the position sensor than run-mode. This is necessary because the "accurate" position sensor provides only incremental position information. The run-mode control circuits are not aligned with the rotor position until the motor is rotating and there is an occurrence of the "index" position signal.

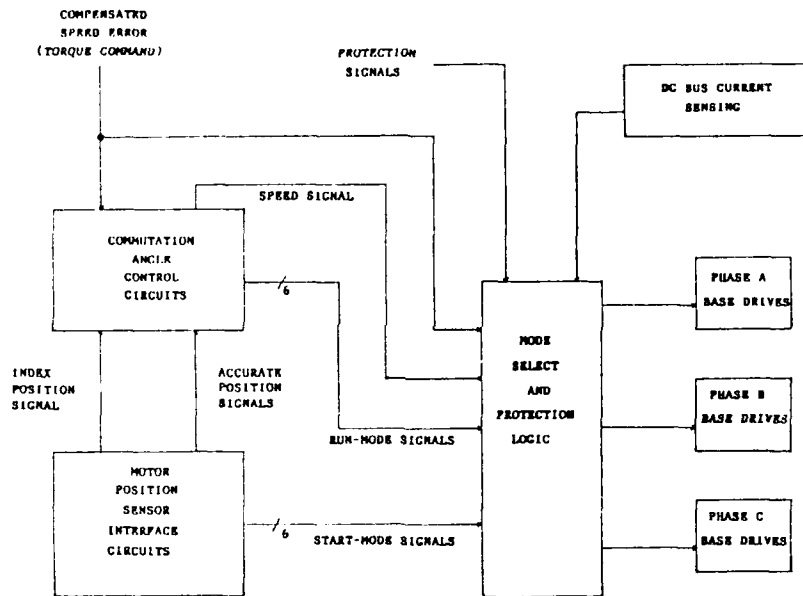


Figure 3.23. Motor Control Block Diagram

At speeds below the normal operating range of PMB there will be no load on the system, and precise control of the motor speed is not needed. Thus the start-mode is used to accelerate the motor to approximately 5000 rpm. Above this speed the run-mode is used and inverter drive signals are provided that are precisely aligned with motor position. The design of the commutation angle control circuits was simplified because of no need to operate at low motor speeds.

The braking mode is used when negative torque is commanded from the motor. During braking mode some energy is sent to the bus. Therefore, a current dump circuit is required to prevent excess charging of the bus capacitors during braking.

3.2.2 Inverter Specifics

The design requirement for the inverter power rating comes from the PMB torque output of 100 in-lb required to support a 95 kVA shock load on the system. The motor current was predicted to be 158 A rms per phase with peaks of 220 A. The Westinghouse DA11503008 darlington transistor was selected to implement the inverter switch. The darlington transistor set, freewheel diode, and snubber diode are included in the switch module. The arrangement of the switch module is shown in Figure 3.24. The complete switch module schematic appears in Figure 3.25. The switch module also includes voltage clamps for the base-emitter junction of each transistor, and a snubber network.

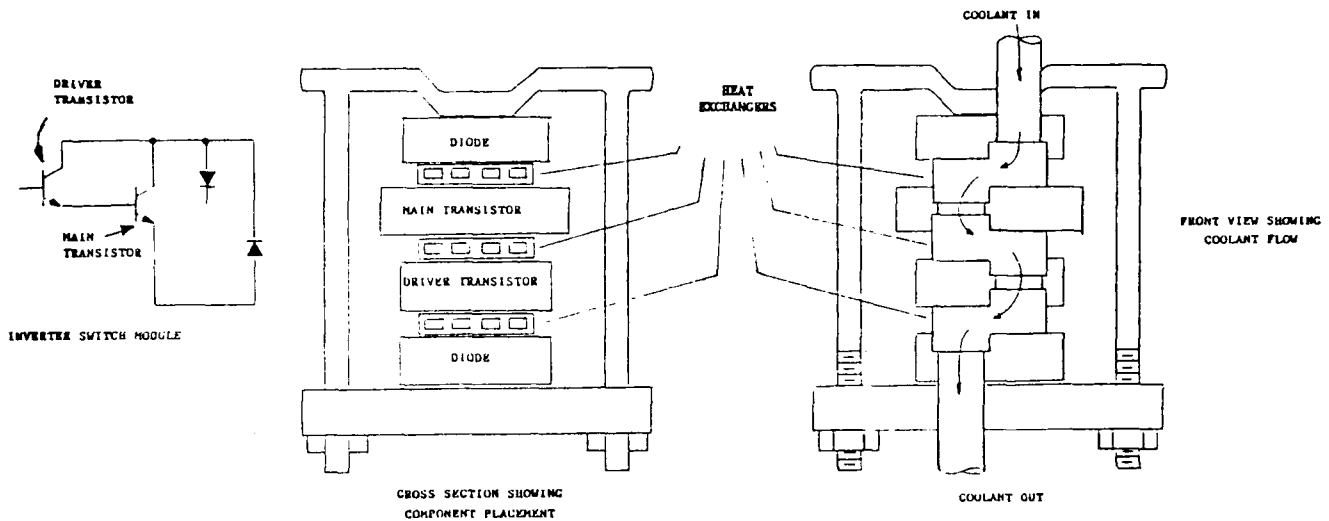


Figure 3.24. Switch Module

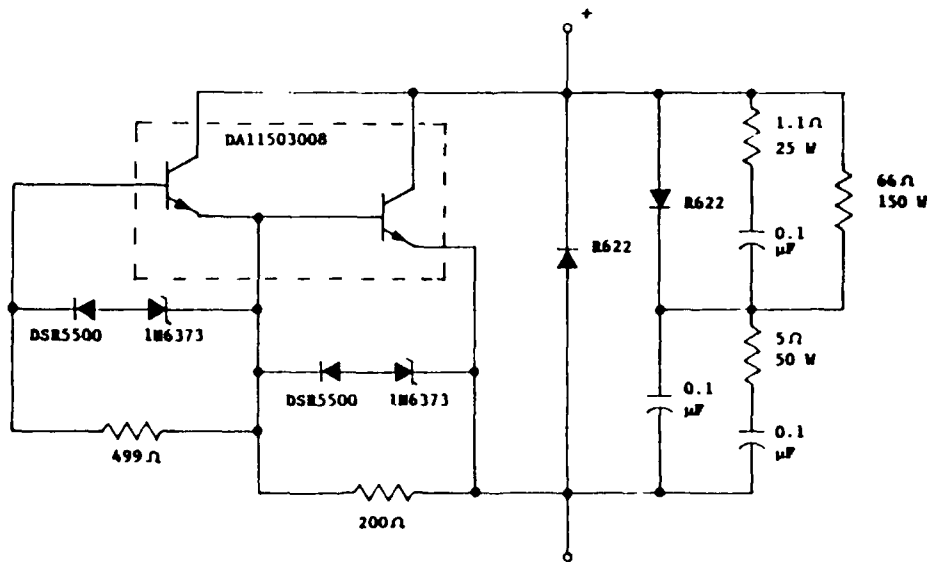


Figure 3.25. Switch Module Schematic

Figure 3.26 is a block diagram representing a single phase of the inverter. The logic block receives the inverter drive signals from the motor control circuits. These signals are then used to activate the switch drive circuits. Each switch drive circuit also sends a signal back to the logic block indicating the present "on" or "off" state of its associated transistor. The logic block uses this information to actively prevent simultaneous conduction of both transistors in its leg of the inverter. Two current transformers are used. One is a proportional drive current transformer that provides base drive current to each transistor that is a fixed fraction of the transistor's total current. The other is a current transformer that provides a signal to the protection logic so that the transistors in that phase are turned off in the case of excessive current. The isolation transformer provides power to each switch drive circuit because the switch drive circuits float with their associated switch modules.

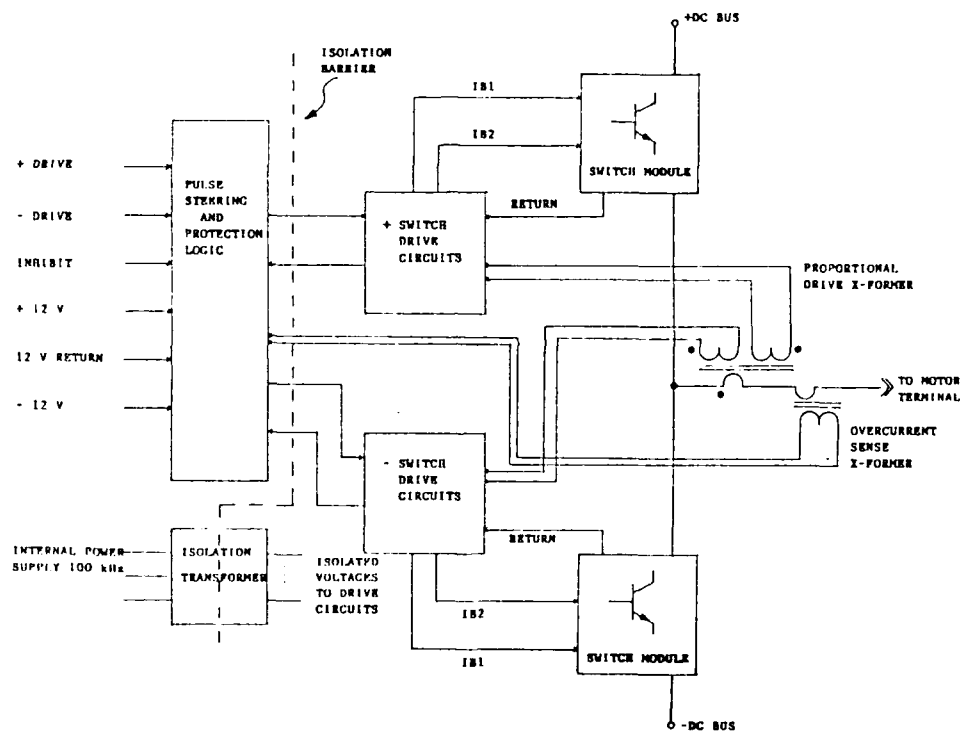


Figure 3.26. Inverter Single Phase

The photograph in Figure 3.27 shows the construction of the inverter. The switch modules are arranged in a "horseshoe" pattern to allow simple connection of the inverter to source and load. The distribution of cooling fluid to each switch module via hoses can also be seen. Figure 3.28 shows the inverter with the switch drive circuits in place.

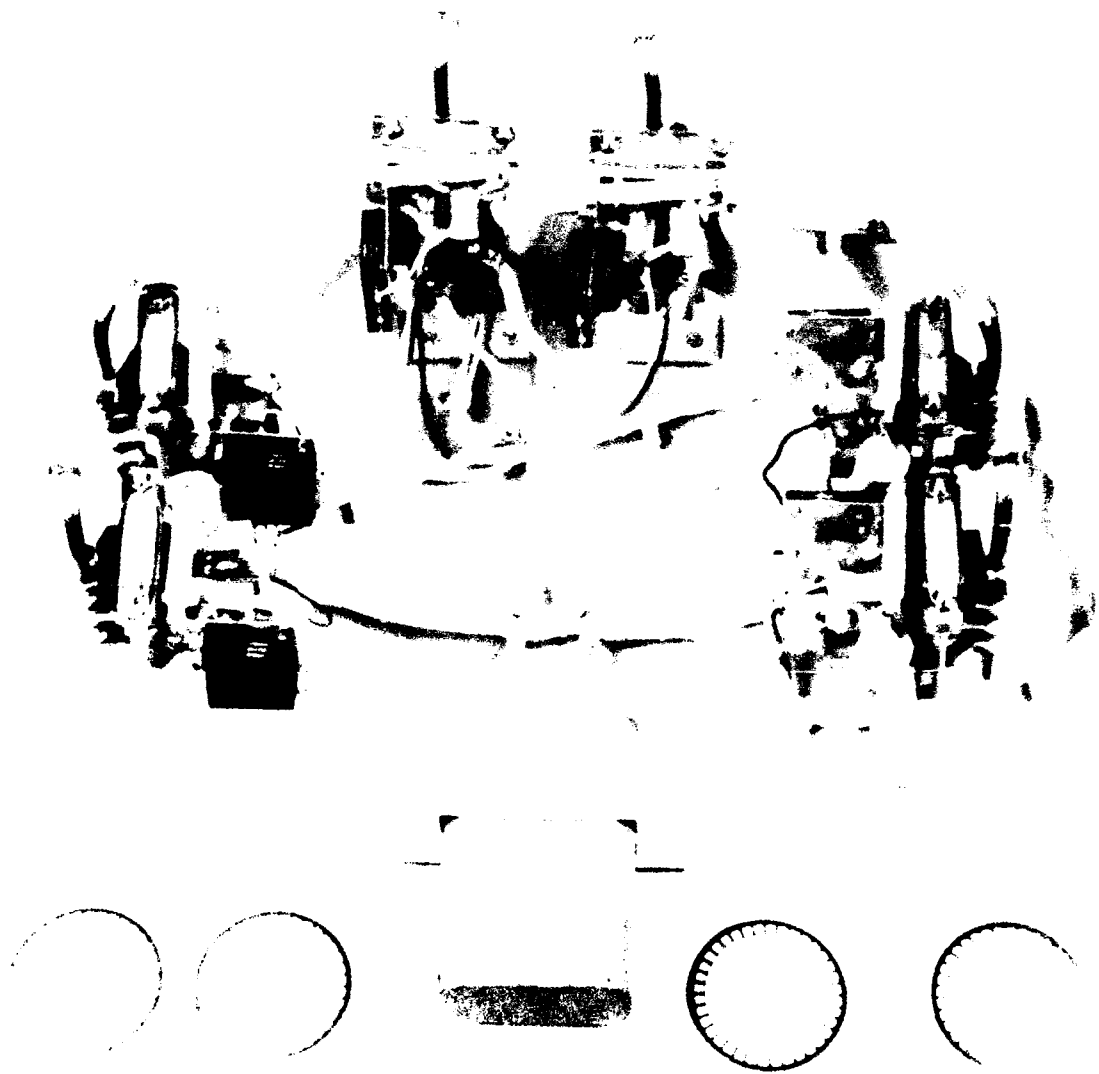


Figure 3.27. Inverter Photo Without Base Drives

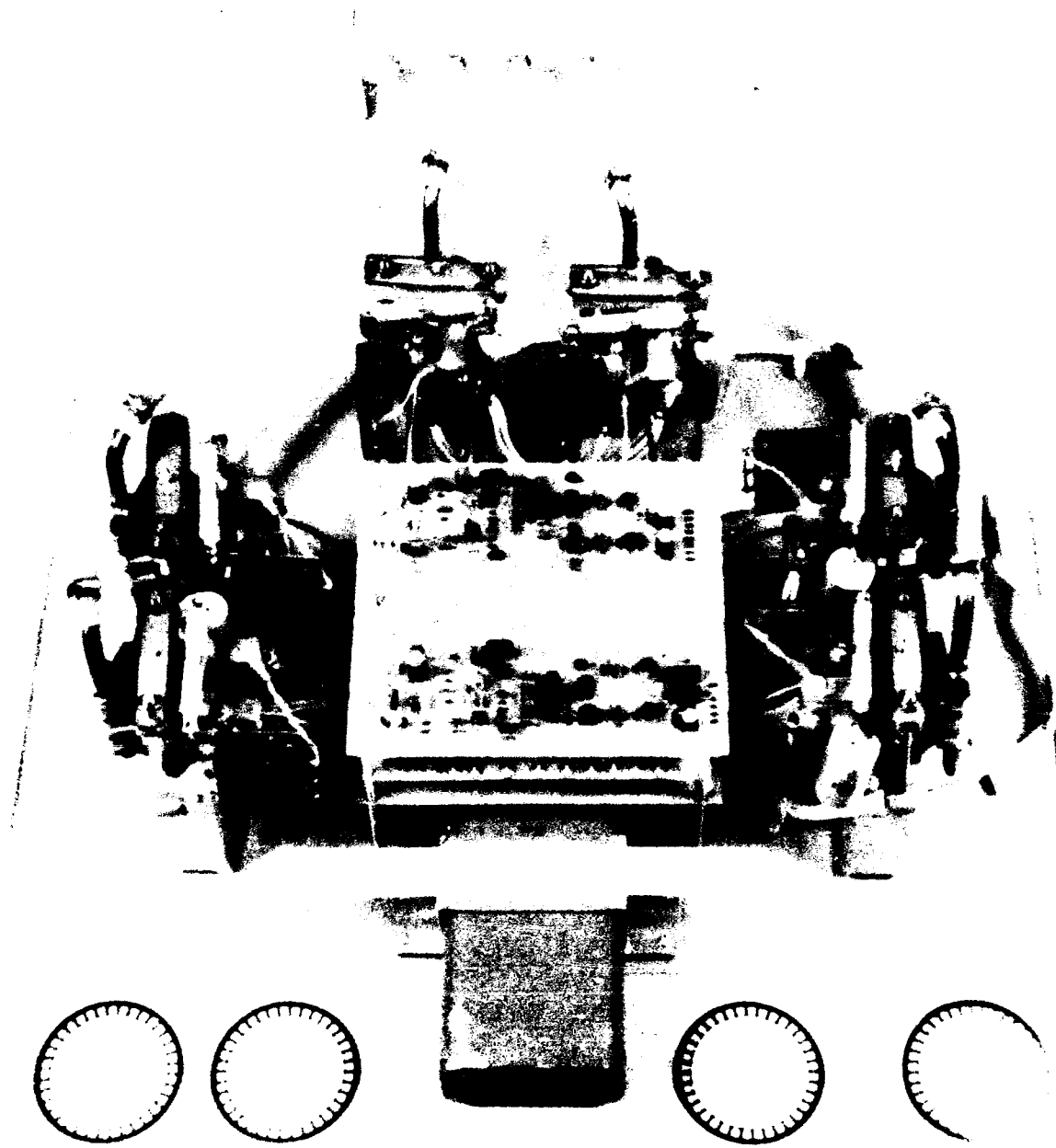


Figure 3.28. Inverter Photo with Base Drives

Simulation of the permanent magnet motor operation was performed during the motor design process. The results of these simulations were used to choose the inverter power transistors, predict inverter power loss, and determine inverter cooling requirements. Some examples of simulation results at 10 krpm, 30 krpm, and 50 krpm are shown in Figure 3.29.

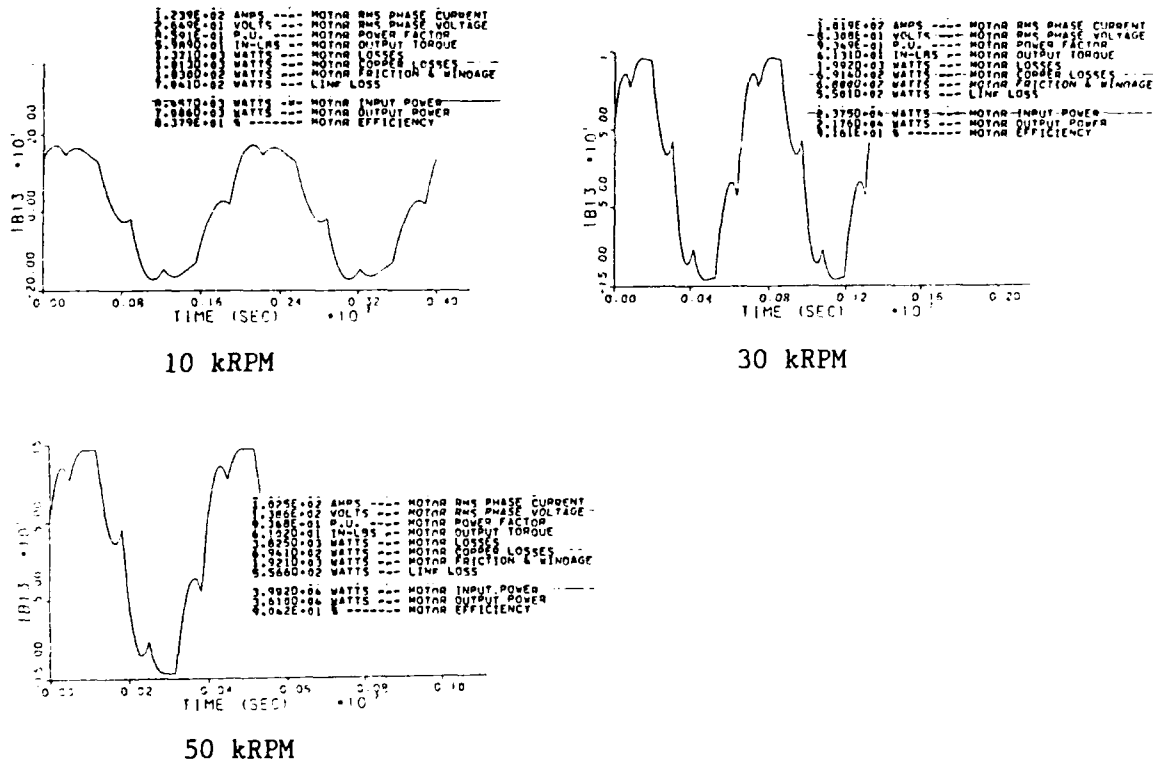


Figure 3.29. PMB Simulation Results

3.2.3 Inverter Testing

The inverter testing progressed through three stages: static test, interim test, and system test. Static testing of the inverter was basically a functional check of the switch modules and drive circuits. Some changes were made to the bus leads, and the snubbers were modified. Some examples of voltage and current waveforms from static testing are shown in Figure 3.30.

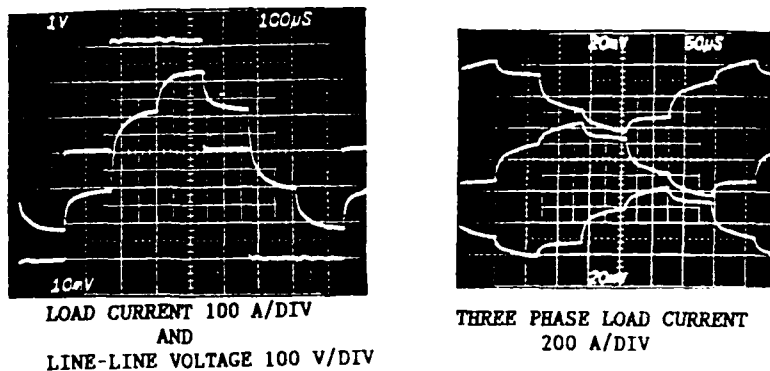


Figure 3.30. Static Test Waveforms

The second stage of testing allowed the inverter to be tested with the motor. Considerable time was spent to get the motor position sensor working as required. A temperature compensation circuit was designed, built, and tested with the position sensor. The interim test set-up is illustrated in Figure 3.31. With this arrangement PMA was used to load PMB above 28 krpm since the PMA/SCR bridge combination is only designed to work above 28 krpm. The inverter and motor were run up to 45 krpm at no-load to check vibration. PMB was run at 30 krpm and 40 krpm with measured input powers of 27.2 kW and 36.8 kW, respectively. An example of PMB motor current at these operating points is shown in Figure 3.32. Because of delays caused by position sensor problems in the early stages of interim testing the interim test was abbreviated so that system testing might begin. This was a reasonable move since the motor, motor controls, and inverter were performing as expected.

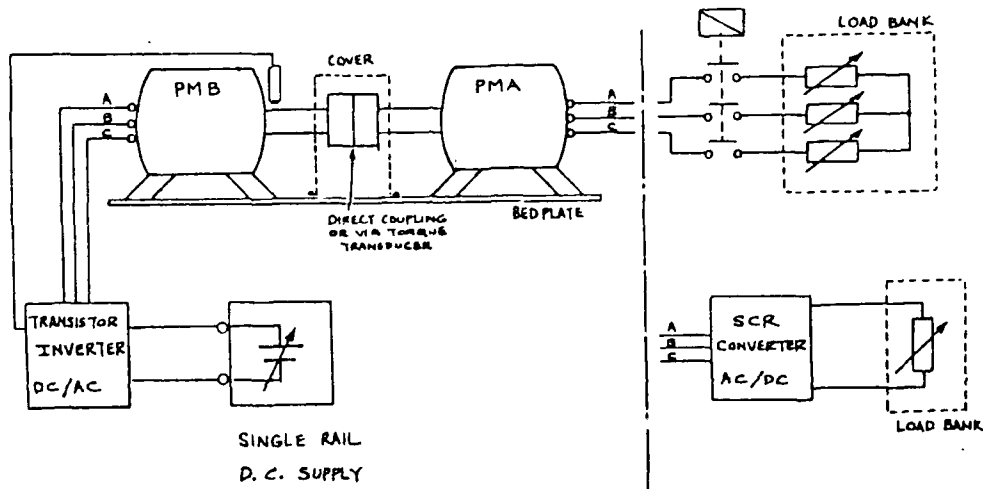


Figure 3.31. Interim Test Setup

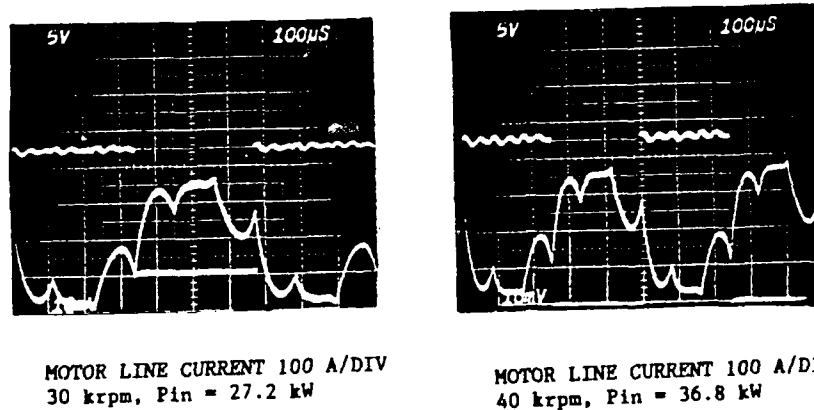


Figure 3.32. Interim Test Motor Currents

Following the interim test PMA and PMB were attached to the system gearbox. At this point the entire ECCSD system was in place for testing. Initially we expected that only brief testing would be necessary to verify operation of the inverter and PMB with the gearbox. At first attempt, however, PMB would not start properly on the gearbox. After correcting a minor flaw in the gearbox the problem was determined to be in the position sensor used with PMB. Side loading of PMB's shaft due to the gear mesh, through which PMB is attached to the gearbox, was causing changes in the position sensor air gap. This caused enough variation in sensor output to have the wrong inverter transistors turned on for a given motor position. As a result PMB would not start reliably or accelerate to normal running speed.

The section of the position sensor used to determine absolute motor position for starting purposes was changed. The new arrangement is not sensitive to small changes in the sensor air gap. A new position sensor interface circuit was designed and built. The sensor was aligned with rotor position, and PMB was remounted on the gearbox. PMB was then run at speeds up to 45 krpm no-load in order to check vibration levels of PMB and the gearbox.

The next step in testing was to run PMB and the gearbox input simultaneously so that the output generator would run at 12000 rpm. For a set gearbox input speed motor speed was adjusted manually to get the gearbox output to 12 krpm. Motor speed was adjusted by setting the inverter voltage to the desired level, and then varying the motor commutation angle as required.

Open loop testing of the output speed control was then performed for motor speeds of 20 krpm, 30 krpm, and 40 krpm. At each of these points the system input speed was such that output speed was 12 krpm. In this way data was taken at actual operating points of the system. Figure 3.33 shows that the control input is the motor commutation angle command, and that the output response is a signal proportional to system output speed.

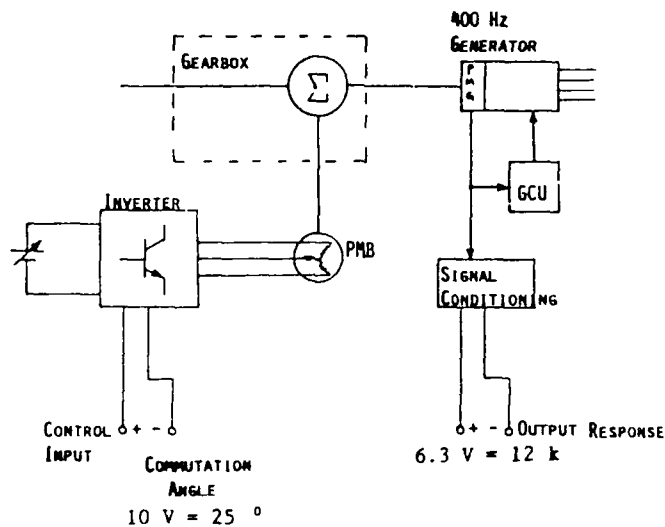
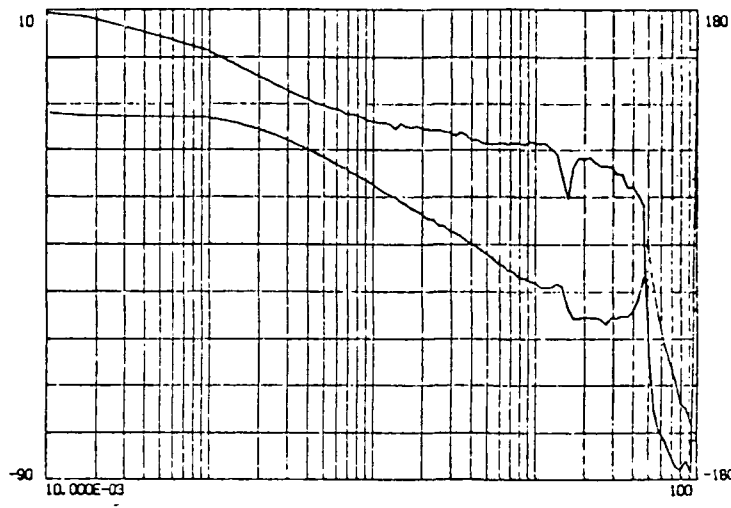
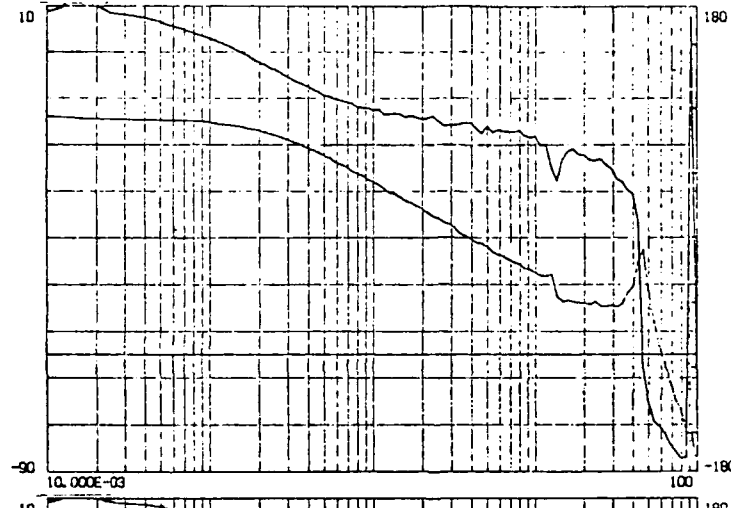


Figure 3.33. Input to Output Responses Measurement

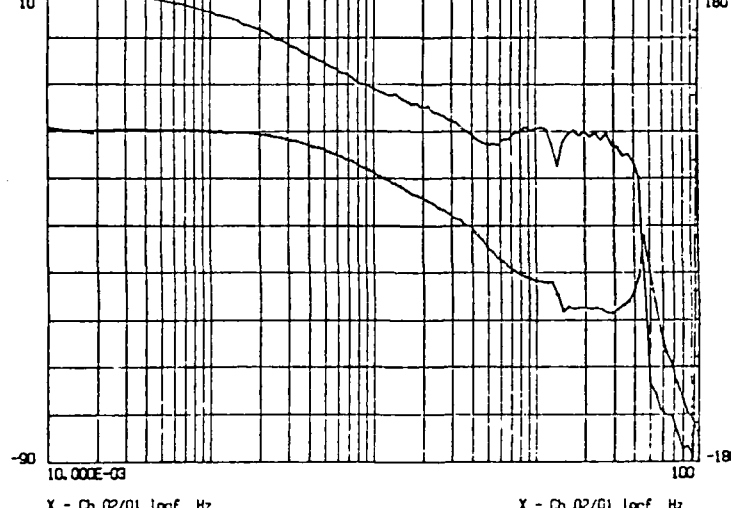
Open loop testing was performed first at no-load and then with load. To load the system the Generator Control Unit (GCU) is activated so that the nominal 115 V l-n appears at the generator terminals. Then a load is placed across the generator terminals. When a load is placed on the system in open loop the output speed will droop, and the motor commutation angle must be adjusted to return the output speed to 12 krpm. This droop in output speed limits the amount of load that can be placed on the system during open loop operation. Figures 3.34 and 3.35 show the bode plots that were obtained during open loop testing.



PMB SPEED = 40 K



PMB SPEED = 30 K

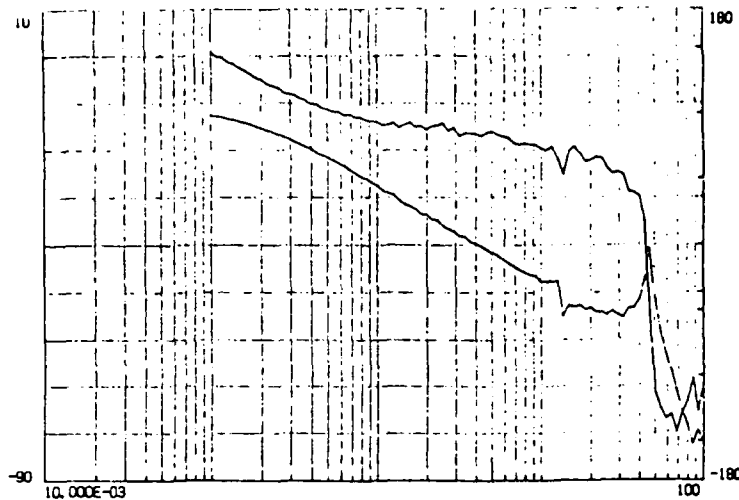


PMB SPEED = 20 K

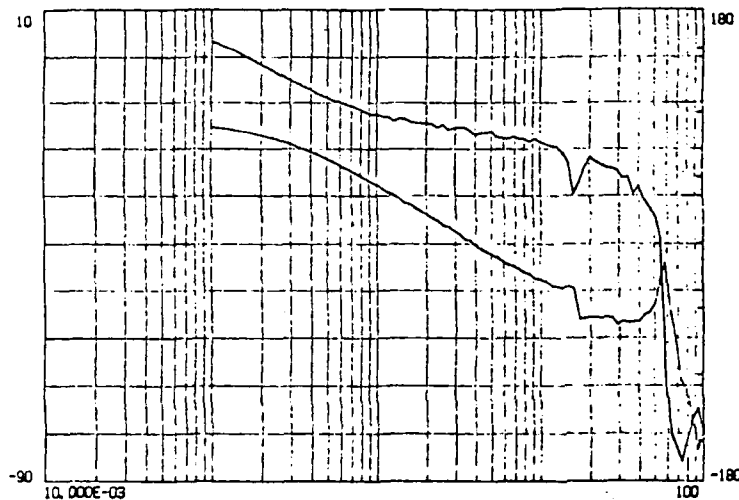
X - Ch 02/01 logf Hz
Y - Ch 02/01 logr dB

X - Ch 02/01 logf Hz
Y - Ch 02/01 theta deg

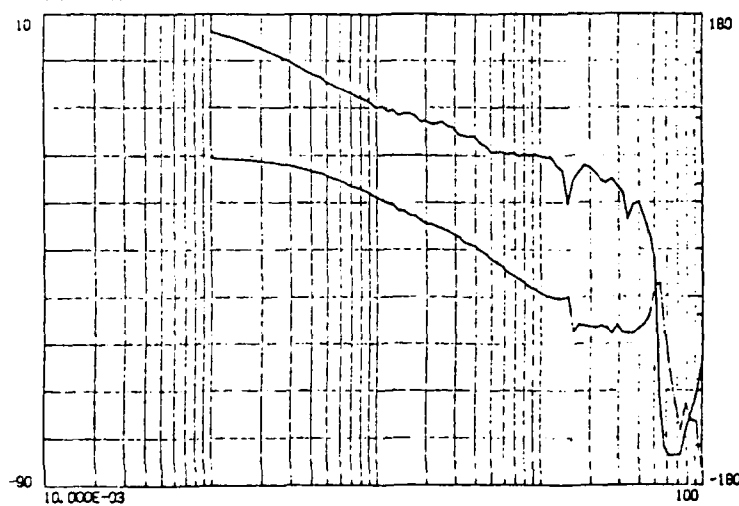
Figure 3.34. Open Loop Bode Plots, No-Load



PMB SPEED = 40 K
400 Hz LOAD = 10 kW



PMB SPEED = 30 K
400 Hz LOAD = 20 kW



PMB SPEED = 20 K
400 Hz LOAD = 30 kW

X - Ch 02/01 logf Hz
Y - Ch 02/01 logr dB

X - Ch 01 logf Hz
Y - Ch 01 theta deg

Figure 3.35. Open Loop Bode Plots, With Load

The output speed control block diagram for the system is shown in Figure 3.36. The compensation function $G_1(S)$ is proportional plus integral (P.I.), and was selected based on results from the system model described in an earlier section of this report. The system transfer function $G_2(S)$ was measured during open loop testing. For closed loop testing the output speed signal is subtracted from the output speed reference and the error is used to drive the system so that PMB speed is increased or decreased as necessary to maintain the desired 12 krpm output speed.

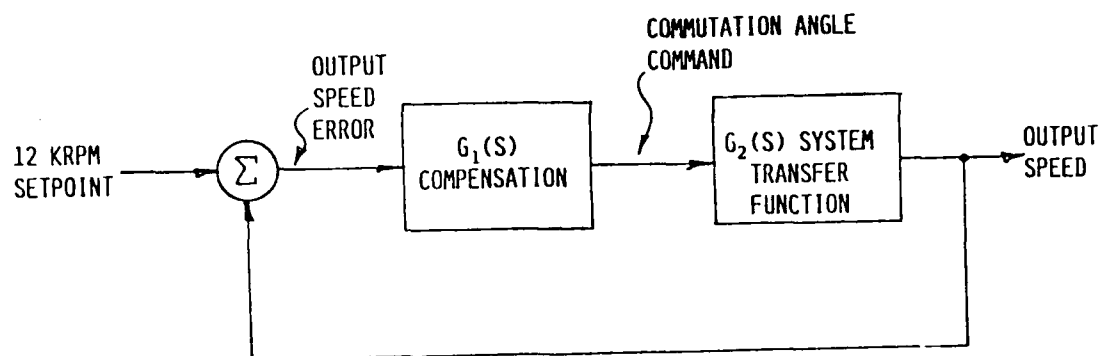


Figure 3.36. Output Speed Control Block Diagram

Initially the proportional gain of $G_1(S)$ was approximately 80(38 db). This high gain amplified the small ripple present in the output speed signal, and caused motor commutation angle command to contain a significant component. As a result the motor current showed undesirable modulation. The proportional gain of $G_1(S)$ was reduced to approximately five (14 db). This allowed the motor speed control to operate smoothly.

The loop response $G_1(S)G_2(S)$ of the system was then measured with the system running under closed loop control of the output speed. An example of the measured system transfer function is shown in Figure 3.37. At this point system testing was begun as explained in a later section of this report.

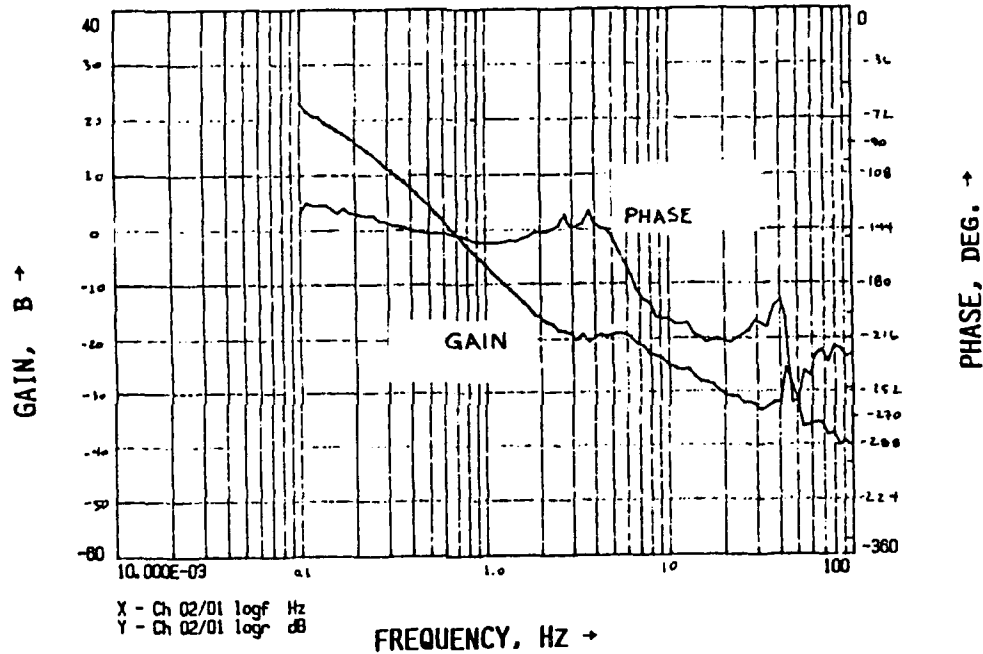


Figure 3.37. Closed Loop Transfer Function Bode Plot

4.0 PERMANENT MAGNET MACHINES

The permanent magnet (PM) machines were tested at speeds up to 45,000 rpm, 100°F oil inlet temperature, for the no-load and continuous load conditions. The electrical, thermal and flow performances are in accordance with our design goals. The maximum operating speed of 50,000 rpm should not be exceeded due to predicted high containment ring stress. The permanent magnet machines are shown in Figures 4.1 and 4.2.

4.1 DESIGN OBJECTIVES

The permanent magnet (PM) machines performance requirements were formulated to suit the concepts for the ECCSD system. The design goals are based on a system rating of 40/60 kva and 95 kva shock load. The design goals are as follows:

- o The generator, PMA, peak power rating is 77.3 kva at 27,778 rpm for 5 seconds duration. PMA continuous rating is 48 kva at 27,778 rpm. PMA required peak power versus speed is shown in Figure 4.3.
- o The motor, PMB, peak power rating is 83.8 hp at 50,000 rpm for 5 seconds. PMB continuous rating is 49.8 hp at 50,000 rpm. PMB required peak power versus speed is shown in Figure 4.3.
- o The machines shall be compatible with MIL-L-7808 and MIL-L-23699.
- o The operating temperature range is 80°F to 275°F.
- o Electrical insulation life of 20,000 hours.
- o Bearing B-10 life of 30,000 hours.
- o Vibration level not to exceed 10 g's.

The design process consisted of electromagnetic, thermal, bearing, rotor critical and stress analyses. State-of-the-art analytical and modeling tools, such as finite elements and PATRAN, were utilized to predict machine parameters and operating performance. MAGNET software was used to perform the electromagnetic finite element analysis. SINDA finite difference computer program was utilized to calculate the machine operating temperatures. ANSYS finite element software was employed to perform rotor containment ring stress analysis.

4.2 ELECTROMAGNETIC ANALYSIS

A preliminary design trade study was performed to determine optimum machine design configuration. This electromagnetic study addressed key design parameters, such as number of poles, operating speed and radial vs

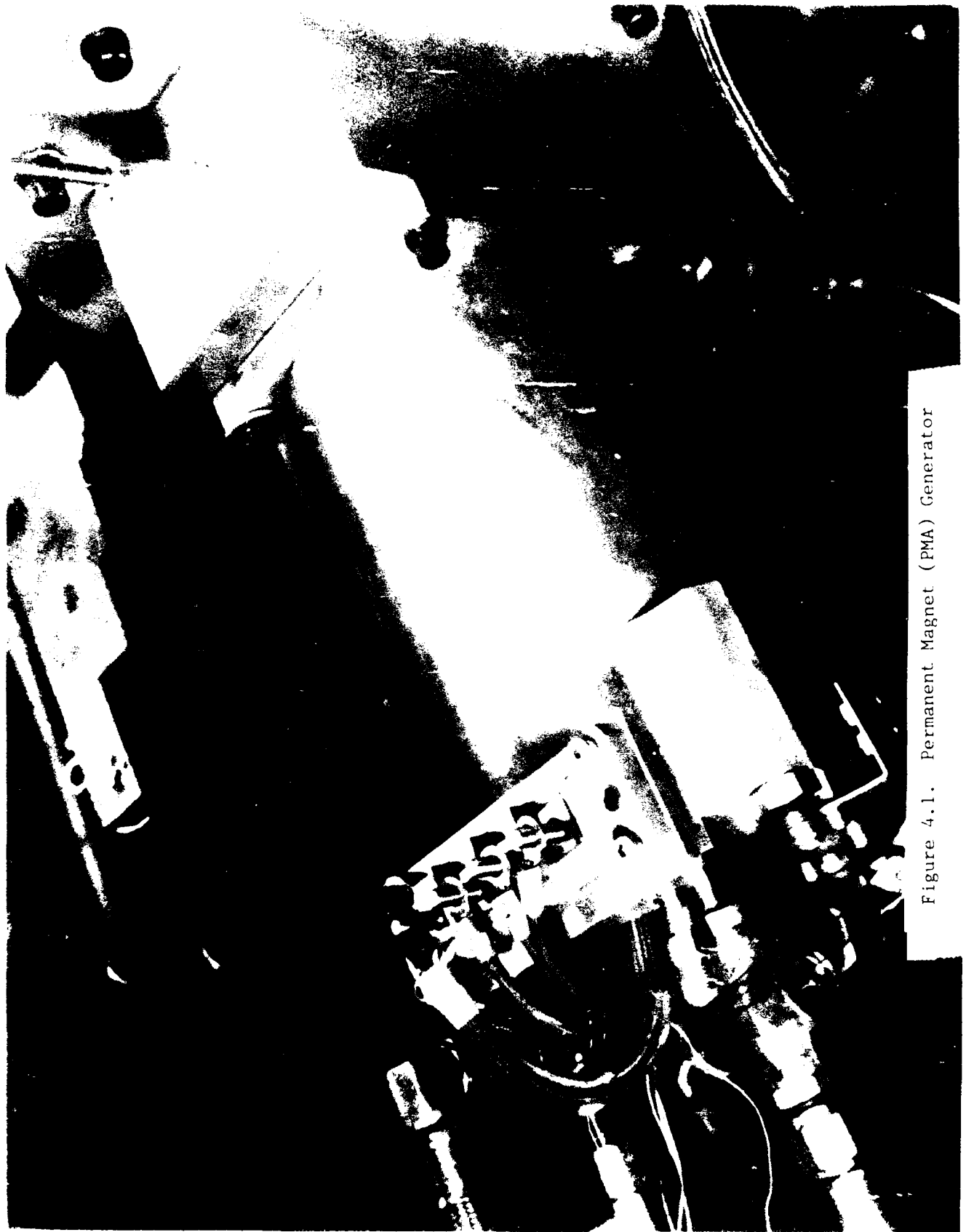


Figure 4.1. Permanent Magnet (PMA) Generator



Figure 4.2. Permanent Magnet (PMB) Motor

PERMANENT MAGNET MACHINES

PEAK POWER REQUIREMENT - 5 SECONDS

41.86
41

$$PMA = 9.2593$$

$$PMB = 8.3333$$

OUTPUT POWER (KW)

80

60

40

20

PMA

PMB

10

20

30

40

50

OPERATING SPEED (KRPM)

Figure 4.3. PMA/PMB Required Output Power vs Speed

tangential direction of magnetization. The objective is to find a combination of the above mentioned parameters which yield the lightest machine within the boundary of design constraints. This trade study is described in detail in Appendix B. The recommended design is a six pole tangential configuration with a maximum operating speed of 50,000 rpm.

Final electromagnetic design was carried out using two dimensional (2D) magnetostatic finite element (FE) analysis. This numerical analysis method solves the electromagnetic field equations taking into account the nonlinearities of the magnetic circuit as well as leakage or fringing fields. Machine parameters are obtained from the vector potential solution: flux, flux densities, inductances and voltage.

->

The vector potential is defined to be a vector A such that the flux density B is derivable from it by the curl operation:

$$\vec{B} = \nabla \times \vec{A} \quad (1)$$

The total flux linked by a path, i.e., the closed contour formed by a coil, is the line integral of A

$$\phi = \oint \vec{A} \cdot d\vec{l} \quad (2)$$

where the line element $d\vec{l}$ follows the wire direction. Because the problem is essentially two-dimensional, the end contribution to the integral in (2) is negligible. The rms generated voltage per phase is then

$$E_{rms} = \frac{2\pi}{\sqrt{2}} f K_w N \phi \quad (3)$$

where f is the frequency, N the number of series turns per phase, K_w the winding factor and ϕ the flux per pole.

Terminal voltage, load angle and/or power factor are determined given the required load point [1]. The reactances are calculated from the no-load and peak load FE solutions: direct axis and quadrature axis armature reactions divided by the corresponding current. The armature reactions are obtained by subtracting the no-load from the peak load solution. Figure 4.4 show plots of the machine flux distribution at no-load and peak load conditions. Table 4.1 lists the calculated and measured no-load voltages. The analysis yielded no-load voltages which are about 6.8 percent higher than the measured values. Note however, that the permanent magnets can have a \pm 2.5 percent variation in BH values within a single lot of material. The

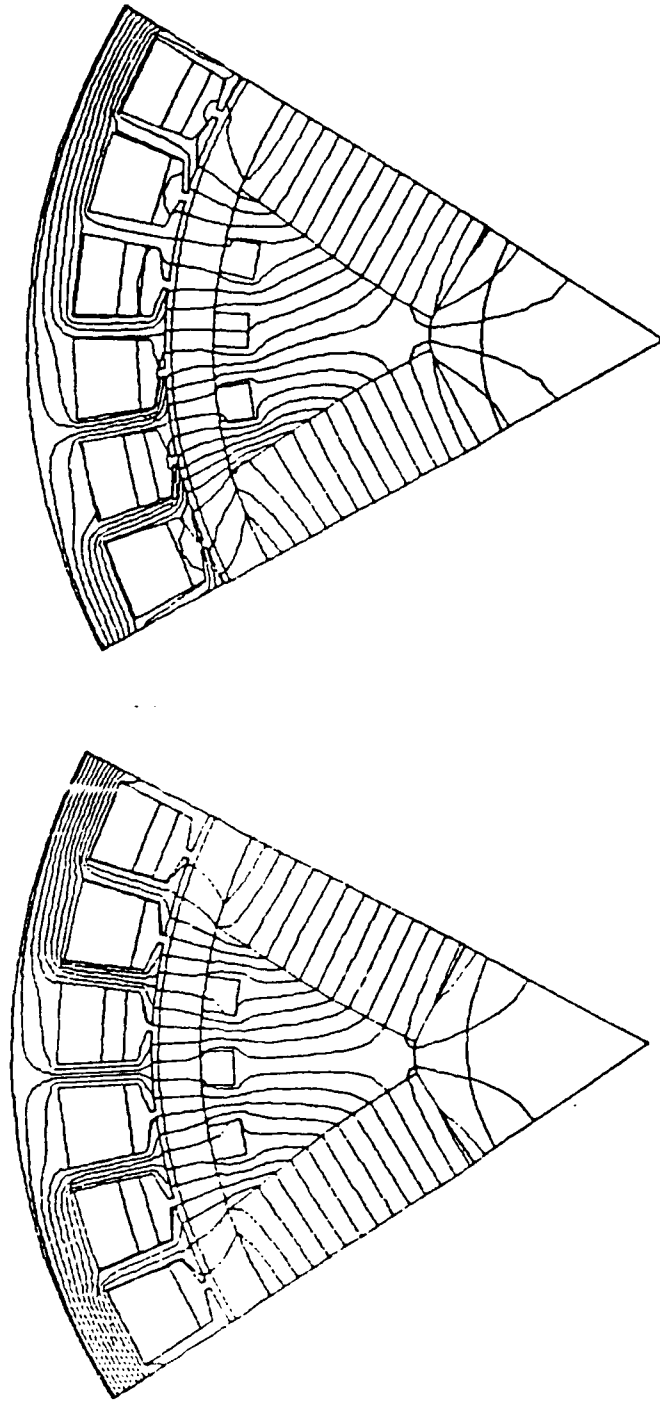


Figure 4.4. F.E. Flux Plots at No-Load and Peak Load Conditions

machines have a

Table 4.1 PMA and PMB No-Load Phase Voltages

NO-LOAD VOLTAGES (VOLTS)				
	PMA		PMB	
MEASURED	128.0	231.0	13.5	40.2
CALCULATED	136.7	227.8	14.4	43.1
SPEED (RPM)	15,000	25,000	5,000	15,000

nearly sinusoidal voltage waveforms. This voltage wave form is given in Figure 4.5. Test results show the third and fifth harmonics being about 2.7 percent and 0.6 percent of the fundamental component, respectively. Table 4.2 lists the fundamental and harmonic components in rms volts for both PMA and PMB. The no-load frequency spectrums are plotted in Figures 4.6 and 4.7.

Table 4.2 No-Load Phase Voltage Frequency Spectrum In Volts (rms)

NO-LOAD PHASE VOLTAGE FREQUENCY SPECTRUM IN VOLTS		
FREQUENCY (HERTZ)	PMA	PMB
FUNDAMENTAL	39.1	13.52
750.	1.0	0.376
1250.	0.25	0.078
1750.	0.15	0.053
2250.	0.08	0.041

PMA load performance correlates very well with the analytical values. Table 4.3 lists calculated versus measured-load performance values. PMA measured phase voltage versus load current is shown in Figure 4.8. PMA has the requirement of 77.3 kva at 27,778 rpm for a 5 second duration. Table 4.3 shows 97. percent accuracy between measured and calculated values. The machine will meet the requirement.

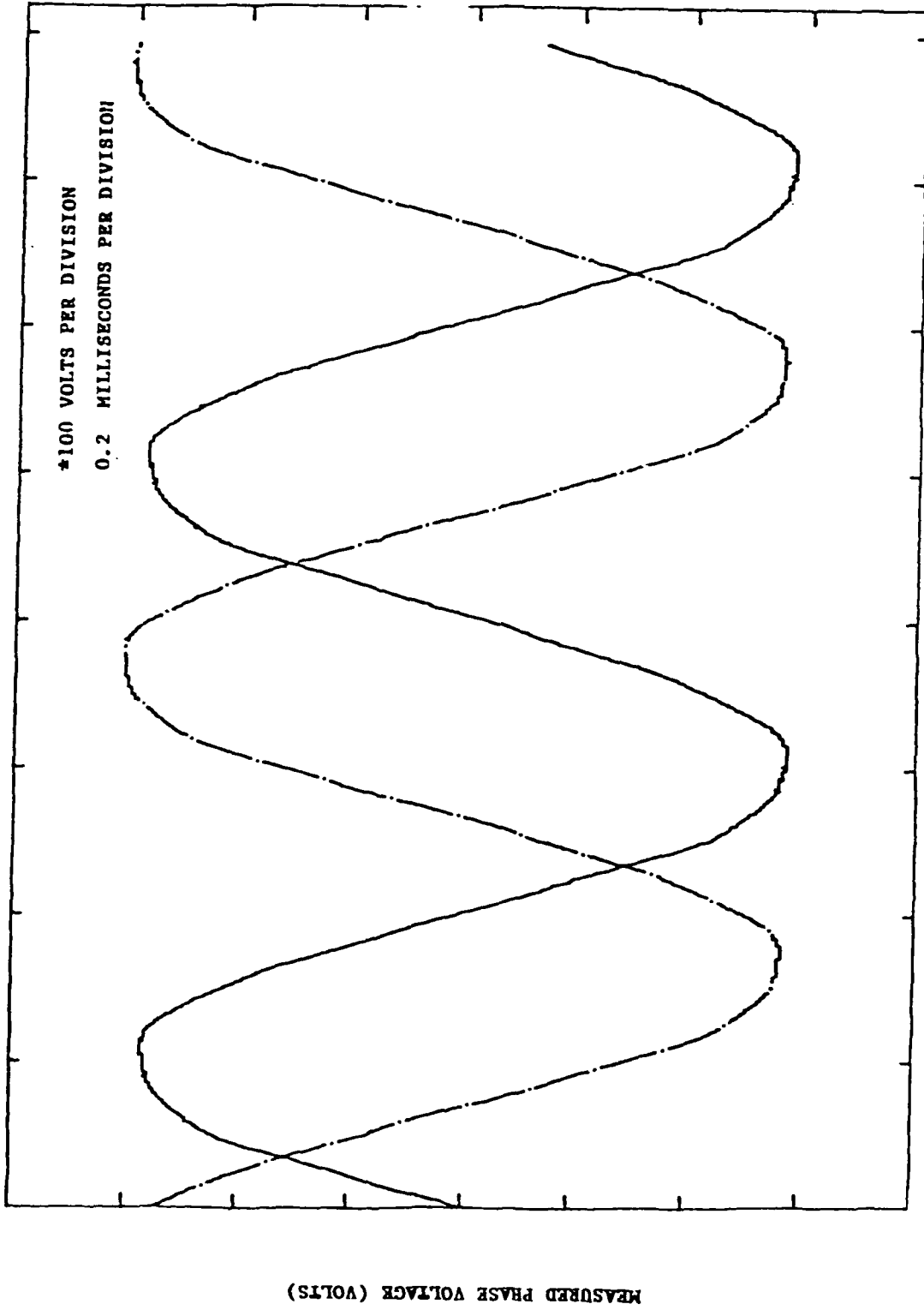


Figure 4.5. PMA No-Load Phase Voltages at 25,000 RPM and 150°F Oil

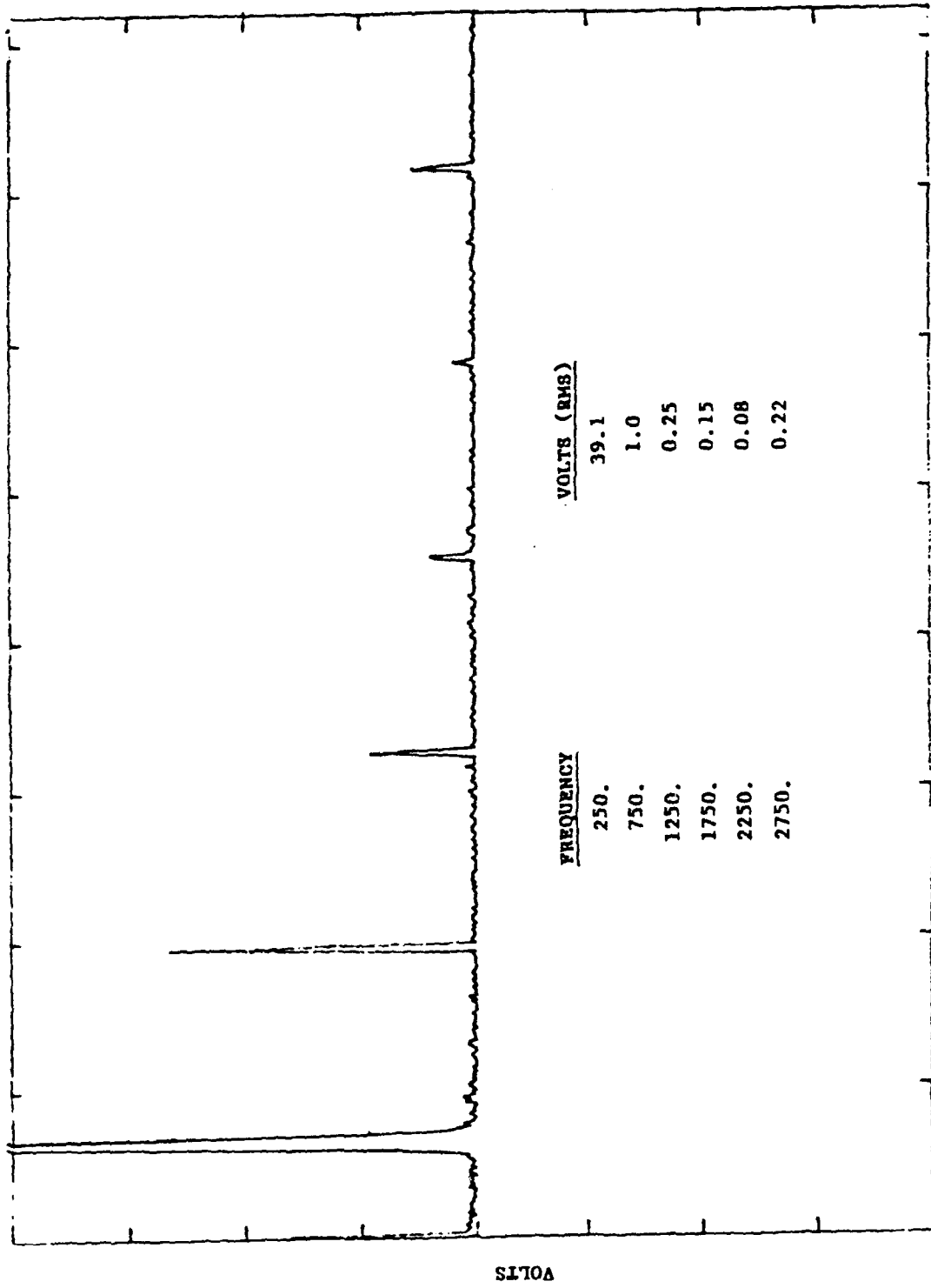


Figure 4.6. PMA Measured No-Load Voltage Frequency Spectrum at 5,000 RPM and 150°F Oil

SI70A

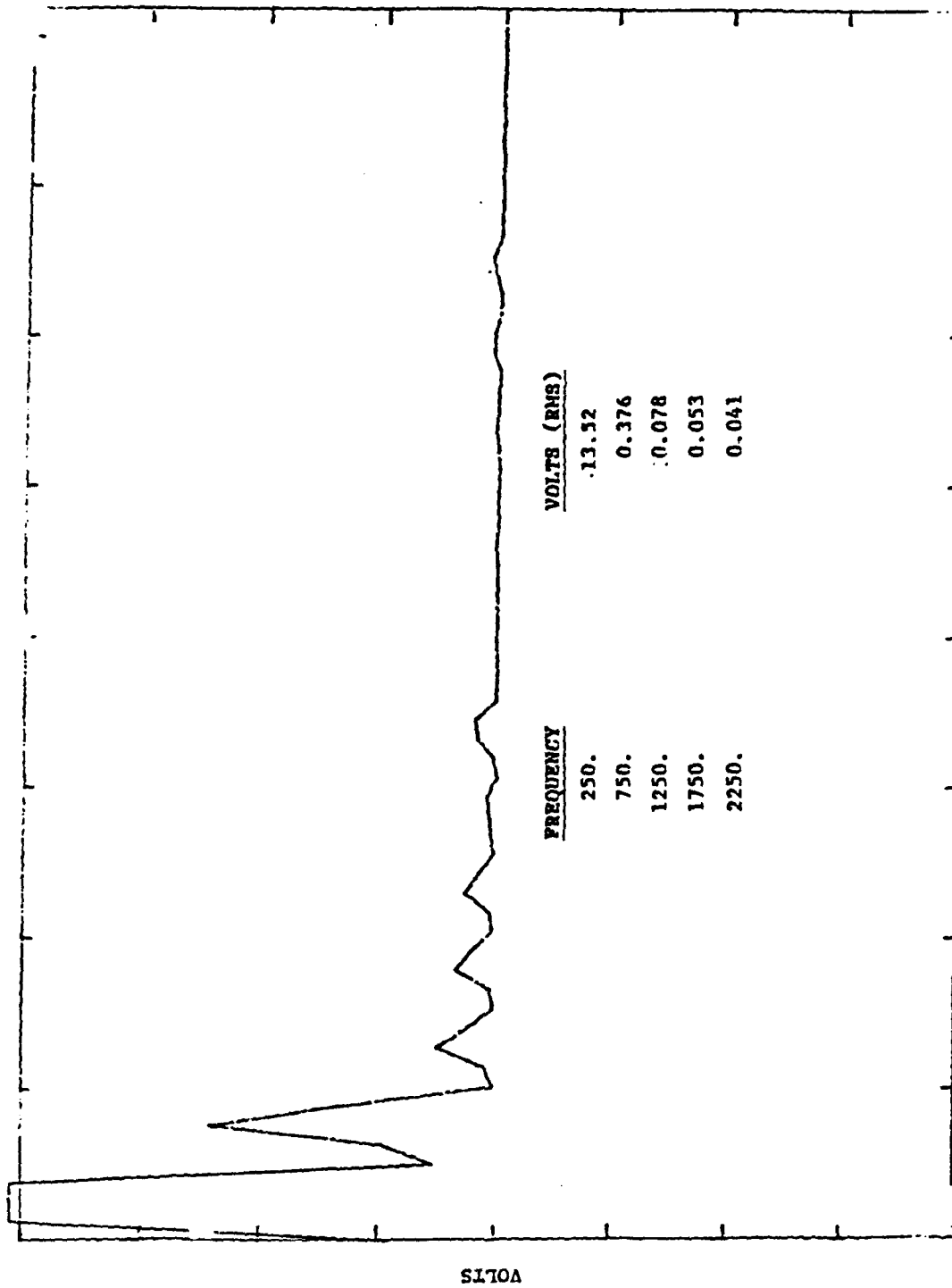


Figure 4.7. PMB Measured No-Load Voltage Frequency Spectrum at 5,000 RPM and 150°F Oil

Table 4.3 PMA Load Performance: Analytical Versus Measured Values

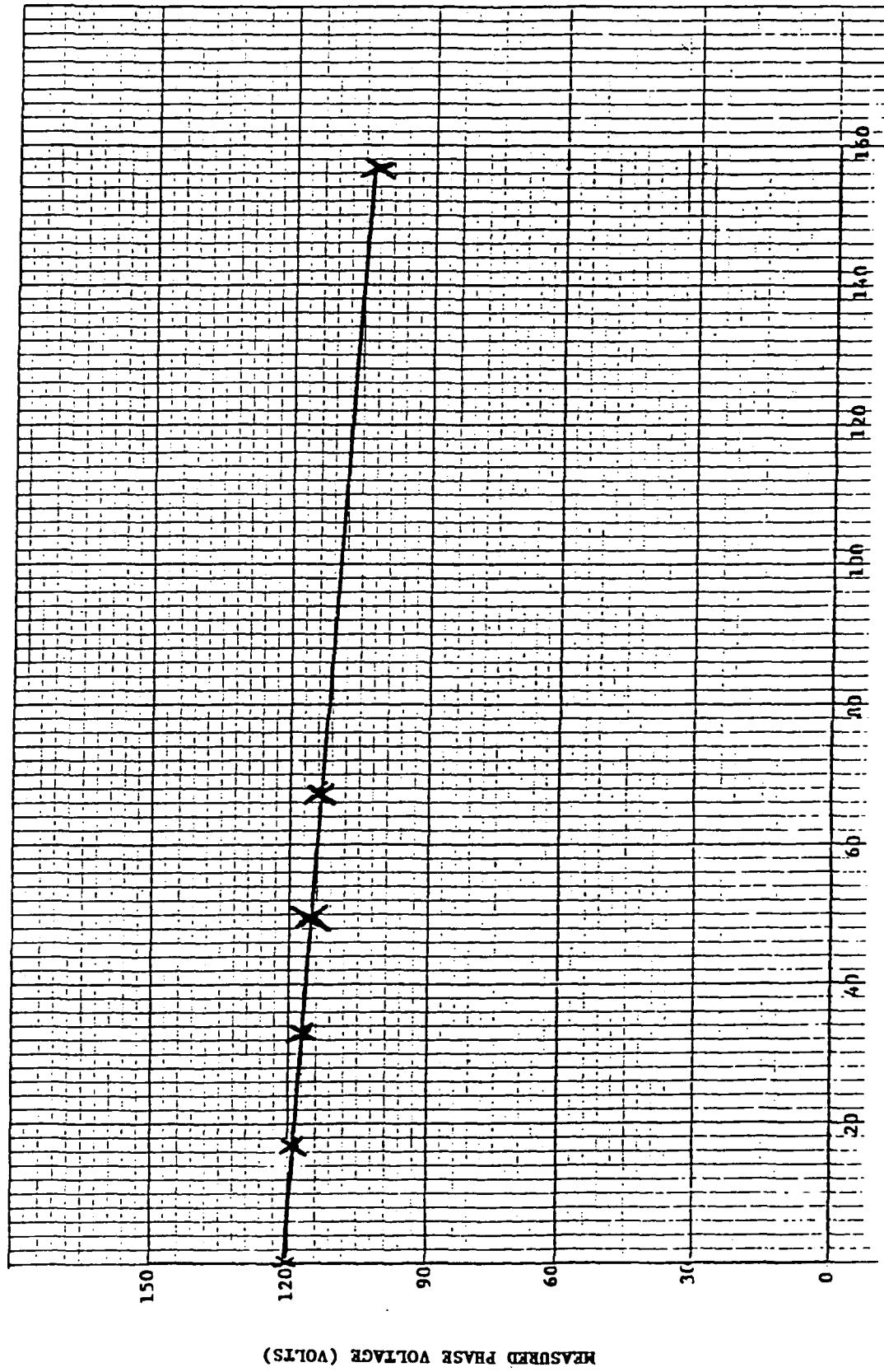
PMA LOAD PERFORMANCE				
MACHINE PARAMETERS	CONTINUOUS LOAD		PEAK LOAD	
	ANALYTICAL	TEST	ANALYTICAL	TEST
SPEED (RPM)	27,778.	27,778.	14,000.	14,000.
VOLTAGE (V)	229.	227.	99.	102.
CURRENT (A)	66.	66.	157.	157.
POWER (KVA)	45.3	45.	46.6	48.

PMB motor performance analysis was carried out using an in-house computer program. This program models the voltage controlled inverter as well as the brushless DC motor. The motor parameters are obtained from the finite element analysis. The user specifies the commutation angle and applied voltage and frequency. The program calculates torque, efficiency, instantaneous voltages and currents, etc. PMB analytical load performance results are listed in Table 4.4. PMB tests were limited to monitoring of terminal voltage and current, without torque measurement. The mounting configuration does not allow for the installation of a torque meter.

Table 4.4 PMB Analytical Load Performance

PMB ANALYTICAL LOAD PERFORMANCE		
PARAMETERS	CONTINUOUS LOAD	PEAK LOAD
VOLTAGE (V dc)	300.	313.
CURRENT (A)	103. RMS	156. RMS
TORQUE (INLB)	61.	100.
SPEED (RPM)	50,000.	50,000.
POWER (KW)	36.1	59.
POWER FACTOR	0.94	0.94
COMMUTATION ANGLE	15.	22.

The electromagnetic design is summarized in Table 4.5. The machine cross sectional view is shown in Figure 4.9.



PHASE CURRENT (AMPS)

Figure 4.8. PMA Phase Voltage vs Load Current at 14,040 RPM and 150°F Inlet Oil

Table 4.5 Electromagnetic Design Summary

PARAMETERS	PMA GENERATOR	PMB MOTOR
o STATOR:		
Lamination Material	Hiperco 50	Hiperco 50
Lamination OD	3.72"	3.72"
Lamination ID	2.92"	2.92"
Thickness	0.006"	0.006"
Number Of Phases	3.	3.
Number Of Slots	36.	36.
Turns Per Coil	1.5	1.
Number Of Wires	4.	11.
Wire Size AWG	#18	#20
Stack Length	5.7"	2.7"
o ROTOR:		
Outside Diameter	2.88"	2.88"
Inside Diameter	1.10"	1.10"
Airgap Mech.	0.020"	0.020"
Number of Poles	6.	6.
Shrink Ring Thick	0.120"	0.120"
Amortisseur Circuit bars/pole	3.	3.
o MATERIALS:		
Pole Piece	Low Carbon Mag. Iron	Low Carbon Mag. Iron
Magnets	SmCo 27 MGOe	SmCo 27 MGOe
Cont. Ring	MP35N (AMS 5845C)	MP35N (AMS 5845C)

4.3 THERMAL ANALYSIS

A finite difference nodal approach was used to determine the temperature distribution in the machine at various speed and load conditions. A modified two-dimensional axisymmetrical heat transfer model was created using PATRAN. The machine was divided into 462 thermal nodes. These nodes represent the various components, such as the rotor and stator assemblies, inner and outer housings, roller bearings, duplex bearing and the shaft. The location of the nodes is given in Figure 4.10. The resulting PATRAN model is illustrated in Figure 4.11.

The Systems Improved Numerical Differences Analyzer (SINDA) program was utilized for solving this model. The computer program is capable of analyzing thermal systems represented in lumped parametric form with conduction and convection between nodes. Subroutines were added to the program for calculating temperature variant parameters: copper losses, convective coefficients between the oil and the various components and viscous losses. Figure 4.12 show the flow schematic and flow rates for PMA and PMB.

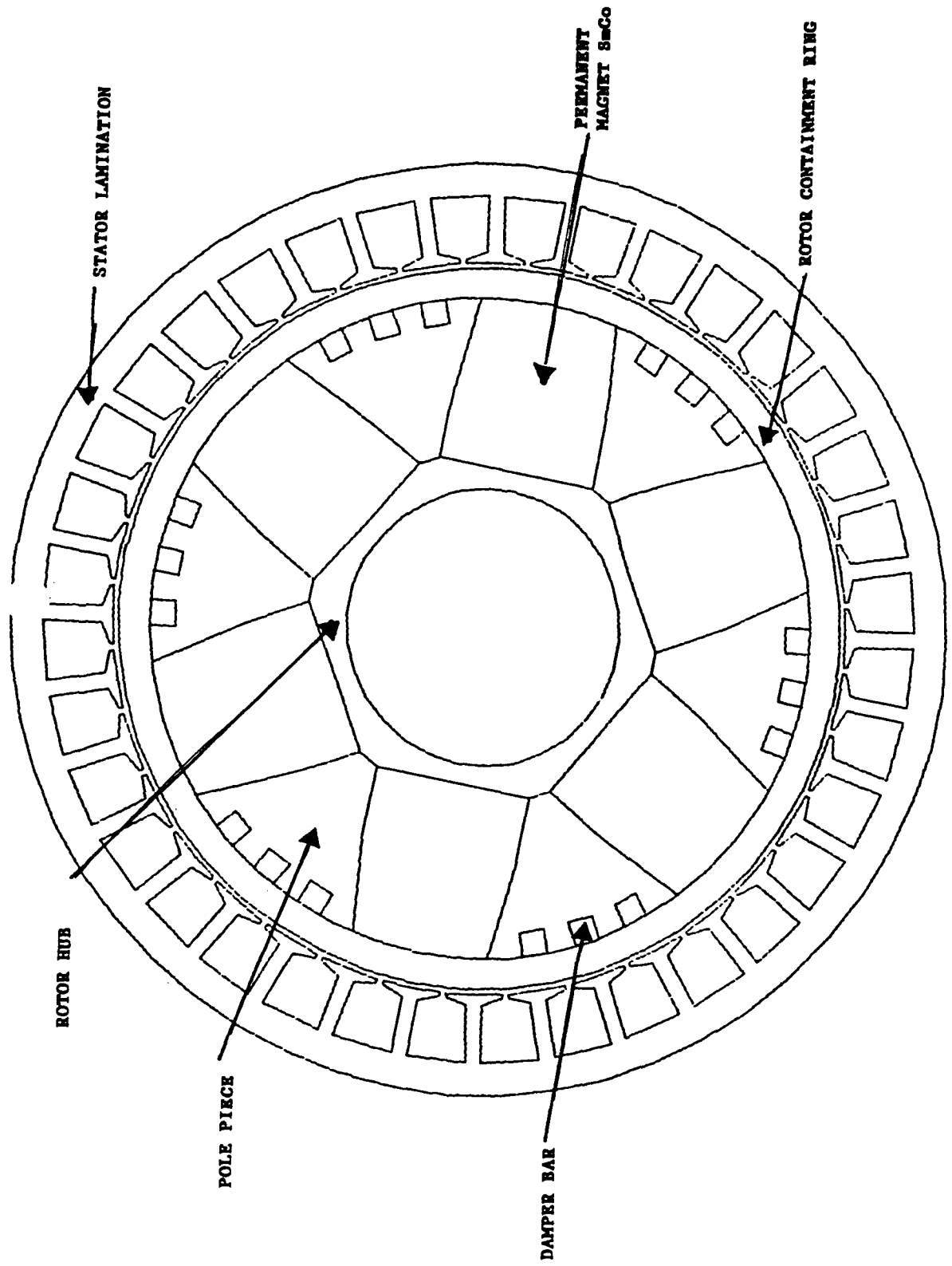


Figure 4.9. PMA and PMB Cross-Sectional View

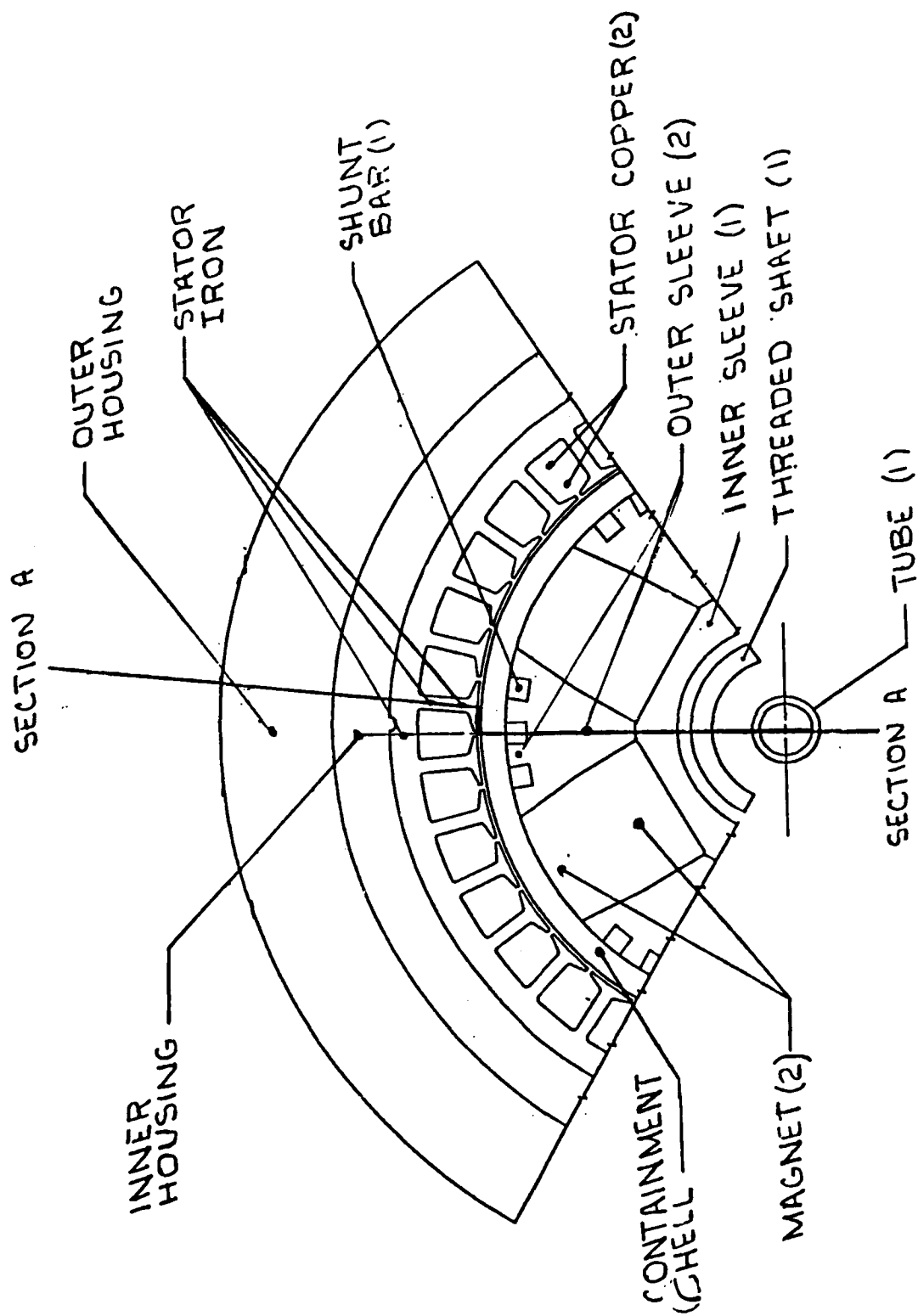


Figure 4.10. Locations of Sinda Nodes for a Typical Cross Section of the Rotor and Stator Assemblies

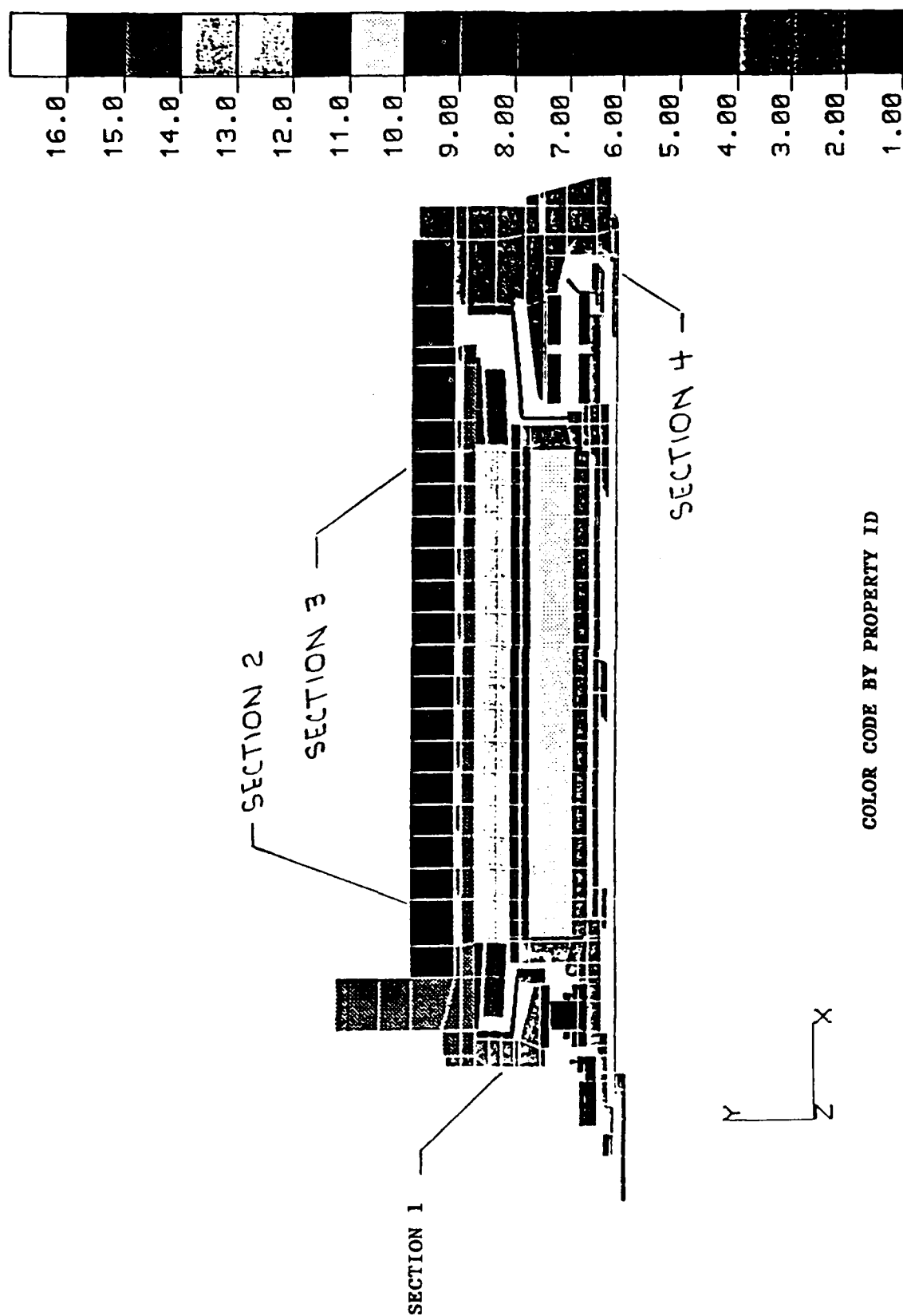
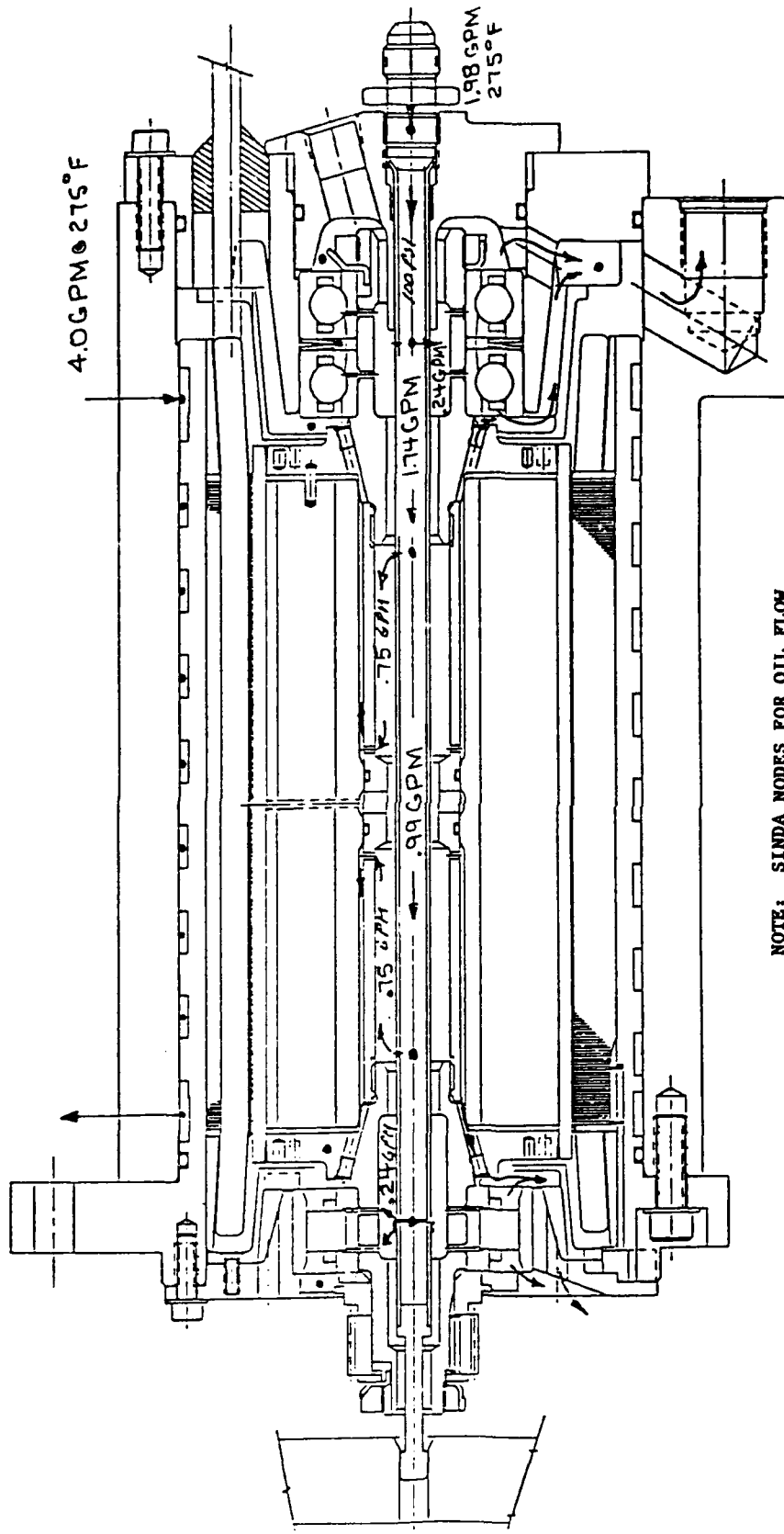


Figure 4.11. Locations of the Thermal Nodes in the Patran Geometric Model - PMA Generator



NOTE: SINDA NODES FOR OIL FLOW

Figure 4.12. PMA/PMB Flow Schematic and Flow Rates

PMA analytical and test results are listed in Table 4.6. The machines performed well under test without any flow or thermal problems. Table 4.6 shows that thermal analysis yielded conservative results. This is because the analysis assumes that there is no convective heat transfer to the surrounding environment as well as that no conductive heat flow between test article and mounting adaptor/gearbox. Our test set up does not reflect the above mentioned assumptions. The analysis also shows that the machine winding temperature is within design goal of 392°F for an inlet oil temperature of 275°F. Table 4.7 contains a summary of PMA calculated temperatures for continuous load and 275°F oil inlet conditions.

Table 4.6 PMA Thermal Analytical Versus Test Results - 1 pu Load

PARAMETERS	<u>ANALYSIS</u>		<u>TEST</u>	
	27,778 RPM	45,000 RPM	27,778 RPM	45,000 RPM
Oil Type	MIL-L-7808	MIL-L-7808	MIL-L-7808	MIL-L-7808
Stator Oil In	100.7°F	107.°F	100.7°F	107.°F
Rotor Oil In	102.°F	109.°F	102.°F	109.°F
Stator Flow	1.9 gpm	1.9 gpm	1.9 gpm	1.9 gpm
Rotor Flow	1.8 gpm	1.8 gpm	1.8 gpm	1.8 gpm
Bearing	172.°F	210.°F	142.°F	184.°F
Winding	282.°F	231.°F	172.°F	156.°F

Table 4.7 Tabulation of Predicted Component Temperatures
 For MIL-L-7808 and MIL-L-23699 Lubricating Oil
 - PMA Generator

Components	Temperature °F	
	Case 1 MIL-L-7808	Case 2 MIL-L-23699
Stator:		
Copper Windings	352°	362°
Iron	344°	355°
Rotor:		
Permanent Magnet	353°	359°
Outer Sleeve	337°	342°
Shunt Bar	352°	358°
Inner Sleeve	316°	321°
Containment Shell	356°	362°
Inner Housing	318°	330°
Outer Housing	310°	320°
Threaded Shaft	302°	306°
Tube	276°	276°
Roller Bearing	305°	309°
Ball Bearings:		
A. Inner Race	338°	348°
B. Balls	326°	336°
C. Outer Race	332°	342°
Inlet Oil	275°	275°
Outlet Oil (Inner Housing)	294°	293°
Outlet Oil (Lube Return Port)	297°	300°

Oil Flows:
 1. Rotor 1.98 gpm
 2. Housing 2.0 gpm

PMB stator winding temperature rise is calculated based on PMA thermal analysis. PMB and PMA have about the same iron losses at their most severe thermal operating conditions. This calculation addresses the difference in copper losses and stack lengths. PMB carries 100 amperes and it has a 0.0113 ohm winding resistance. PMA carries 66 amperes with a 0.043 ohm resistance. PMA stack length is 5.7 inch compared to PMB's 2.7 inch length. PMA thermal analysis yielded a 77°F winding temperature rise. PMB stator winding temperature rise is

$$77^{\circ}\text{F} \times \frac{100^2}{66} \times \frac{0.0113}{0.043} \times \frac{5.7 \text{ inch}}{2.7 \text{ inch}} = 98^{\circ}\text{F}$$

or PMB maximum winding temperature is $98^{\circ}\text{F} + 275^{\circ}\text{F} = 373^{\circ}\text{F}$ for an inlet oil temperature of 275°F .

Table 4.8 contains a summary of PMB measured temperatures at rated current and 40,000 rpm for an inlet oil temperature of 100°F :

Table 4.8 PMB Measured Temperatures at Rated Current, 40,000 RPM and 100°F Inlet Oil

PARAMETERS	TEST RESULTS
INLET OIL TEMP. ($^{\circ}\text{F}$)	100°F
SPEED (RPM)	40,000.
WINDING TEMP. ($^{\circ}\text{F}$)	205.
BEARING TEMP ($^{\circ}\text{F}$)	183.
ROTOR FLOW	1.5 GAL/MIN
STATOR FLOW	1.5 GAL/MIN

4.4 BEARING ANALYSIS

Various sets of roller and duplex ball bearings for the PM machines were analyzed for fatigue life, power loss, and spring rate at various applied loads and rotor speeds. The design goal is to achieve 30,000 hr minimum B10 life as well as to minimize power loss while using large enough bearings to keep the first critical speed of the rotor above the maximum operating speed. The calculations were performed using Sundstrand's in-house computer programs for ball and roller bearings.

The resulting design utilizes a 205 roller bearing on the machines drive end and a pair of 205 duplex bearings at the anti-drive end. The duplex bearings are angular contact type with an axial preload of 130 pounds. The bearing geometrical parameters are listed in Table 4.9. The combined power loss curve for the 205 roller and duplex pair of 205 bearings is shown in Figure 4.13. The calculated B10 lives, at continuous rated load are 1,000,000 hours for the roller and 50,000 hours for the ball bearings. These numbers are in excess of the minimum design goals. PMA and PMB have the same bearings.

Table 4.9 PMA/PMB Bearing Parameters

SIZE OF BEARING	205 SIZE	
	ROLLER	BALL
TYPE OF BEARING	ROLLER	BALL
NUMBER OF ROLLERS/BALLS	12	13
ROLLER/BALL DIAMETER (INCH)	.3150	5/16
LENGTH OF ROLLER (INCH)	.3150	—
PITCH DIAMETER (INCH)	1.5158	1.5158
RACE CURVATURE RATIOS	—	52%
INTERNAL DIAMETRAL CLEARANCE (INCH)	.0010	.0015
MATERIAL LIFE MULTIPLIER	10	10

4.5 ROTOR CRITICAL SPEED

An in-house computer program was used for determining critical speed for the PM rotors. This program, based on the transfer matrix approach, takes into account the magnitude and location of the applied loads, the bearing stiffness and shaft geometry. The transfer matrix method solves steady state dynamic problems in the frequency domain. This method treats a continuous

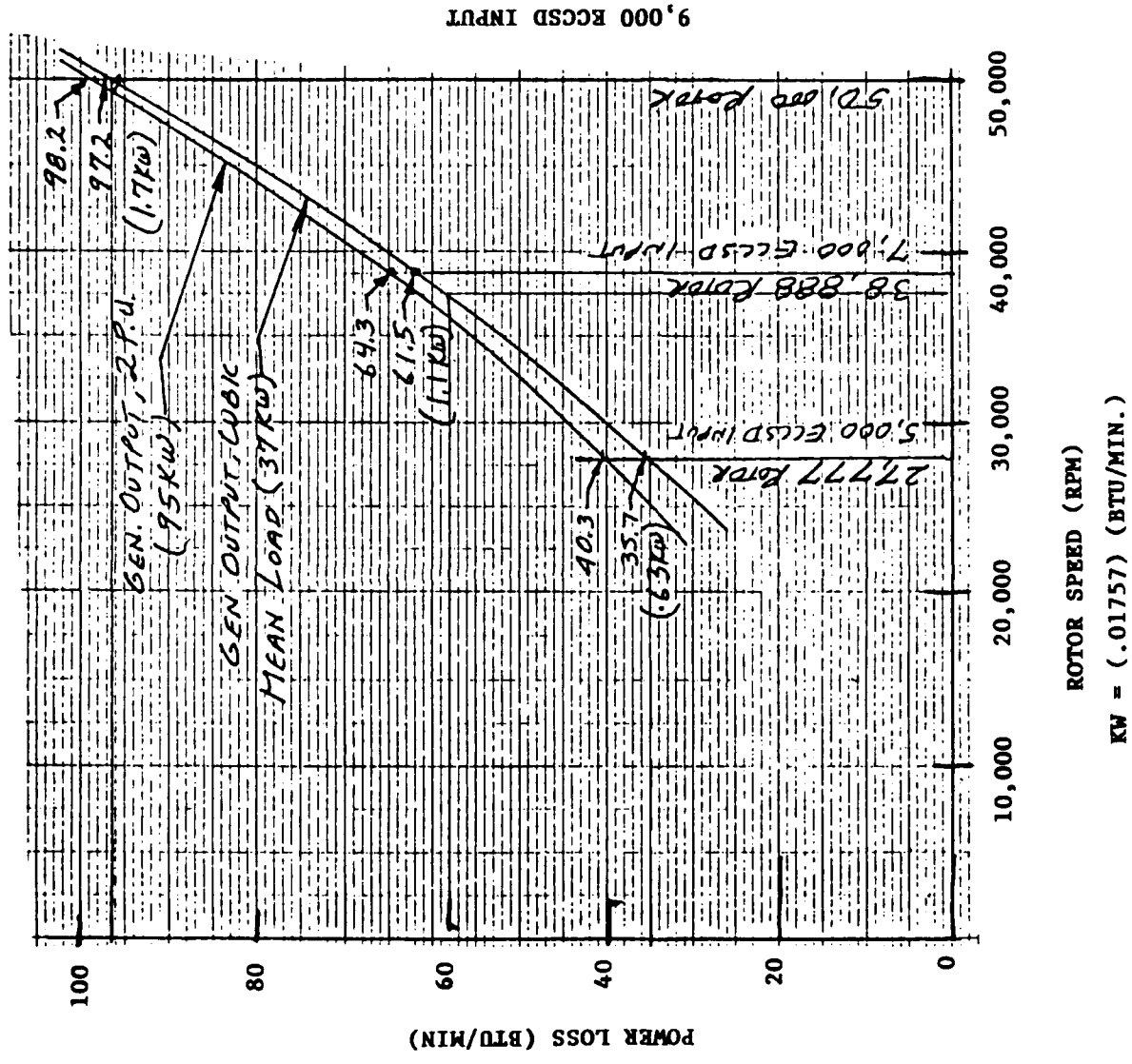


Figure 4.13. Machine Bearings Total Power Loss for MIL-L-7808 at 275°F

system as a lumped system with N concentrated masses at N points called stations. The shaft section which connects one lumped mass station to the next is assumed massless and of uniform stiffness. The differential equations of the continuous system are approximated by two sets of finite difference equations. One set relates the change in forces across a rigid mass station and the other set relates deflections and forces between two adjacent lumped mass stations. Figure 4.14 is a drawing of the rotor and the 15 stations. The results of the analysis showed all critical speeds to be above the maximum operating speed of 50,000 rpm. The results are tabulated in Table 4.10. The mode shapes are shown in Figures 4.15 and 4.16.

Table 4.10 PM Machines Calculated Critical Speeds

Mode	PMA Rotor	PMB Rotor
1st	59,780 rpm	74,560 rpm
2nd	149,270 rpm	202,900 rpm

The analysis results were later confirmed through extensive spin tests. The tests were limited to 45,000 rpm to minimize the risk of mechanical failure prior to system testing and proof of concept. The machines performed very well under dynamic conditions: no-load and load states. The maximum measured, one per revolution rms, vibration is under 3 g. This is well below our design goal of 10 g maximum. Figures 4.17 and 4.18 are plots of machine vibration as a function of speed at no-load condition.

4.6 ROTOR STRESS ANALYSIS

To insure that the containment ring stresses were within the permissible limit, a finite element analysis was performed. An ANSYS 2-D finite element model was developed to evaluate the rotor component stresses and deflections. The design goals are not to exceed the containment ring material yield strength and to prevent the permanent magnet to lift-off from the shaft at 50,000 rpm at 70°F. Temperature effects (350°F) and overspeed (110% base speed) were also addressed.

The rotor design consists of six magnets located around a hexagonal shaft separated by wedges or poles. The assembly is held together by a containment ring with an interference fit. During rotation, magnet retention is aided by a 5° partial slope in the wedges (poles). The analysis shows that the optimum radial interference range for the containment ring to

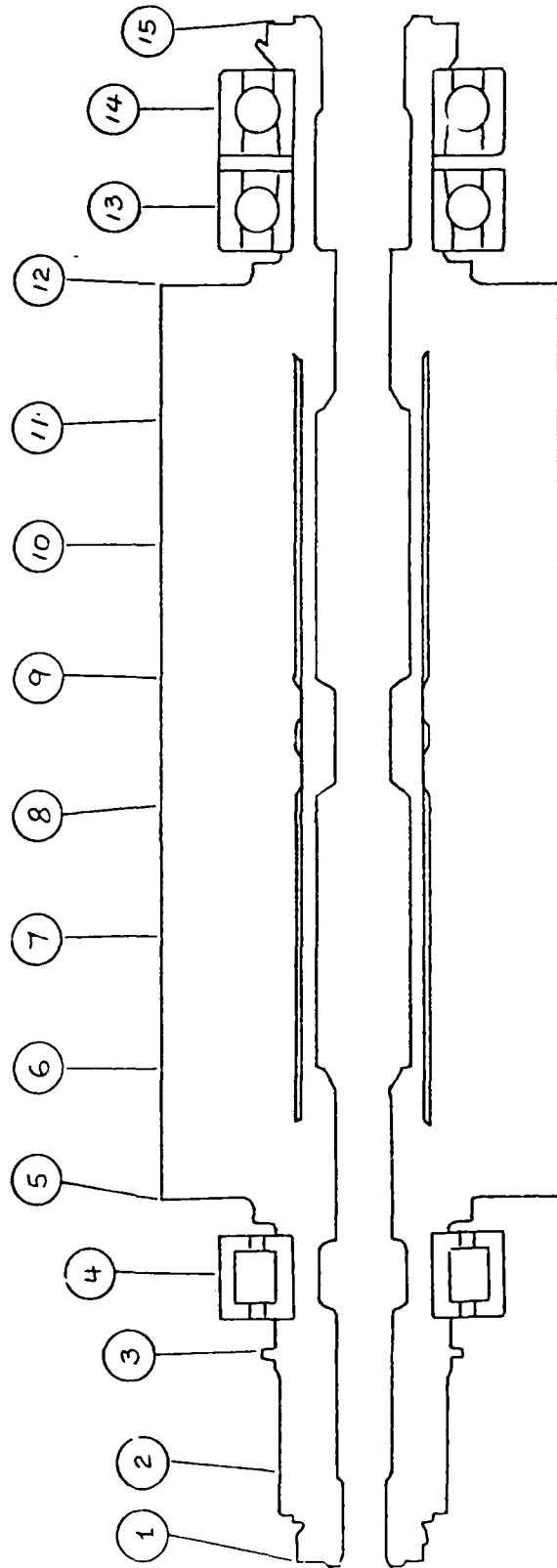


Figure 4.14. Rotating Assembly of PMA and Station Numbers

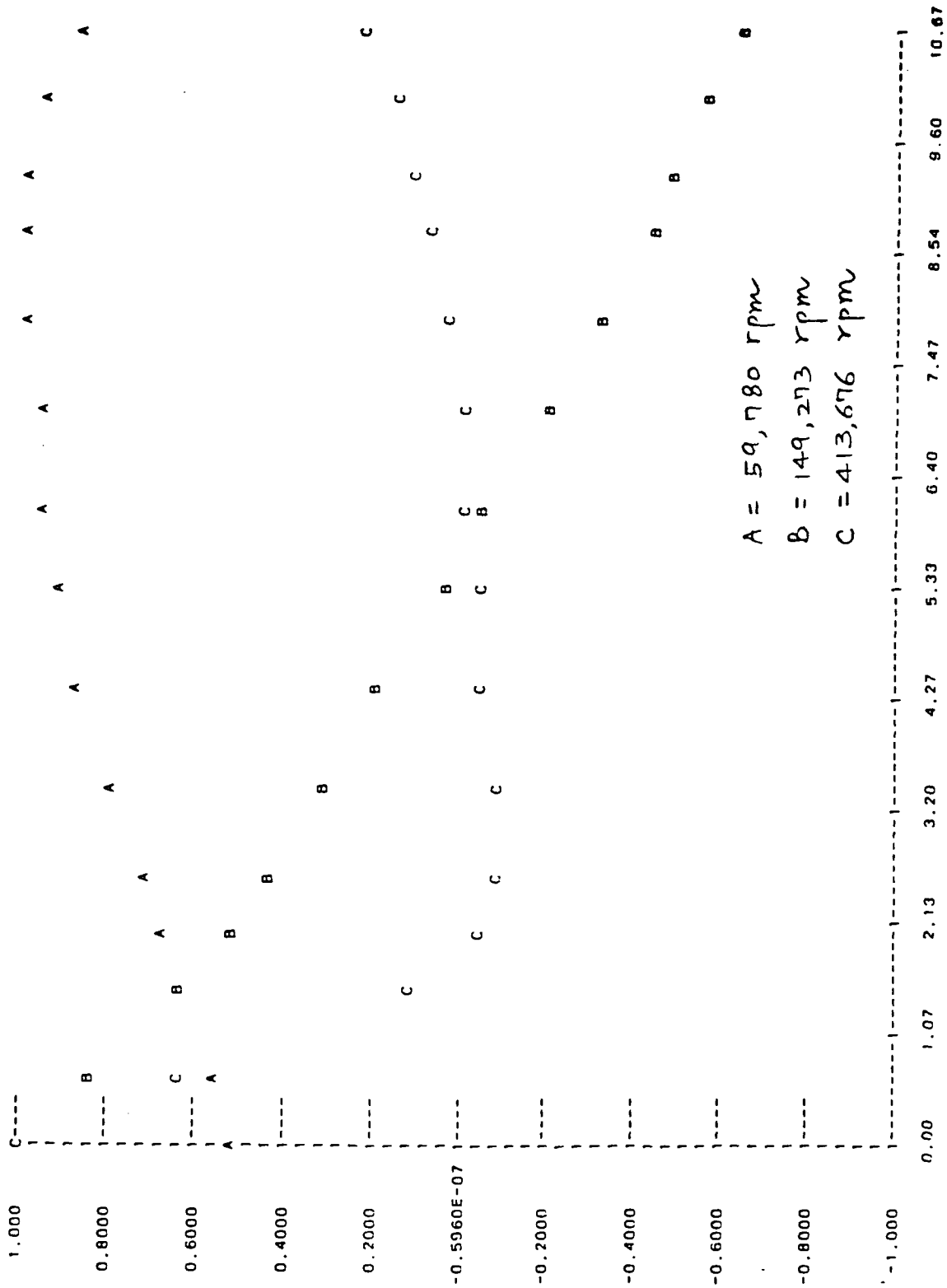


Figure 4.15. Mode Shapes of the PMA Rotor

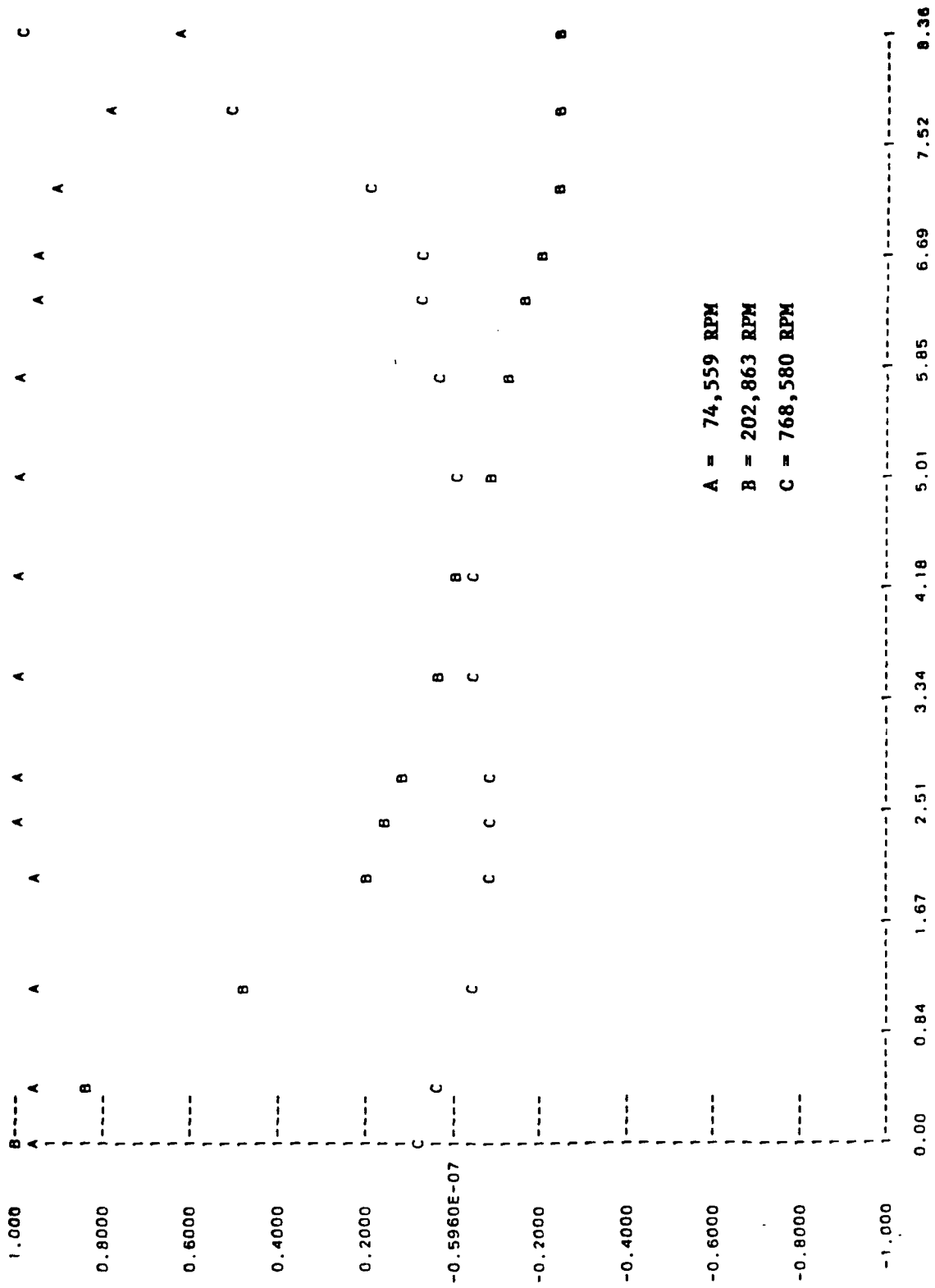


Figure 4.16. Mode Shapes of the MB Rotor

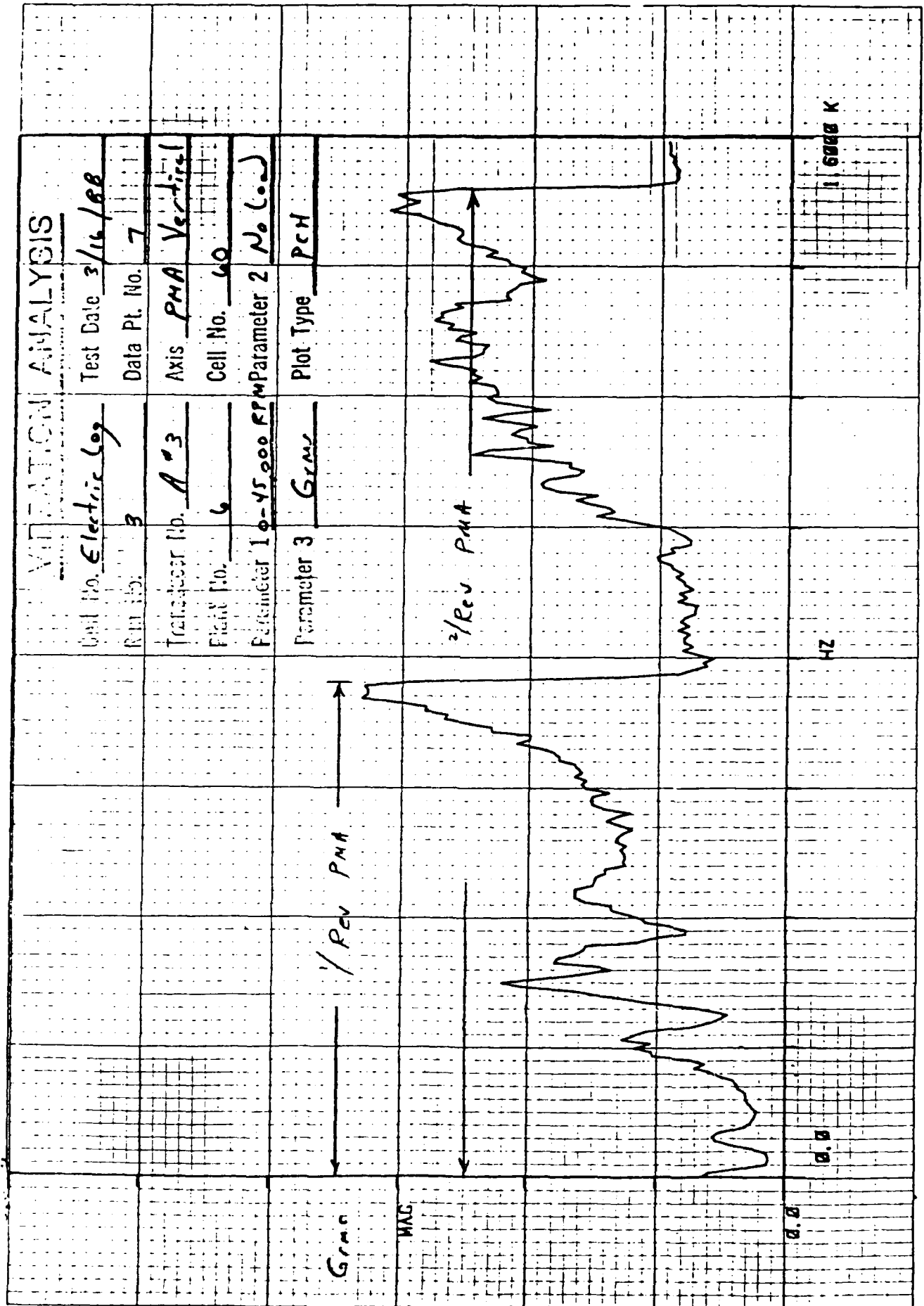
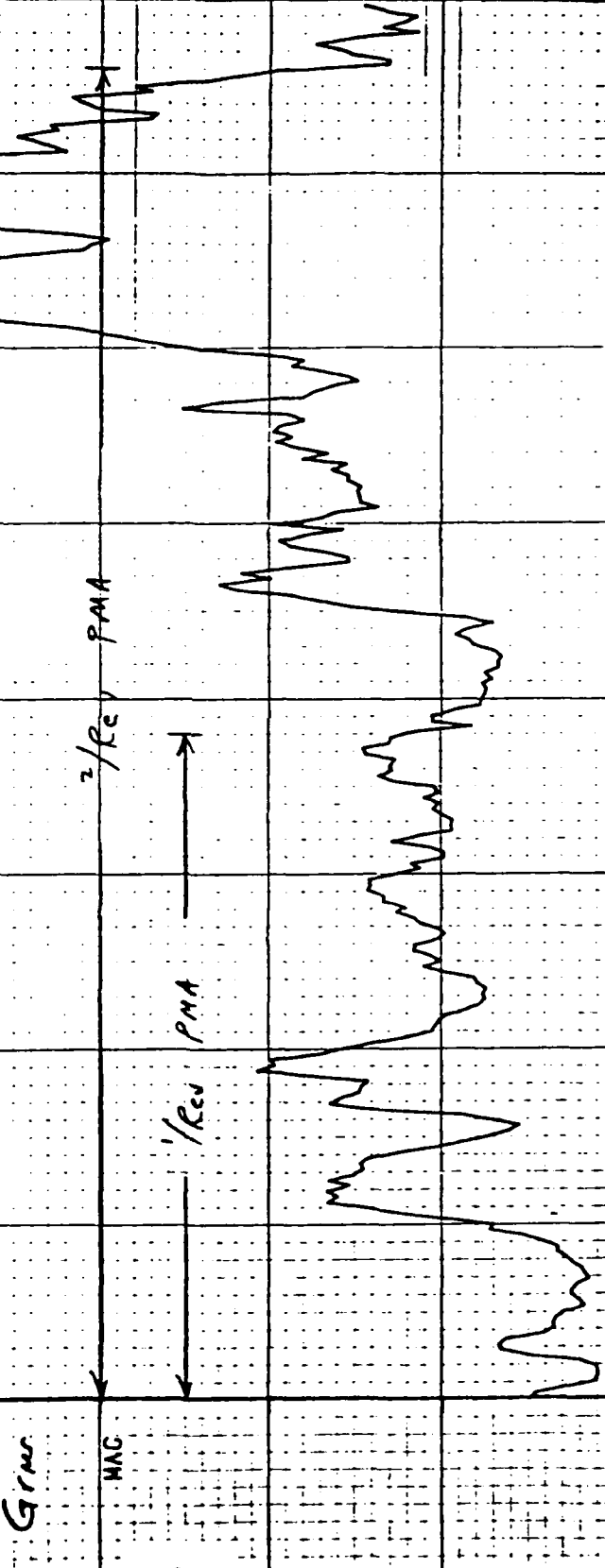


Figure 4.17a. PMA Vertical Vibration Frequency Spectrum - No Load

VIBRATION ANALYSIS

Unit No. Electric Log
 Run No. 3
 Transducer No. A-4
 Plot No. 6
 Parameter 1 0-4000 RPM
 Parameter 2 No Load
 Parameter 3 Grav
 Plot Type PCH

Test Date 3/16/88
 Data Pt. No. 7
 Axis PMA Lateral
 Cell No. 60



0.5
 1.0
 1.5
 2.0
 2.5
 3.0
 3.5
 4.0
 4.5
 5.0
 5.5
 6.0
 6.5
 7.0
 7.5
 8.0
 8.5
 9.0
 9.5
 10.0
 10.5
 11.0
 11.5
 12.0
 12.5
 13.0
 13.5
 14.0
 14.5
 15.0
 15.5
 16.0
 16.5
 17.0
 17.5
 18.0
 18.5
 19.0
 19.5
 20.0
 20.5
 21.0
 21.5
 22.0
 22.5
 23.0
 23.5
 24.0
 24.5
 25.0
 25.5
 26.0
 26.5
 27.0
 27.5
 28.0
 28.5
 29.0
 29.5
 30.0
 30.5
 31.0
 31.5
 32.0
 32.5
 33.0
 33.5
 34.0
 34.5
 35.0
 35.5
 36.0
 36.5
 37.0
 37.5
 38.0
 38.5
 39.0
 39.5
 40.0
 40.5
 41.0
 41.5
 42.0
 42.5
 43.0
 43.5
 44.0
 44.5
 45.0
 45.5
 46.0
 46.5
 47.0
 47.5
 48.0
 48.5
 49.0
 49.5
 50.0
 50.5
 51.0
 51.5
 52.0
 52.5
 53.0
 53.5
 54.0
 54.5
 55.0
 55.5
 56.0
 56.5
 57.0
 57.5
 58.0
 58.5
 59.0
 59.5
 60.0
 60.5
 61.0
 61.5
 62.0
 62.5
 63.0
 63.5
 64.0
 64.5
 65.0
 65.5
 66.0
 66.5
 67.0
 67.5
 68.0
 68.5
 69.0
 69.5
 70.0
 70.5
 71.0
 71.5
 72.0
 72.5
 73.0
 73.5
 74.0
 74.5
 75.0
 75.5
 76.0
 76.5
 77.0
 77.5
 78.0
 78.5
 79.0
 79.5
 80.0
 80.5
 81.0
 81.5
 82.0
 82.5
 83.0
 83.5
 84.0
 84.5
 85.0
 85.5
 86.0
 86.5
 87.0
 87.5
 88.0
 88.5
 89.0
 89.5
 90.0
 90.5
 91.0
 91.5
 92.0
 92.5
 93.0
 93.5
 94.0
 94.5
 95.0
 95.5
 96.0
 96.5
 97.0
 97.5
 98.0
 98.5
 99.0
 99.5
 100.0
 100.5
 101.0
 101.5
 102.0
 102.5
 103.0
 103.5
 104.0
 104.5
 105.0
 105.5
 106.0
 106.5
 107.0
 107.5
 108.0
 108.5
 109.0
 109.5
 110.0
 110.5
 111.0
 111.5
 112.0
 112.5
 113.0
 113.5
 114.0
 114.5
 115.0
 115.5
 116.0
 116.5
 117.0
 117.5
 118.0
 118.5
 119.0
 119.5
 120.0
 120.5
 121.0
 121.5
 122.0
 122.5
 123.0
 123.5
 124.0
 124.5
 125.0
 125.5
 126.0
 126.5
 127.0
 127.5
 128.0
 128.5
 129.0
 129.5
 130.0
 130.5
 131.0
 131.5
 132.0
 132.5
 133.0
 133.5
 134.0
 134.5
 135.0
 135.5
 136.0
 136.5
 137.0
 137.5
 138.0
 138.5
 139.0
 139.5
 140.0
 140.5
 141.0
 141.5
 142.0
 142.5
 143.0
 143.5
 144.0
 144.5
 145.0
 145.5
 146.0
 146.5
 147.0
 147.5
 148.0
 148.5
 149.0
 149.5
 150.0
 150.5
 151.0
 151.5
 152.0
 152.5
 153.0
 153.5
 154.0
 154.5
 155.0
 155.5
 156.0
 156.5
 157.0
 157.5
 158.0
 158.5
 159.0
 159.5
 160.0
 160.5
 161.0
 161.5
 162.0
 162.5
 163.0
 163.5
 164.0
 164.5
 165.0
 165.5
 166.0
 166.5
 167.0
 167.5
 168.0
 168.5
 169.0
 169.5
 170.0
 170.5
 171.0
 171.5
 172.0
 172.5
 173.0
 173.5
 174.0
 174.5
 175.0
 175.5
 176.0
 176.5
 177.0
 177.5
 178.0
 178.5
 179.0
 179.5
 180.0
 180.5
 181.0
 181.5
 182.0
 182.5
 183.0
 183.5
 184.0
 184.5
 185.0
 185.5
 186.0
 186.5
 187.0
 187.5
 188.0
 188.5
 189.0
 189.5
 190.0
 190.5
 191.0
 191.5
 192.0
 192.5
 193.0
 193.5
 194.0
 194.5
 195.0
 195.5
 196.0
 196.5
 197.0
 197.5
 198.0
 198.5
 199.0
 199.5
 200.0
 200.5
 201.0
 201.5
 202.0
 202.5
 203.0
 203.5
 204.0
 204.5
 205.0
 205.5
 206.0
 206.5
 207.0
 207.5
 208.0
 208.5
 209.0
 209.5
 210.0
 210.5
 211.0
 211.5
 212.0
 212.5
 213.0
 213.5
 214.0
 214.5
 215.0
 215.5
 216.0
 216.5
 217.0
 217.5
 218.0
 218.5
 219.0
 219.5
 220.0
 220.5
 221.0
 221.5
 222.0
 222.5
 223.0
 223.5
 224.0
 224.5
 225.0
 225.5
 226.0
 226.5
 227.0
 227.5
 228.0
 228.5
 229.0
 229.5
 230.0
 230.5
 231.0
 231.5
 232.0
 232.5
 233.0
 233.5
 234.0
 234.5
 235.0
 235.5
 236.0
 236.5
 237.0
 237.5
 238.0
 238.5
 239.0
 239.5
 240.0
 240.5
 241.0
 241.5
 242.0
 242.5
 243.0
 243.5
 244.0
 244.5
 245.0
 245.5
 246.0
 246.5
 247.0
 247.5
 248.0
 248.5
 249.0
 249.5
 250.0
 250.5
 251.0
 251.5
 252.0
 252.5
 253.0
 253.5
 254.0
 254.5
 255.0
 255.5
 256.0
 256.5
 257.0
 257.5
 258.0
 258.5
 259.0
 259.5
 260.0
 260.5
 261.0
 261.5
 262.0
 262.5
 263.0
 263.5
 264.0
 264.5
 265.0
 265.5
 266.0
 266.5
 267.0
 267.5
 268.0
 268.5
 269.0
 269.5
 270.0
 270.5
 271.0
 271.5
 272.0
 272.5
 273.0
 273.5
 274.0
 274.5
 275.0
 275.5
 276.0
 276.5
 277.0
 277.5
 278.0
 278.5
 279.0
 279.5
 280.0
 280.5
 281.0
 281.5
 282.0
 282.5
 283.0
 283.5
 284.0
 284.5
 285.0
 285.5
 286.0
 286.5
 287.0
 287.5
 288.0
 288.5
 289.0
 289.5
 290.0
 290.5
 291.0
 291.5
 292.0
 292.5
 293.0
 293.5
 294.0
 294.5
 295.0
 295.5
 296.0
 296.5
 297.0
 297.5
 298.0
 298.5
 299.0
 299.5
 300.0
 300.5
 301.0
 301.5
 302.0
 302.5
 303.0
 303.5
 304.0
 304.5
 305.0
 305.5
 306.0
 306.5
 307.0
 307.5
 308.0
 308.5
 309.0
 309.5
 310.0
 310.5
 311.0
 311.5
 312.0
 312.5
 313.0
 313.5
 314.0
 314.5
 315.0
 315.5
 316.0
 316.5
 317.0
 317.5
 318.0
 318.5
 319.0
 319.5
 320.0
 320.5
 321.0
 321.5
 322.0
 322.5
 323.0
 323.5
 324.0
 324.5
 325.0
 325.5
 326.0
 326.5
 327.0
 327.5
 328.0
 328.5
 329.0
 329.5
 330.0
 330.5
 331.0
 331.5
 332.0
 332.5
 333.0
 333.5
 334.0
 334.5
 335.0
 335.5
 336.0
 336.5
 337.0
 337.5
 338.0
 338.5
 339.0
 339.5
 340.0
 340.5
 341.0
 341.5
 342.0
 342.5
 343.0
 343.5
 344.0
 344.5
 345.0
 345.5
 346.0
 346.5
 347.0
 347.5
 348.0
 348.5
 349.0
 349.5
 350.0
 350.5
 351.0
 351.5
 352.0
 352.5
 353.0
 353.5
 354.0
 354.5
 355.0
 355.5
 356.0
 356.5
 357.0
 357.5
 358.0
 358.5
 359.0
 359.5
 360.0
 360.5
 361.0
 361.5
 362.0
 362.5
 363.0
 363.5
 364.0
 364.5
 365.0
 365.5
 366.0
 366.5
 367.0
 367.5
 368.0
 368.5
 369.0
 369.5
 370.0
 370.5
 371.0
 371.5
 372.0
 372.5
 373.0
 373.5
 374.0
 374.5
 375.0
 375.5
 376.0
 376.5
 377.0
 377.5
 378.0
 378.5
 379.0
 379.5
 380.0
 380.5
 381.0
 381.5
 382.0
 382.5
 383.0
 383.5
 384.0
 384.5
 385.0
 385.5
 386.0
 386.5
 387.0
 387.5
 388.0
 388.5
 389.0
 389.5
 390.0
 390.5
 391.0
 391.5
 392.0
 392.5
 393.0
 393.5
 394.0
 394.5
 395.0
 395.5
 396.0
 396.5
 397.0
 397.5
 398.0
 398.5
 399.0
 399.5
 400.0
 400.5
 401.0
 401.5
 402.0
 402.5
 403.0
 403.5
 404.0
 404.5
 405.0
 405.5
 406.0
 406.5
 407.0
 407.5
 408.0
 408.5
 409.0
 409.5
 410.0
 410.5
 411.0
 411.5
 412.0
 412.5
 413.0
 413.5
 414.0
 414.5
 415.0
 415.5
 416.0
 416.5
 417.0
 417.5
 418.0
 418.5
 419.0
 419.5
 420.0
 420.5
 421.0
 421.5
 422.0
 422.5
 423.0
 423.5
 424.0
 424.5
 425.0
 425.5
 426.0
 426.5
 427.0
 427.5
 428.0
 428.5
 429.0
 429.5
 430.0
 430.5
 431.0
 431.5
 432.0
 432.5
 433.0
 433.5
 434.0
 434.5
 435.0
 435.5
 436.0
 436.5
 437.0
 437.5
 438.0
 438.5
 439.0
 439.5
 440.0
 440.5
 441.0
 441.5
 442.0
 442.5
 443.0
 443.5
 444.0
 444.5
 445.0
 445.5
 446.0
 446.5
 447.0
 447.5
 448.0
 448.5
 449.0
 449.5
 450.0
 450.5
 451.0
 451.5
 452.0
 452.5
 453.0
 453.5
 454.0
 454.5
 455.0
 455.5
 456.0
 456.5
 457.0
 457.5
 458.0
 458.5
 459.0
 459.5
 460.0
 460.5
 461.0
 461.5
 462.0
 462.5
 463.0
 463.5
 464.0
 464.5
 465.0
 465.5
 466.0
 466.5
 467.0
 467.5
 468.0
 468.5
 469.0
 469.5
 470.0
 470.5
 471.0
 471.5
 472.0
 472.5
 473.0
 473.5
 474.0
 474.5
 475.0
 475.5
 476.0
 476.5
 477.0
 477.5
 478.0
 478.5
 479.0
 479.5
 480.0
 480.5
 481.0
 481.5
 482.0
 482.5
 483.0
 483.5
 484.0
 484.5
 485.0
 485.5
 486.0
 486.5
 487.0
 487.5
 488.0
 488.5
 489.0
 489.5
 490.0
 490.5
 491.0
 491.5
 492.0
 492.5
 493.0
 493.5
 494.0
 494.5
 495.0
 495.5
 496.0
 496.5
 497.0
 497.5
 498.0
 498.5
 499.0
 499.5
 500.0
 500.5
 501.0
 501.5
 502.0
 502.5
 503.0
 503.5
 504.0
 504.5
 505.0
 505.5
 506.0
 506.5
 507.0
 507.5
 508.0
 508.5
 509.0
 509.5
 510.0
 510.5
 511.0
 511.5
 512.0
 512.5
 513.0
 513.5
 514.0
 514.5
 515.0
 515.5
 516.0
 516.5
 517.0
 517.5
 518.0
 518.5
 519.0
 519.5
 520.0
 520.5
 521.0
 521.5
 522.0
 522.5
 523.0
 523.5
 524.0
 524.5
 525.0
 525.5
 526.0
 526.5
 527.0
 527.5
 528.0
 528.5
 529.0
 529.5
 530.0
 530.5
 531.0
 531.5
 532.0
 532.5
 533.0
 533.5
 534.0
 534.5
 535.0
 535.5
 536.0
 536.5
 537.0
 537.5
 538.0
 538.5
 539.0
 539.5
 540.0
 540.5
 541.0
 541.5
 542.0
 542.5
 543.0
 543.5
 544.0
 544.5
 545.0
 545.5
 546.0
 546.5
 547.0
 547.5
 548.0
 548.5
 549.0
 549.5
 550.0
 550.5
 551.0
 551.5
 552.0
 552.5
 553.0
 553.5
 554.0
 554.5
 555.0
 555.5
 556.0
 556.5
 557.0
 557.5
 558.0
 558.5
 559.0
 559.5
 560.0
 560.5
 561.0
 561.5
 562.0
 562.5
 563.0
 563.5
 564.0
 564.5
 565.0
 565.5
 566.0
 566.5
 567.0
 567.5
 568.0
 568.5
 569.0
 569.5
 570.0
 570.5
 571.0
 571.5
 572.0
 572.5
 573.0
 573.5
 574.0
 574.5
 575.0
 575.5
 576.0
 576.5
 577.0
 577.5
 578.0
 578.5
 579.0
 579.5
 580.0
 580.5
 581.0
 581.5
 582.0
 582.5
 583.0
 583.5
 584.0
 584.5
 585.0
 585.5
 586.0
 586.5
 587.0
 587.5
 588.0
 588.5
 589.0
 589.5
 590.0
 590.5
 591.0
 591.5
 592.0
 592.5
 593.0
 593.5
 594.0
 594.5
 595.0
 595.5
 596.0
 596.5
 597.0
 597.5
 598.0
 598.5
 599.0
 599.5
 600.0
 600.5
 601.0
 601.5
 602.0
 602.5
 603.0
 603.5
 604.0
 604.5
 605.0
 605.5
 606.0
 606.

VIBRATION ANALYSIS

Unit No. Electric Log CSA Test Date 3/24/88

Run No. 4

Data Pt. No. 10

Transducer No. A⁰¹

Axis PMB Vertical

Plant No. 6

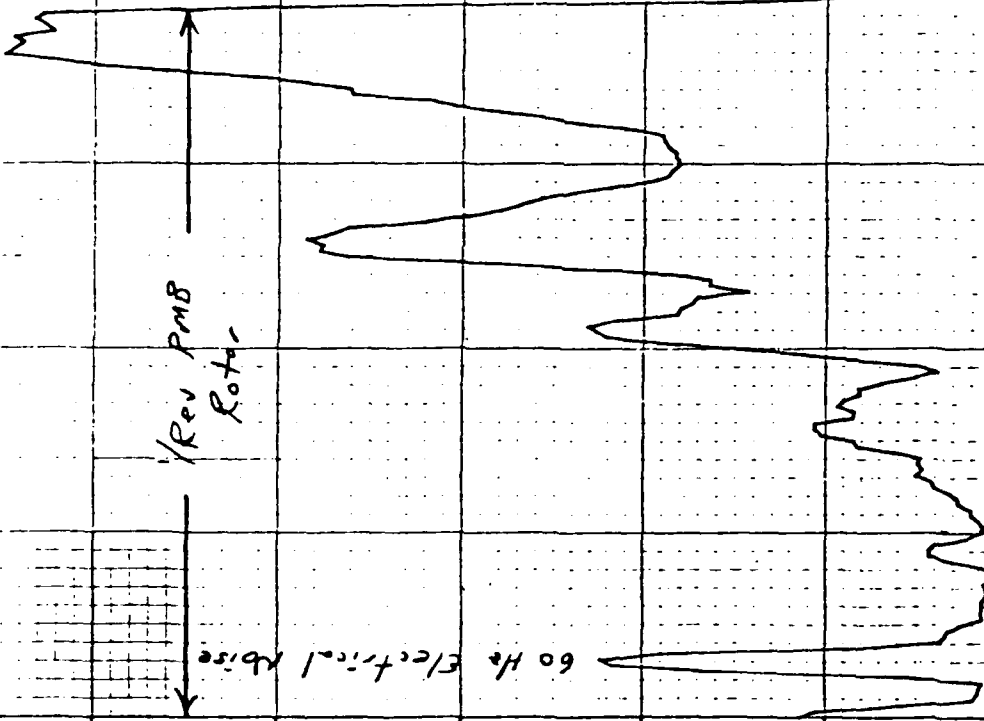
Cell No. 60

Parameter 1 0-45000 RPM

Parameter 2 No Load

Parameter 3 Grms

Plot Type PCH



Grms

MAG

0.0

0.0

HZ

1.60000 K

Figure 4.18a. PMB Vertical Vibration Frequency Spectrum - No Load

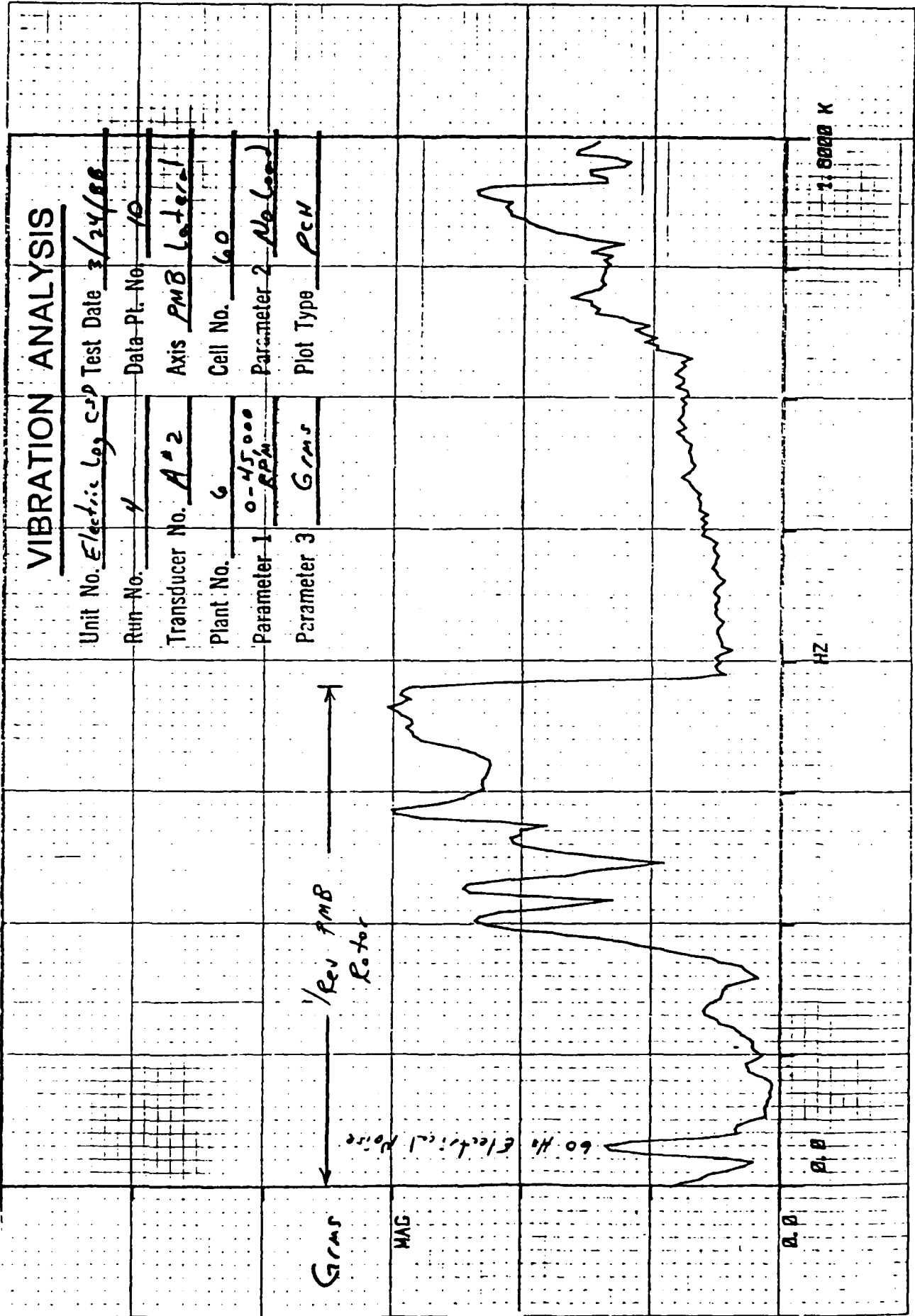


Figure 4.18b. PMB Lateral Vibration Frequencies Spectrum - No Load

be 0.008 inch to 0.0085. The maximum effective stress for each component at 50,000 rpm and 70°F is as follows:

Containment Ring	219. ksi
Wedge	12. ksi
Magnet	18. ksi
Shaft	7. ksi

The stresses for the shaft, wedge and magnet are all compressive. These are well within material limits. The stress on the containment ring is 219 ksi where as the material measured yielded strength is 242.5 ksi at 70°F. The material is MP35N nonmagnetic steel aged and work hardened.

The effects of temperature and overspeed on containment ring stress are summarized in Table 4.11. These calculated results show that the yield strength of the material is not exceeded, but permanent magnet lift-off occurs at 55,000 rpm at 70°F and 350°F condition. Therefore, it is recommended not to exceed the 50,000 rpm operating speed.

Table 4.11 Containment Ring Calculated Stress
For Various Speed and Temperatures

ROTOR COMPONENTS	CONTAINMENT RING INTERFERENCE = 0.008 INCH			
	70°/50 K	70°/55 K	350°/50 K	350°/55 K
MAGNET SEP.	NO SEP	FULL SEP (=.0005 IN)	PARTIAL SEP	FULL SEP (=.0008 IN)
CONT. RING STRESS	207.3 KSI	217.7 KSI	190.6 KSI	214.3 KSI
WEDGE STRESS	11.3 KSI	11.6 KSI	10.1 KSI	11.2 KSI
MAGNET STRESS	17.1 KSI	23.1 KSI	17.7 KSI	25.7 KSI
CONTAINMENT RING INTERFERENCE = 0.0085 IN				
MAGNET SEP.	NO SEP	FULL SEP (=.0002 IN)	PARTIAL SEP	FULL SEP (=.0005 IN)
CONT. RING STRESS	219.1 KSI	223.4 KSI	200.4 KSI	216.5 KSI
WEDGE STRESS	12.1 KSI	11.9 KSI	11.4 KSI	11.9 KSI
MAGNET STRESS	18.0 KSI	20.6 KSI	18.3 KSI	24.1 KSI

The rotors were inspected and measured after several hours of operation at speeds up to 45,000 rpm and 150°F oil temperature. No abnormalities or growth were observed.

To assure the quality of the MP35N material, Sundstrand tested the material tubing for tensile strength at several temperatures. The material has exceptional strength up to 350°F and no loss in ductility was found. The test results are shown in Table 4.12.

Table 4.12 MP35N Tensile Test Results

Sample No.	Test Temp., °F	YS (ksi)	UTS (ksi)	% El	% RA
MPR 31449	RT	242.5	243.0	—	51.0
1	150°	242.0	245.0	9.3	45.0
2	150°	242.4	244.8	8.8	43.3
3	150°	233.7	241.8	11.6	46.2
Avg.	150°	239.4	243.9	9.9	44.8
4	250°	231.7	236.4	11.6	48.9
5	250°	224.8	236.4	10.5	48.9
6	250°	226.5	234.2	15.5	45.3
Avg.	250°	227.7	235.7	12.5	47.7
7	350°	223.4	229.5	10.0	50.5
8	350°	226.6	228.1	9.3	42.4
9	350°	226.8	231.4	9.3	44.4
Avg.	350°	225.6	229.7	9.5	45.8

4.7 TEST SETUP

The permanent magnet machines were assembled on to the differential gearbox and mounted on the drive stand. The test setup is shown in Figure 4.19. Stator and rotor oil flows and pressures were independently controlled. The accelerometers, mounted on the anti-drive end enable recording of the vibration level. The machines temperatures were monitored using iron constantine thermocouples. The thermocouples were potted, 120° apart, in the stator slots and the winding end turn area. Bearing temperatures were also monitored with the thermocouples embedded and potted into the end bells. Electrical voltages, currents and power were measured using high frequency power meters.



Figure 4.19. RCSPH System Test Setup

The limits established for the test were as follows:

Maximum vibration at antidrive end	10 g
Maximum stator winding temperature	392 °F
Maximum rotor speed	45,000 RPM
Maximum oil inlet temperature	150 °F

5.0 GEAR BOX

5.1 DESIGN OBJECTIVES

The gear box is a functional prototype of the gear train to be used in a production electrically compensated constant speed drive (CSD). Although the gears are not of final production configuration, they are made with the correct gear ratios and have representative inertias. The box, lubrication, cooling, and gears are sized for durability and manufacturability.

5.2 DESIGN PARAMETERS

- o B10 life for F-16 type load conditions is well in excess of 30,000 hours.
- o Cubic mean load is 37 kw (from F-16 qual endurance test conditions).
- o Proof load is 5,600 in-lb (maximum input shaft shear section torque).
- o When two gears mesh with a common gear, the gear stresses at the larger of the two ratios are balanced.

5.3 GEAR BOX INTERFACE (See Figure 5.1 and 5.2)

The gear box envelop dimensions are available on Sundstrand Drawing #EP2833-411. The input face of the gear box includes a F-16 V-band pad. The required input speed is 5,000 to 9,000 RPM counter clockwise looking at the pad. The input torque is limited by an input shaft shear section designed to shear at 5,000 to 5,600 in-lb. The output pad of the gear box accepts a Sundstrand generator (Model #60EG04, Outline #724846, Assembly #724847). The generator pad speed is 12,000 RPM clockwise looking at the gear box pad. This face of the gear box also provides pads for the two electromagnetic machines (PMA (CCW), and PMB (CW) looking at the gear box pads).

5.4 HOUSING DESIGN

The gear box housing is designed as a heavy wall (.75 inch thick) steel weldment. This type of construction was selected as the most economical method of reliably achieving the required bearing bore size and locational tolerance.



Figure 5.1. Gear Box Input Pad

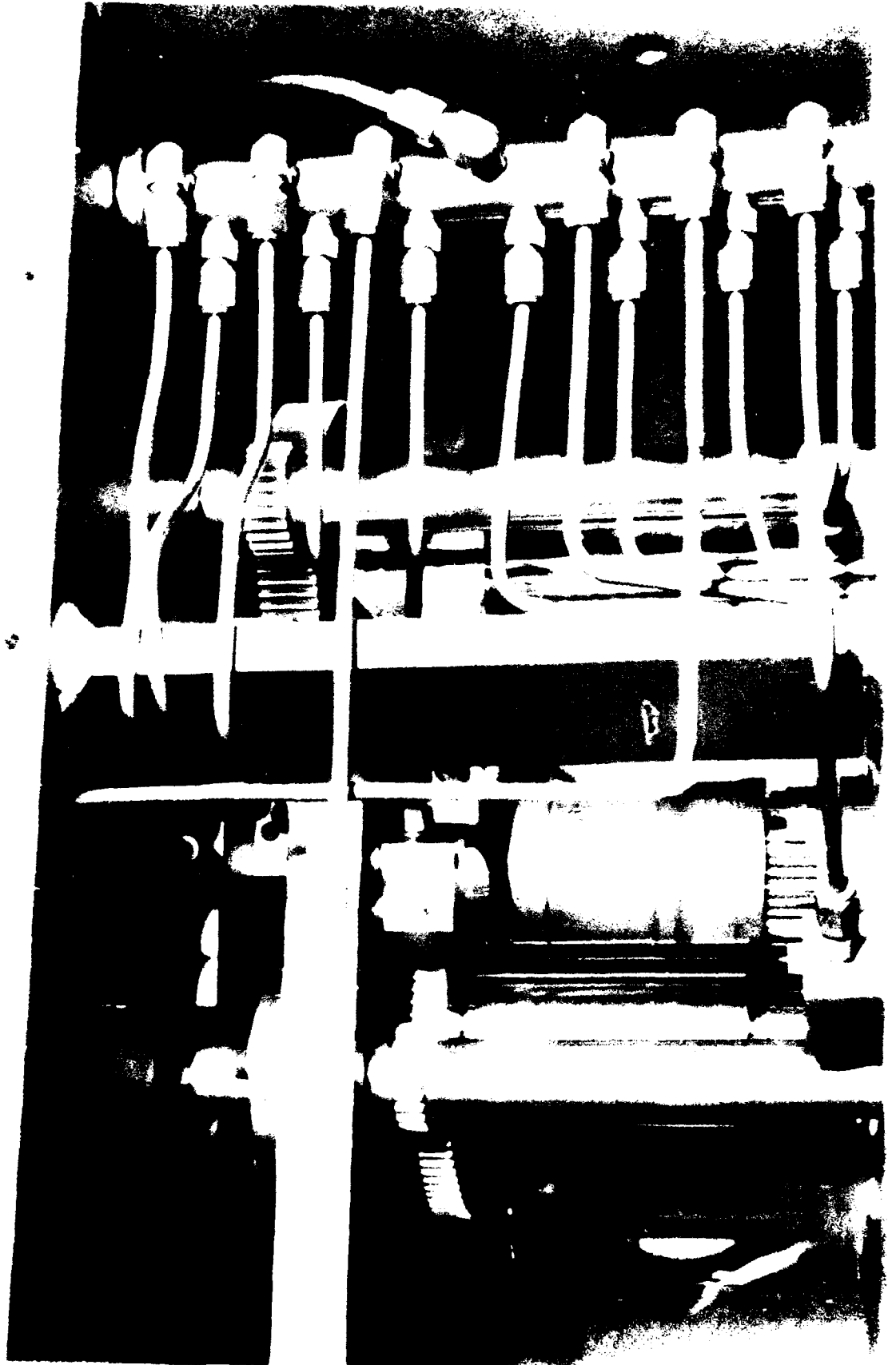


Figure 5.2. Gear Box, Cover Removed

5.5 GEAR DESIGN (See Figure 5.3 through 5.13 and Tables 5.1 through 5.3)

The gears, especially the lower speed gears, have little impact on the system inertia. As a result they are designed for life rather than weight. The gear train as designed can be safely run at 95 kw (2 p.u.) for 26 hours. Because of the very high pitch line velocity (15,000 ft/min), the gear mesh at the electromagnetic machines (PMA & PMB) are precision spur gears. A helical gear set is recommended for a production configuration. The differential is a standard F-15 differential assembly, Sundstrand Part #744382 with an oversized drive gear welded onto the input ring gear. This differential was chosen because it was readily available and was designed for the proper rating. A nomogram of rotational speeds for each leg of the differential is shown in Figure 5.4. Inspection of the nomogram shows that to compensate for decreased input speed, the PMB speed must increase. The journal bearing velocity of the differentials planet gears is very high, but, it is deemed acceptable for this application. A production drive would be based on a different type of differential. A proposed production design is shown in Figure 5.6.

To protect against inadvertently driving PMB in the reverse rotational direction, a grounding one way clutch was added to the PMB jack shaft.

The gear train schematic for the prototype CSD and accompanying data charts are shown on Figures 5.5, 5.7, and Table 5.1. Gear train input loads are listed in Table 5.2. A chart of gear tooth tip modifications is shown on Table 5.3. Figures 5.8 through 5.13 show computer print outs of the gear profiles for detail gear data charts, see Sundstrand Drawing #EP2833-402.

5.6 BEARING DESIGN (See Table 5.4)

The bearing life analysis is based on a mean load of 37 kw (F16 endurance test) and a shock load condition of 95 kw. Since the electromagnetic generator (PMA) has the highest loads, only PMA bearings were analyzed. The prototype CSD bearings were analyzed using the Sundstrand in-house D17X ball bearing program and the D18 roller bearing program. The DN number for the electromagnetic machines is high, 1.25×10^6 at a speed of 50,000 rpm. The B-10 life for the 2 p.u. condition is good with the minimum life occurring at the electromagnetic machine roller bearing (11,000 hours). A spot check of the lower speed bearings showed that they have very high B-10 lives. The differential bearings were not analyzed at this time since they are loaded at a lower level than in their production F-15 application. In the production application, all of the CSD power flows through the differential. In this prototype CSD there is an input splitter gear that diverts all the PMA (generator) power directly to PMA rather than taking it out of the differential carrier gear.

The diametal fits between the bearings and the adjacent shafts or bores are given on Sundstrand Drawing #EP2833-402.

5.7 GEAR BOX LUBRICATION & COOLING (See Figure 5.14)

Each bearing is lubricated by a separate jet and is installed with provisions for adequate drainage. The gears are cooled by a spray of oil with sufficient volume such that the oil temperature does not rise more than 40°F assuming a 1 percent loss per mesh and operating at 95 kw. The gear cooling flow is directed to the back side of each mesh so that the oil tends to be pulled into the opening gear mesh. A lubrication and cooling manifold pressure of 50 psi was chosen. Figure 5.2 shows a view of the gear box lube lbj/in² for psi distribution plumbing. A 0.030 in-diameter orifice was chosen for bearing lubrication. This resulted in a flow of 0.12 gal/min. A 0.040 diameter orifice was chosen for the gear tooth cooling. This resulted in a flow of .22 gal/min. The differential gears and bearings are lubricated and cooled in the same way as on the standard CSD. Flow is ported to the differential from the generator through a small transfer tube.

5.8 GEAR BOX TEST HISTORY

The gear box performed well. There were, however, a few start up problems. At first the gear box would not drain properly. It was determined that the facilities scavage pump had excess capacity and was pulling air up the drain pipe. Increasing the gear box ventilation solved this problem.

Next, excessive drag was observed in the PMB drive train. It was eventually traced to a slight interference between the gear retaining screw head on the PMB jack shaft and one of the PMB cover attached screws. A small notch was ground in the head of the cover attach screw to eliminate the interference.

The test facilities set up made it difficult to change the input spline (dog bone). During testing, the spline lubricating grease was centrifuged out. Late in the test sequence the gear box was pulled and the spline shaft removed. Excessive spline wear was observed; input drive misalignment was suspected. Correct alignment should give satisfactory performance. If prolonged testing is expected, some attention should be given to this spline; either plan to pull and relubricate the spline on a regular basis, apply a thicker spline grease, or add a snap ring to act as a dam.

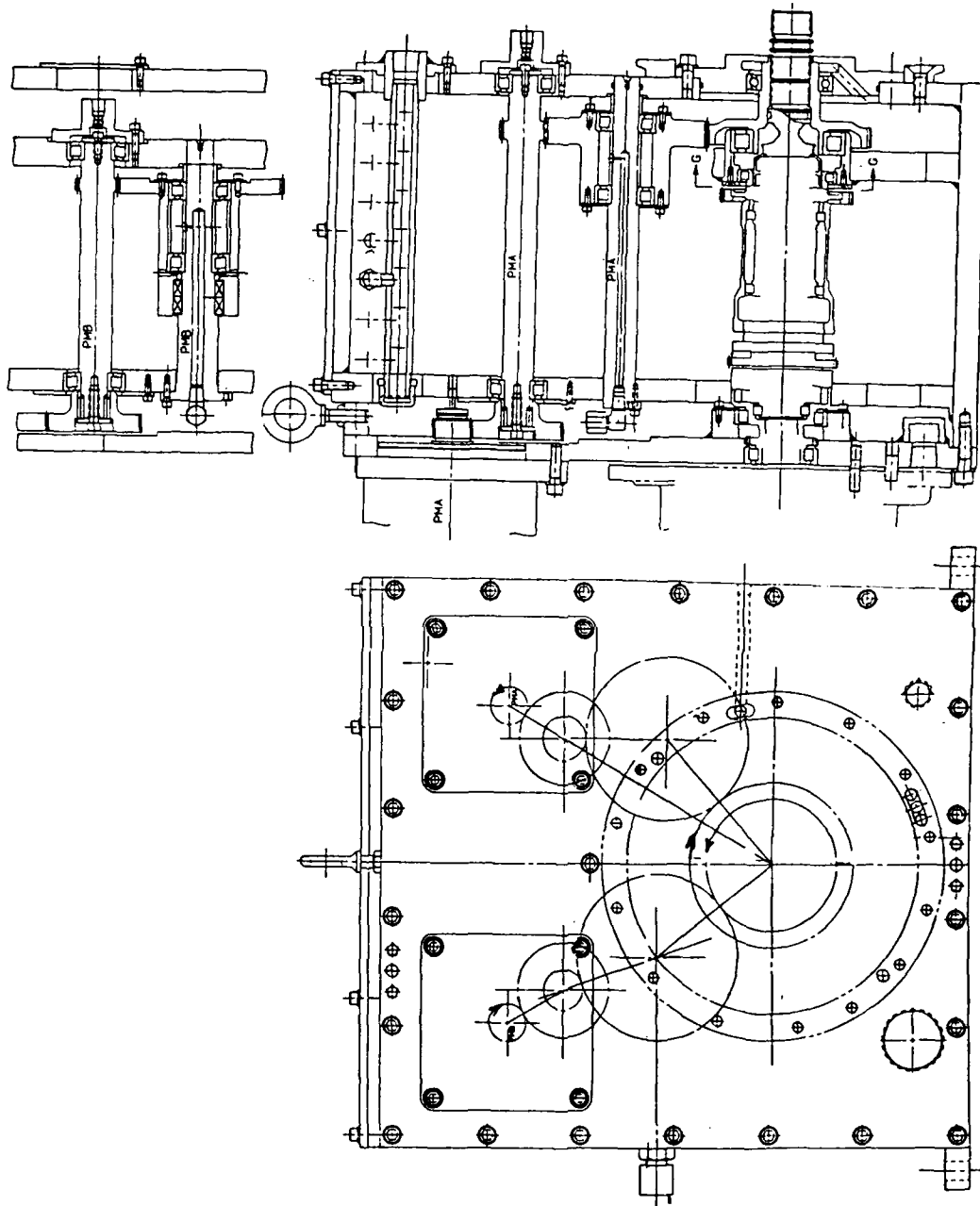


Figure 5.3. Differential Gear Box

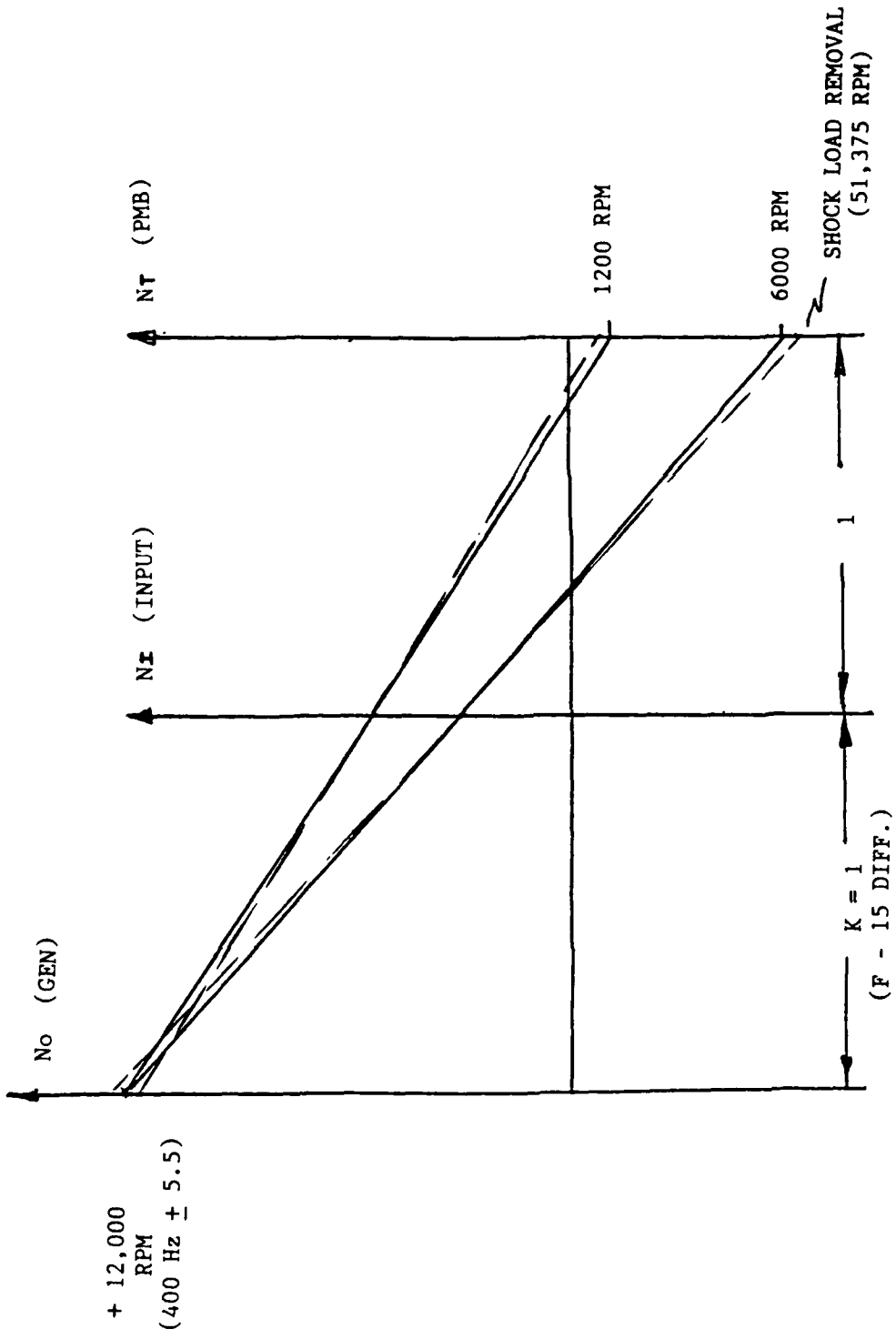
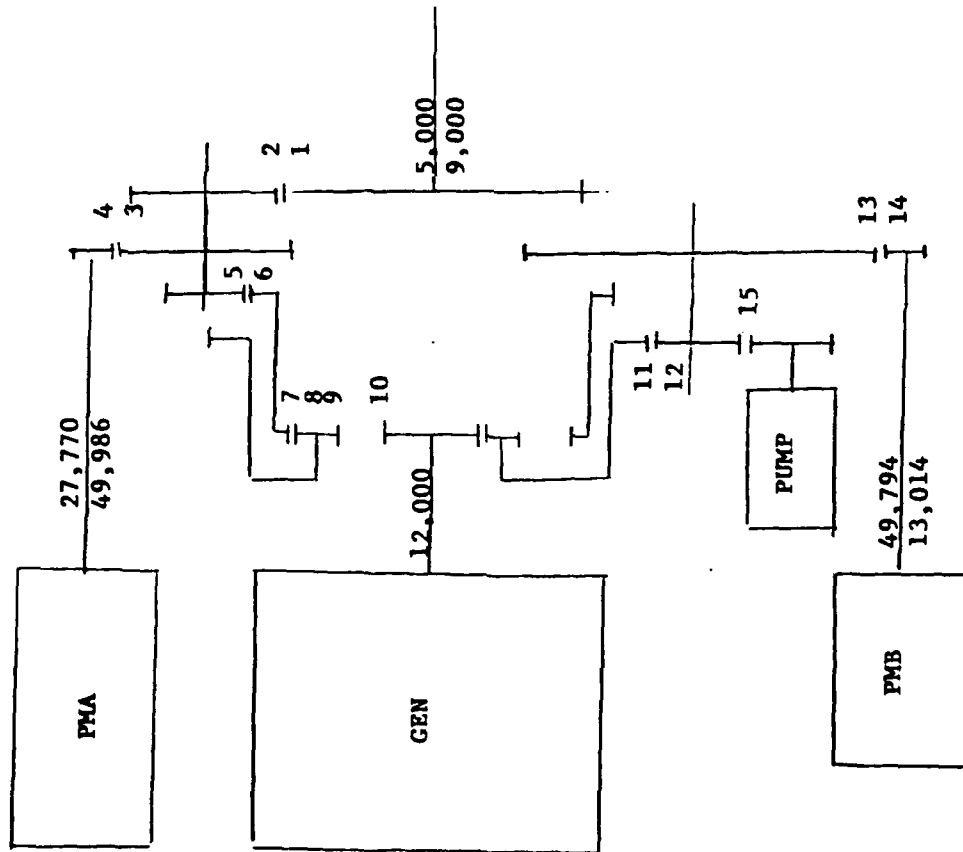


Figure 5.4. Differential Gear Speed Diagram

ELECTRIC LOG
SINGLE SIDED - BELOW STRAIGHT THRU



GEARING

NO.	NO. OF TEETH	D.P.	P.D.	SPEED RPM	
				MIN.	MAX.
1	54	14	3.86	5,000	9,000
2	37	14	2.64	7,297	13,135
3	137	32	4.28		
4	36	32	1.13	27,770	49,986
5	38	20	1.90	7,297	13,135
6	92	20	4.5	3,014	5,425
7	60	20	3.0		
8	52	20	1.04	6,087	1,357
9	34	20	1.70		
10	20	20	1.00	12,000	
11	99	20	4.95	6,087	1,357
12	39	20	1.95	-15,453	-4,038
13	116	20	5.80		
14	36	32	1.13	-49,794	-13,014
15	38	32	1.19	-15,859	-4,144

Figure 5.6. Proposed Production Gear Train

GEAR DESIGN

INPUT DATA:

- . MATERIAL TO BE 9310, CARBURIZED.
- . 10 H-MIN LIFE @ 2 PU SHOCKLOAD (95 KS ASSUMING GENERATOR EFF. 85%.
- . CUBIC MEANLOAD (CML) = 36.9 KW BASED ON F-16 MSIP ENDURANCE TEST, TABLE III, SPEC 16ZE228B. THIS INPUT WAS RUN THROUGH PROGRAM SIMILAR TO RE86/205.

ANALYSIS:

GEAR MESH 1/2 HAS A HIGH-PITCH LINE VELOCITY - 15,000 FT-MIN AS A RESULT 32 PITCH AND CLASS P1 GEARING WAS CHOSEN - ALL OTHER GEARS ARE 20 PITCH CLASS 3.

METHOD:

SUNDSTRAND IN-HOUSE C-25 GEAR ANALYSIS PROGRAM.

RESULTS:

CALCULATED G-10 LIFE BASED ON CML, ALL GEARS $> 10^6$ H. G-10 LIFE BASED ON 2PU, SHOCKLOAD, THE MINIMUM LIFE OF ALL THE GEARS (PMA IDLER) IS 26 H.

ASSUMPTIONS:

2 PU LOAD IS THE MOST SEVERE LOADING CONDITION AND ACCELERATION REQUIREMENTS WILL NOT ADVERSLEY AFFECT THE SYSTEM.

REFERENCE INFORMATION: AT INPUT ACCEL RATE OF 20% MINUTE INPUT SPEED (5000 RPM X 0.2 = 1,000 RPM/S). THE SYSTEM SHALL REGULATE WITHIN SPEC; AT 40% THE SYSTEM SHALL NOT INCURE DAMAGE. THIS CONVERTS TO A PMA MAX ACCELERATED RATE OF 11,111 RPM/S, USING A PMA ROTOR INERTIA OF APPROXIMATELY 0.04 IN-LB S². THE DRIVE TORQUE REQUIRED IS APPROXIMATELY 46 IN-LB. FOR PMB, MAX ACCEL RATE IS 20,000 RPM/S AND INERTIA IS APPROXIMATELY 0.02 IN-LB S² RESULTING IN A DRIVE TORQUE OF APPROXIMATELY 42 IN-LB.

Figure 5.7. Gear Design

2 P.U. CONDITION

Table 5.1. Gear Summary Differential Gear Box

	<u>PMA</u>			<u>PMB</u>		
MESH NO.	1/2 ***	3/4	4/5	67 ***	8/9	9/10
NO. TEETH	32/90	27/99	99/100	36/90	24/99	99/80
PITCH	32	20	20	32	20	20
CLASS	P1	3	3	P1	3	3
FACE WIDTH	0.53/0.53	0.56/0.81	0.81/0.61	0.53/0.53	0.35/0.4	0.47/0.37
LIFE HR *	69/106	50/26	591/2000	LARGE/LARGE	41/38	684/12,000
CONTACT RATIO	1.35	1.36	1.56	1.35	1.38	1.55
LOAD (IN LB)	210	524	1942	100	249	829
SPEED (RPM) **	28,000	11,200	3,024	50,000	20,000	6,000

* BASED ON BENDING
 ** USED IN LIFE ANALYSIS
 *** THIS IS A PRECISION GEAR ST.

Table 5.2. Gear Load

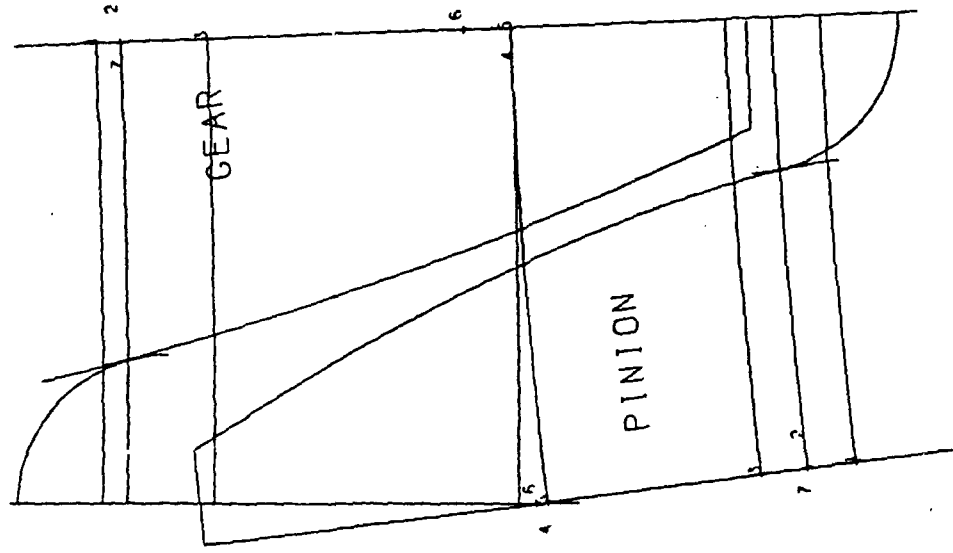
INPUT SPEED (RPM)	PMA (RPM)	POWER (KW)
3,000	27,777	69.55
4,200	38,888	42.18
5,400	50,000	15.59

PMA
(75 KW SHOCK LOAD)

INPUT SPEED (RPM)	PMA (RPM)	POWER (KW)
3,000	50,000	58.80
4,200	30,000	35.28
5,400	10,000	11.76

PMB
(75 KW SHOCK LOAD)

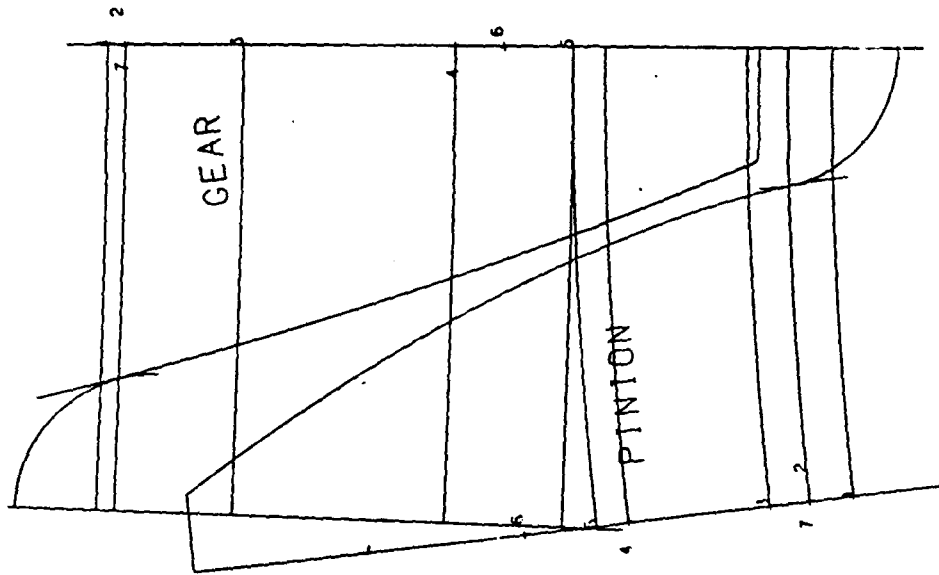
1 --MAX. STRESS CIRCLE 2 --SWEEPOUT
 3 --TIF 4 --P. D.--STD
 5 --P. D.--OPER. 6 --PARABOLA VERTEX
 7 --MAX. UNDERCUT SCALE .80 X
 09.17.35-C25



PMA GEAR 1-2
 (32 PITCH)

Figure 5.8. Gear Profile

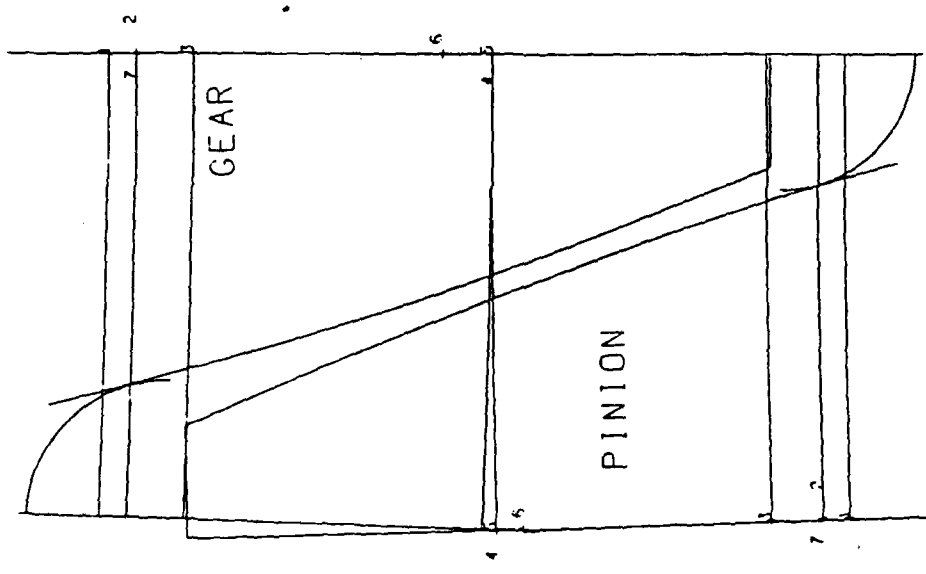
1 --MAX. STRESS CIRCLE 2 --SWEEPOUT
 3 --TIF 4 --P. D.--STD
 5 --P. D.--OPER. 6 --PARABOLA VERTEX
 7 --MAX. UNDERCUT SCALE 50 X
 09.17.35-C25



PMA GEAR 3-4
(20 PITCH)

Figure 5.9. Gear Profile

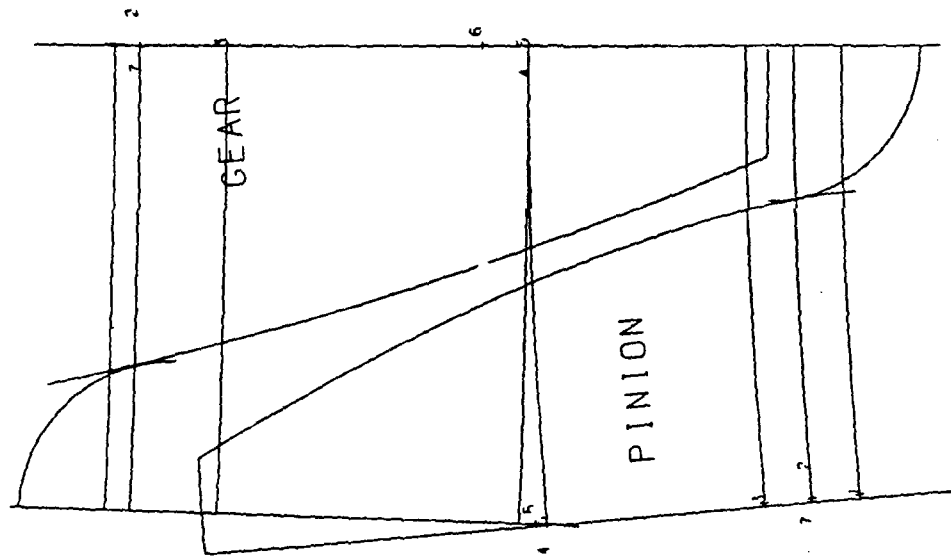
1 --MAX. STRESS CIRCLE 2 --SWEEPOUT
 3 --TIF 4 --P. D.--STD
 5 --P. D.--OPER. 6 --PARABOLA VERTEX
 7 --MAX. UNDERCUT SCALE 50 X
 09.17.35-C25



PMA GEAR 4-5
 (20 PITCH)

Figure 5.10. Gear Profile

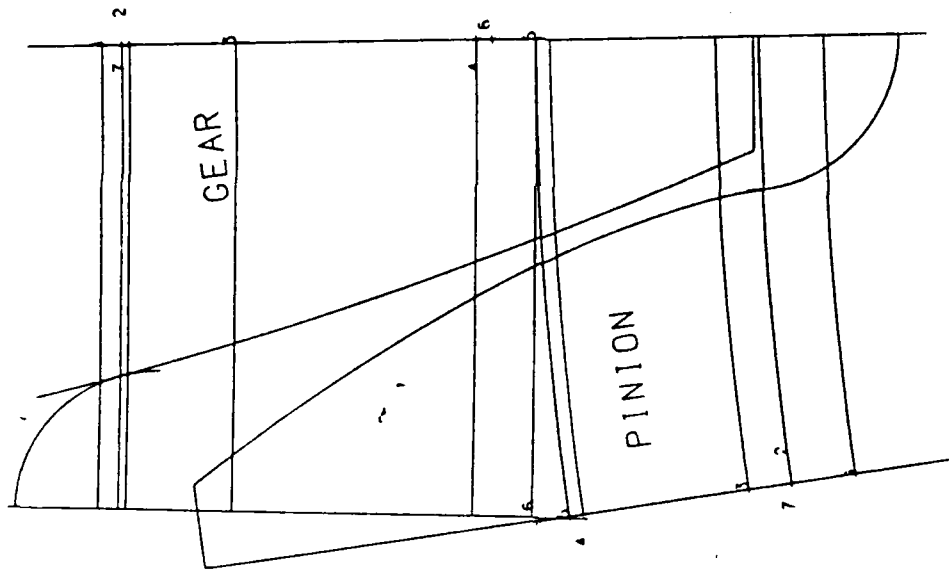
1 --MAX. STRESS CIRCLE 2 ---SWEEPOUT
 3 --TIF 4 --P. D.--STD
 5 --P. D.--OPER. 6 --PARABOLA VERTEX
 7 --MAX. UNDERCUT SCALE 80 X
 09.17.36-C25



PMB GEAR 6-7
 (32 PITCH)

Figure 5.11. Gear Profile

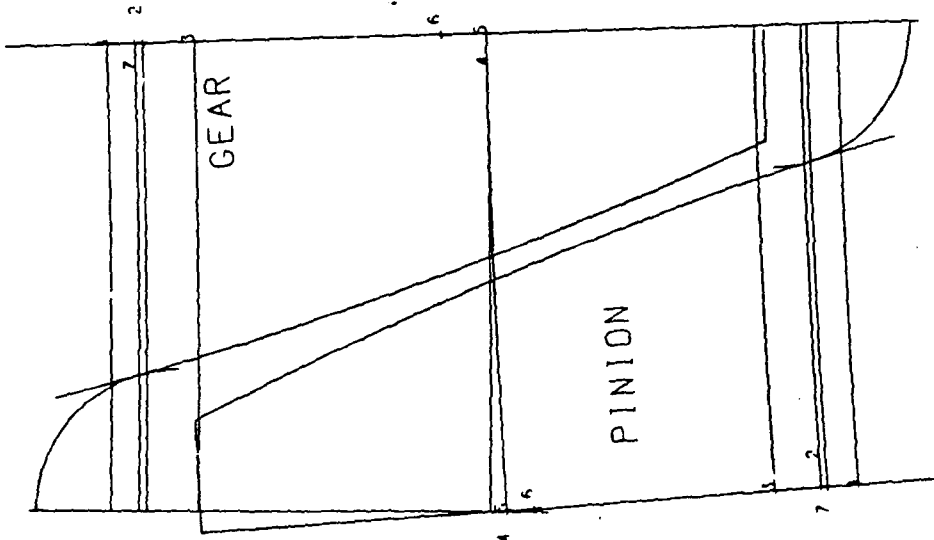
1 --MAX. STRESS CIRCLE 2 --SWEEP:POUT
 3 --TIF 4 --P. D.--STD
 5 --P. D.--OPER. 6 --PARABOLA VERTEX
 7 --MAX. UNDERCUT SCALE 50 X
 09.17.36-C25



PMB GEAR 8-9
 (20 PITCH)

Figure 5.12. Gear Profile

1 --MAX. STRESS CIRCLE 2 --SWEEPOUT
 3 --TIF 4 --P. D.--STD
 5 --P. D.--OPER. 6 --PARABOLA VERTEX
 7 --MAX. UNDERCUT SCALE 50 X
 09.17.36-C25



PMB GEAR 9-10
 (20 PITCH)

Figure 5.13. Gear Profile

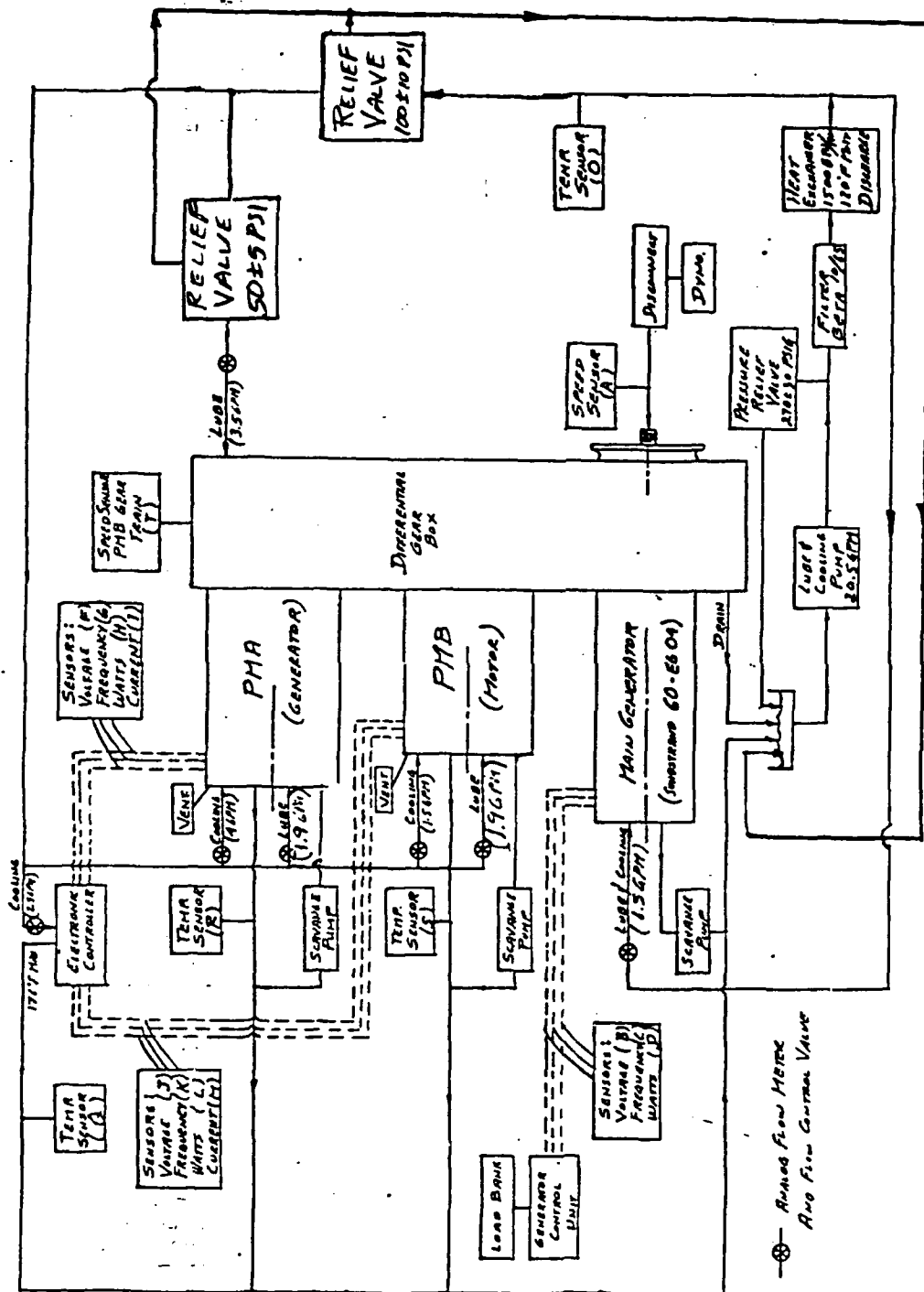


Figure 5.14. Differential Gear Box Test Schematic

Table 5.3. Gear Tooth Tip Modification

PMA POWER FLOW <-----	SAME GEAR										PMB POWER FLOW ---->	
	1	2	3	4 (3)	4 (5)	5	6	7	8	9 (8)		9 (10)
GEAR	36T	90T	27T	99T	99T	100T	36T	90T	24T	99T	99T	80T
DRIVER	/	/	/	/	/	/	/	/	/	/	/	/
DRIVEN	/	/	/	/	/	/	/	/	/	/	/	/
DEFLECTION	0.00030	0.00030	0.00055	0.00054	0.00049	0.00049	0.00014	0.00014	0.00050	0.00049	0.00044	0.00044
COMPUTER REC. TIP TOL. @ C	0.0000 0.0006	STD.	+0.0000 -0.0006	STD.	+0.0000 -0.0006	STD.	STD.	+0.0000 -0.0006	STD.	+0.0000 -0.0006	STD.	+0.0000 -0.0006
COMPUTER REC. TIP TOL. @ D	0.0002 0.0008	+0.0003 -0.0003	-0.0005 -0.0011	+0.0003 -0.0003	-0.0005 -0.0011	+0.0003 -0.0003	-0.0003 -0.0003	-0.000L -0.000B	+0.0003 -0.0003	-0.0005 -0.0011	+0.0003 -0.0003	-0.0005 -0.0011
TIP TOL. @ C	STD.	STD.	+0.0000 -0.0006	STD.	+0.0000 -0.0006							
TIP TOL. @ D	STD.	STD.	-0.0005 -0.0011	STD.	-0.0005 -0.0011							

Table 5.4. Bearing Information

APPLICATION	PMA/PMB ROLLER	PMA/PMB DUPLEX	JACK SHAFT/IDLER	INPUT SPLITTER GEAR END	INPUT SPLITTER INPUT END
PART NUMBER	EP2833-156	EP2833-36	4330-04UL-3AP	4320-11UL-3AP	5900892
SIZE/TYPE	205/ROLLER	2-205/ANG. CONT.	204/ROLLER	111/ROLLER	009/CONRAD
MANUFACTURER	SBB	SBB	SUNDSTRAND	SUNDSTRAND	SBB
CLASS	RBEC 5	ABEC 5	RBEC 1	RBEC 1	ABEC 1
ELEMENTS	10-9X9	12-.312 DIA.	12-7.5X9	20-9.5X12	15-.281 DIA.
INT. CLEARANCE	0.0015/0.0025	0.0008/0.0020	0.0010/0.0022	0.0018/0.0035	0.0014/0.0020
MAT. RACE/ELEM.	M-50	52100	52100	52100	52100
MAT. CAGE	4340 PLATED	AMS 6415	AL BRONZE	AL BRONZE	BRONZE
DYNAMIC LAB LB.	~5,500	~4,500/SET	~4,500	~13,000	~6,000
DN MAX	1.25X10 ⁶	1.25X10 ⁶	0.4X10 ⁶ @ J.S.	0.3X10 ⁶	0.2X10 ⁶
B-10 LIFE (HR) PMA SHOCK LOAD	11,000 HR @ MIN SPEED	32,000 HR @ MAX SPEED	*	*	*
B-10 LIFE (HR) PMB CML	300,000 HR @ MIN SPEED	32,000 HR @ MAX SPEED	*	*	*

* SPOT CHECK SHOWS CONSERVATIVE DESIGN

6.0 SYSTEM TEST

The performance goals for the ECCSD system of this report were taken from the constant speed drive requirements of the F-16 aircraft, General Dynamics specification no. 16ZEO27B. These requirements are summarized in Table 6.1.

Table 6.1 System Spec Summary

Output Speed:	12000 ± 120 rpm steady state 12000 ± 900 rpm shock load
Input Speed Range:	5000 - 9000 rpm (1.8:1)
Continuous Rating:	40/60 kVA
Shock Load:	95 kVA
Input Accel/Decel:	1000 rpm/s, perform to spec. 2000 rpm/s, no damage to result

With input gearing the normal range of input speed to the gearbox is 3,000 to 5,400 rpm. For this range of speeds both PMA and PMB will attain their maximum operating speed of 50,000 rpm. For the early stages of system testing the operating speed of PMA or PMB is being limited to 45,000 rpm. Thus, the gearbox input speed is restricted to be between 3,300 and 4,860 rpm.

System testing of the ECCSD began once the output speed control loop was working properly with the inverter driving PMB. At that point a regulated output speed of 12000 rpm was available to drive the 400 Hz generator. System testing involved two stages: the first stage used a static power supply for the inverter while the second stage involved connection of the SCR bridge to the inverter.

6.1 TESTING WITH STATIC DC SUPPLY

The first stage of testing allowed testing of the output speed controls without the complication of running the entire ECCSD system. The goal of this testing was simply to verify operation of the motor drive and output speed controls over a range of speeds and loads. The system input speed determines the required speed, and thus voltage, of PMB. The voltage applied to PMB is set by the inverter bus voltage. It is not possible to accurately track changes in system input speed by manually controlling the supply voltage. For this reason only testing at single speed points is possible with the inverter connected to a static supply.

Testing with a static power supply was done at input speeds of 4800, 4200, and 3600 rpm. These conditions correspond to PMB speeds of 20 krpm, 30 krpm, and 40 krpm, respectively. At each of these points the 400 Hz generator was subjected to 10 kW and 30 kW loads. The results of these tests are listed in Table 6.2.

Table 6.2 Test Results

Input Speed rpm	--4800--		--4200--		--3600--	
400 Hz Load* kW	10	30	10	30	10	30
PMB Speed rpm	-20,000-		-30,000-		-40,000-	
Inverter Voltage	117	117	177	177	236	236
Inverter Current	52	95	56	100	59	100
PMB Phase Volts rms	53.8	53.7	80.7	80.4	107.9	107.4
PMB Phase amperes rms	56.0	84.0	58.3	84.0	59.9	84.1
PMB Input Power	5.8	10.6	9.2	16.4	13.3	22.5
400 Hz Gen. Volts rms	121.0	121.2	120.9	121.3	120.9	121.2
400 Hz Gen. amperes rms	28.8	86.0	28.8	86.2	28.8	85.9
Output Speed Transient	114	267(rpm)	114	267	114	267

*nominal load @ 115 V rms

System response at 4,200 rpm for two load points is shown in Figure 6.1. This response is typical of that observed at other speeds. At this point in testing the output speed control algorithm has not been optimized. The oscilloscope waveforms in Figure 6.1 were recorded at 1 second per division, and the output speed is observed to recover in approximately two seconds.

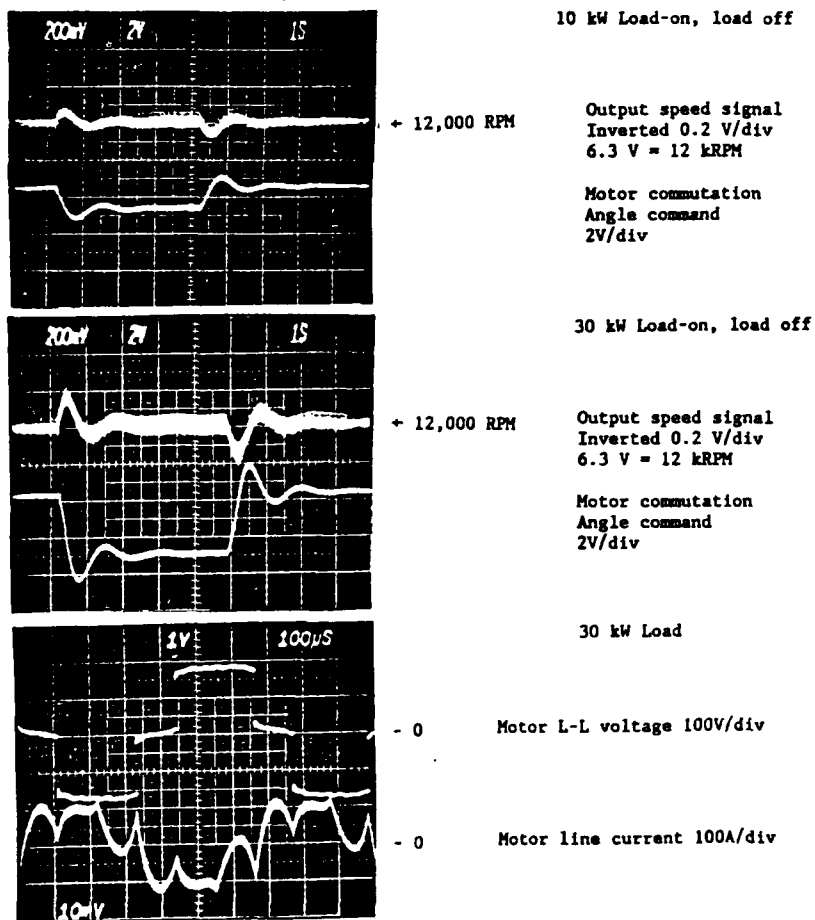


Figure 6.1. Typical System Response, 4200 RPM

The goal of testing with a static source is not to optimize output speed control. Instead proper operation of the motor, inverter, and speed control circuit is verified. Also, behavior of the system up to this point is in agreement with that predicted by the model. Because system response may be different when a nonideal source is used, further work on the controls at this point was not warranted.

6.2 SCR BRIDGE AND INVERTER COMBINED TESTING

In the interest of proceeding with full system testing as quickly as possible, testing with a static power supply was ended. The output speed control loop is stable with reasonable gain and phase margins. This allows testing at the system level to continue with effort focused on performance of the power converters.

The next step in testing of the system was to change over to the actual system configuration. That involved connection of the inverter bus to the SCR bridge output. Previous testing of the system was done using a very stiff source for the inverter driving PMB. Thus, there was little or no interaction of the inverter with the bus. Changing over to using the PMA and SCR bridge combination as the source of power for the inverter represents the first real test of the entire ECCSD system. Peculiarities of the system may be observed that were previously masked by the nearly ideal power source that was used.

The first tests focused on the inverter start mode to be sure that the motor would pass smoothly through the start mode and into the run-mode. Transients in the motor currents during motor start were observed. At one point two inverter transistors failed due to excessive current. The problem was traced to two areas; the bus current sensor and the inverter switching pattern.

Changes were made to the bus current sense circuit to increase its noise immunity and stop erroneous overcurrent trips.

The photo of Figure 6.2 documents misfiring of the inverter and the resultant motor current transient. As the bus voltage was increased the transients became large enough to trip the PMB protection circuit causing the inverter to be shutoff. The inverter misfiring was seen to occur at approximately the same point in the cycle of the six-step motor current waveform. Figure 6.3 shows the transients occurring on a once per revolution basis (6-pole motor). Because the inverter pattern was in error at only one portion of the motor revolution, the motor position sensor was determined to be the source of the problem. Drift in the output of the position sensor is responsible for the erroneous motor position signals.

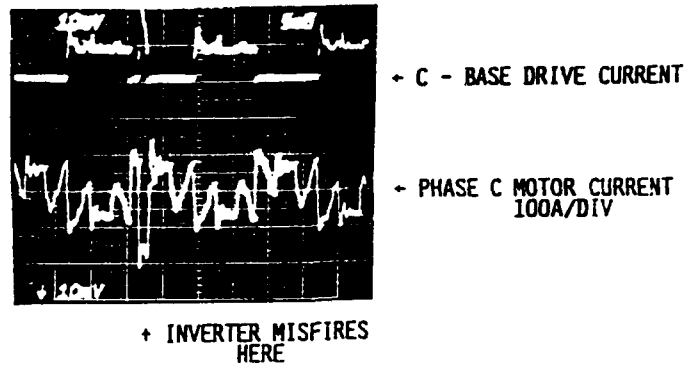


Figure 6.2. Inverter Current Showing Misfiring

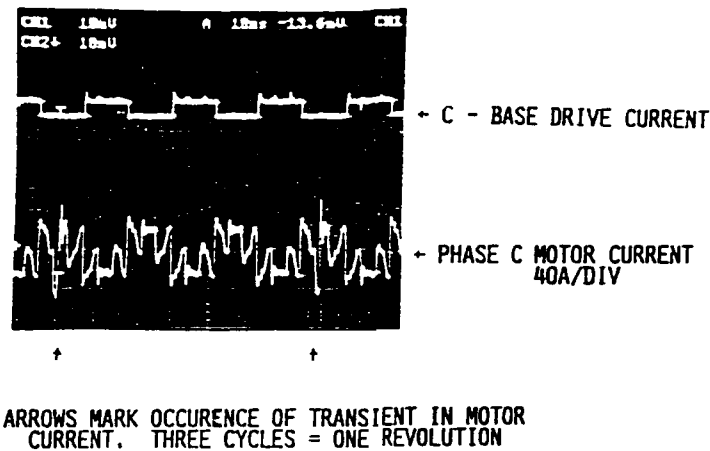


Figure 6.3. One Per Revolution Transients

Changes were made to the position sensor interface circuit to account for the changes in the position sensor output pattern. This was partially successful in that the motor current transients were reduced to the point where testing could continue. Figure 6.4 shows the motor current transient that occurs as the motor speed approaches the point where the motor control switches to run-mode and a different position sensor is used. Figure 6.5 shows smooth operation of the motor after the transition to run-mode.

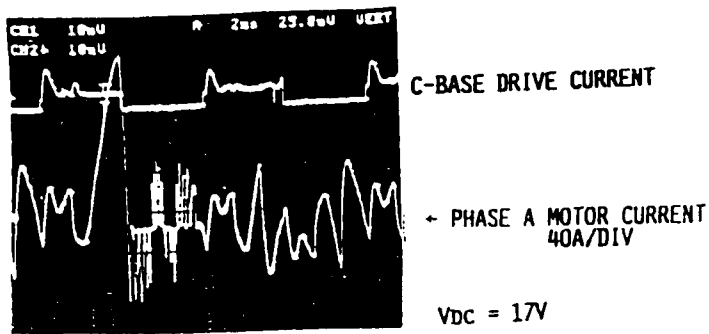


Figure 6.4. Motor Current Transient

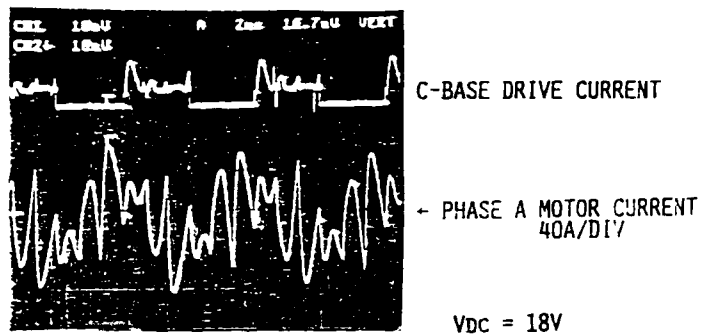


Figure 6.5. Motor Current in Run Mode

Once in the run-mode no problems were seen until the bus voltage approached 75 V. Wide variations in the magnitude of the motor current were observed. These variations were seen even though the motor commutation angle command (compensated error signal) was quite steady as shown in Figure 6.6. Figure 6.7 documents the excessive motor current and the resultant shutdown of the inverter by the PMB protection circuit. The cause of the problem seems to be in the portion of the motor control circuit that sets the commutation angle in response to the compensated error signal. This circuitry is apparently being upset by noise picked up from the SCR bridge commutation. Reconstruction of a portion of the motor control circuitry to improve its noise immunity would solve the problem.

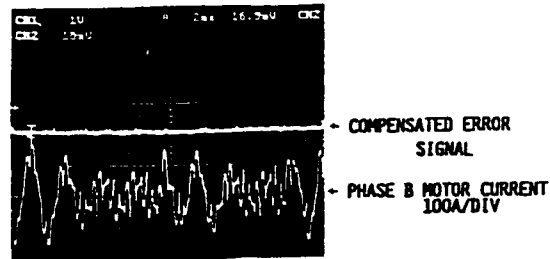


Figure 6.6. Motor Current Variations

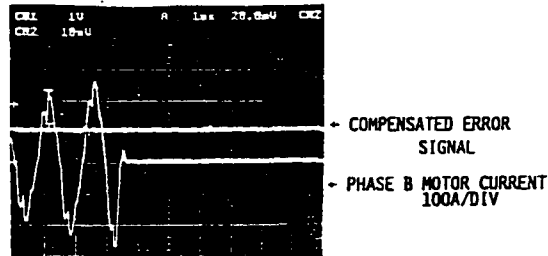


Figure 6.7. Excessive Current Causes Shut-down

At this point testing was stopped to prepare for demonstration of the system during an Air Force visit to Sundstrand in early July, 1988.

6.3 SYSTEM DEMONSTRATION

Testing of the full system with the output of the PMA/SCR bridge combination supplying the PMB/inverter combination advanced to the point of PMB spinning with no-load. The output speed control loop has not been closed with PMA supplying power to PMB.

In order to continue system testing, changes must be made to the Electric Power Processor. Rather than making changes and introducing unknowns that could interfere with a demonstration of progress made so far, testing was stopped. The decision was made to return to the configuration where PMB and the inverter are supplied by a static source. In this way the SCR bridge and inverter are demonstrated separately.

The demonstration of the system was performed for Air Force personnel on July 8, 1988. The demonstration of PMA and the SCR bridge showed regulation of the bridge output in response to rapid changes of input speed and step changes in load current. Details of SCR bridge operation are covered in section 3.1 of this report. PMB and the inverter were demonstrated by running the system under closed loop speed control with 10 kW and 30 kW loads at each of three input speeds. Operation of PMB and the

inverter at these points is described more thoroughly in section 6.1 of this report. Figure 6.8 shows the electronics test area during system test.

Both the PMA/SCR bridge and the PMB/inverter combinations were shown to perform as required at representative operating conditions. Therefore, two PM machines, the Electric Power Processor, the Gearbox, and Output Speed Control of the ECCSD system are all demonstrated. Additional development is required before the entire system can be demonstrated as a single unit.



Figure 6.8. System Test Area

7.0 CONCLUSIONS AND RECOMMENDATIONS

All of the major subsystems required in the ECCSD system have been demonstrated. The two permanent magnet machines, gearbox, SCR bridge, and inverter have all been tested at representative operating points. System output speed control has been demonstrated with 10 kW and 30 kW loads at 3600, 4200, and 4800 rpm.

No inherent barriers to operation of the full ECCSD system were uncovered during development. The full system was run no-load, open loop for motor speeds up to 14 krpm. Further development should focus on operation of the SCR bridge, inverter, and output speed controls if all performance goals for the system are to be achieved.

Component efficiencies and the resulting system efficiency were predicted during the design process. Simulation revealed that the desired performance goals can be met by the ECCSD system described in this report. Further testing of the complete ECCSD system is required before actual efficiency and performance limitations can be verified.

The section of the position sensor for PMB that provides absolute motor position for motor starting requires further development. The high speed, high accuracy sensor used to operate the brushless motor, PMB at normal running speeds worked properly during the entire period of testing. Thus, the key portion of the position sensor used with PMB performs as required.

Because of the high output voltage from PMA at high speeds (970 V peak to peak), a converter employing thyristors is used for to conversion. This is a proven technology at Sundstrand and the risk is low. Switching losses are low in this converter circuit because natural commutation is used. This converter is more efficient than circuits using hard switching techniques. A major disadvantage of the controlled rectifier system is that the input power factor varies with delay angle. In this application, input power factor is lowest at high PMA output voltage with low output voltage from the converter.

Input voltage distortion can disturb the proper operation of the controlled rectifier via the synchronization circuit for phase delay control. Additional circuitry required by the converter to operate on a distorted voltage source inevitably affects and degrades the dynamic performance of the controlled-rectifier system. It would be desirable to have a separate 3 phase low-voltage output on the PMA. This arrangement would be similar to a position sensor where the low-voltage output is aligned (in phase) with the output from the main three-phase winding on the generator. The low-voltage output would be used to provide thyristor turn-on timing information. Since this signal is a clean sine wave and not affected by the voltage distortion at the generator terminals, problems caused by the interaction of the nonlinear load with the generator source

impedance will be completely eliminated. This will further simplify the design of the electronics as no special circuitry is required for the processing of a distorted timing reference signal.

If there is a need to further improve the dynamic response of the controlled-rectifier system, synchronization of the thyristor turn-on timing signals to all three-input phases is desirable. This approach will increase the speed of response by at least a factor two at the expense of component count.

The dynamic performance of the inverter drive system operating on a weak voltage supply has not been fully investigated. System stability will be largely affected by the degree of decoupling of the inverter from the rectifier. Due to the constraint of having minimum storage elements in the power circuit, the PMA/controlled rectifier system can not provide a stiff voltage source characteristic that is desirable for the PMB/inverter drive system. Both the inverter drive and the thyristor converter desire a low impedance source to ensure stable operation over a wide speed range.

A stiff voltage source characteristic is difficult to implement due to

- (a) a ratio, of the system fault level to the equipment rating, that is low and
- (b) source (PMA) impedance that increases with operating speed.

If there is no constraint on the filter size, the inverter drive system can be effectively decoupled from the thyristor converter by adding a very large capacitance to the link to approximate an ideal voltage source. This, however, increases the interaction of the thyristor converter with the generator impedance and could cause instability in the total system.

A more sophisticated control scheme for the inverter/PMB combination would reduce undesirable harmonics present in the motor currents. This would have little benefit at higher loads, but could improve system efficiency at light loads.

The approach taken for the development of the power converters for the ECCSD is considered low risk. The always below straight through configuration has high efficiency at the upper end of the input speed range. It suffers from a weight disadvantage, though, because the speed compensation components are designed to carry more power than for a midrange system.

An ECCSD system operating with a speed range including straight through would minimize power flow in the speed compensation path and greatly reduce the required power rating of the PM machines. A significant development

effort is required, however, to produce a suitable bidirectional power converter that is both simple (highly reliable) and efficient.

Other features of the ECCSD concept remain to be investigated in detail. Inclusion of features such as emergency power or engine starting has the potential of making the ECCSD competitive with existing aircraft power generation schemes.

APPENDIX A

DESIGN CONSTRAINTS

1.0 STUDY DESIGN CONSTRAINTS

The design constraints given are those developed to meet the requirements of the study, and establish those guidelines needed to complete the comparative trades and complete a breadboard design. As design progresses, additions will be added as needed. Further definition is required.

1.1 DEVELOPMENT COMPONENTS

Development components will consist of one breadboard set of hardware consisting of two motor/generators and one controller.

1.1.1 MOTOR/GENERATOR DRAWINGS

Layout, and detail drawings shall be produced to provide documentation details sufficient to produce prototype units.

1.1.2 CONTROLLER

Controller schematics and parts identification shall be in detail sufficient to define the breadboard construction.

2.0 APPLICATION DATA AND ASSUMPTIONS

2.1 SPEED RANGE

The input speed range shall be 1.9/1.0.

2.1.2 SPEED LIMITS

The input shaft speed range shall be 4666-8438 RPM with overspeed to 8860 RPM.

3.0 OIL SYSTEM

The oil system used for both cooling and lubrication of motor/generator and controller shall operate under the following conditions.

3.1 OIL TEMPERATURE

Cooling oil temperature limits are 275°F maximum with excursions to 285°F for all rotating components. Minimum oil inlet temperature will be no lower than -65°F. Oil cooling temperature for the controller shall have a maximum limit of (TBD°F) and a minimum limit of -65°F.

3.1.1 OIL TYPE

The oil type shall be MIL-L-7808 on MIL-L-23699.

3.1.2 OIL FLOW

Oil flow for lubrication and cooling shall not exceed 2.5 gal/min.

3.1.3 OIL PRESSURE DROP

Pressure drop across any cooling circuit shall not exceed 75 lb /in.

3.1.4 CHANGE PRESSURE

Cooling oil pressure shall be a maximum of 240-280 lbf/in.

4.0 COOLING

Oil cooling shall be such that drag losses of rotating components are minimized and oil deterioration of components is minimized.

4.1 AMBIENT AIR

Ambient air temperatures are to be used for proof of principle development testing. These limits can be assumed to be a minimum of 65°F and a maximum of 100°F.

4.1.1 AMBIENT PRESSURE

Ambient pressure for development will be sea level pressure.

5.0 PERFORMANCE GOALS

The components being analyzed shall be developed to function with a system having the following requirements.

5.1 RATING

A system output kVA at the generator terminals shall be 30/40-kVA with a P.F. range of 0.75 to 1.0.

5.2 FREQUENCY CHARACTERISTICS

The frequency characteristics shall be in accordance with Figure A-1.

5.2.1 FREQUENCY MODULATION

Frequency modulation shall not exceed the limits of Figure A-2.

5.3 SYSTEM EFFICIENCY

The system efficiency for electric drive shall be similar to a greater than the efficiency of a constant speed drive. The mechanical efficiency of a CSD excluding the generator is maximum of 88% for the straight through condition. For a speed range of 1.8:1 the system efficiency excluding generator is 80-82 percent at upper and lower speed point.

5.4 CONTROLLER

- 5.4.1 Maximum current density in conductors at 2.0 per unit load: TBD.
- 5.4.2 Maximum flux density in transformers and chokes: TBD.
- 5.4.3 MOSFET technology will be used for switching elements.
- 5.4.4 Maximum working voltage in the controller: 450 V.
- 5.4.5 Maximum switching elements currents: TBD.
- 5.4.6 Maximum switching frequency: TBD.
- 5.4.7 Maximum semiconductor junction temperature: 1125°C.
- 5.4.8 Cooling fluid temperature: TBD.
- 5.4.9 Ambient laboratory air temperature: 65° to 100°F.

6.0 CONFIGURATIONS

The five basic configurations for differential, motor/generator and controller are illustrated in Figures I, II, III, IV and V.

7.0 DYNAMIC SIMULATION

8.0 MOTOR/GENERATORSeu

- 8.1 Maximum speed not to exceed 40,000 RPM.
- 8.2 Armature current density not to exceed 26 kA/in² at 2.0 p.u. load.
- 8.3 All machines are 6-pole permanent magnet.
 - 8.3.1 Magnets used are to be 27 MGOe samarium cobalt.
 - 8.3.2 Machines are all to be three phase.
- 8.4 Motor/generators shall use common laminations.
- 8.5 Back iron fluid cooling will be used.
- 8.6 The conduction angle for the 3-phase full wave inverter bridge will be 180°.

8.6.1 Control circuitry shall provide the needed commutation angle to support proper motor operation for the required output.

8.6.2 Minimum operating power factor of 0.9 is assumed.

9.0 CONTROLLER

10. FUNCTIONAL TESTING

10.1 Motor/generator output voltage vs RPM to determine back E.M.F.

10.1.1 Motor/generator vs load characteristic to establish units power source capability.

10.1.2 Motor/generator machine constants, resistance, inductance.

10.1.3 Dielectric integrity of phase and phase to ground insulation. Test voltages will be 1000 volts pulse 2 times highest line to line voltage.

10.1.4 Rotor position tests. A series of test shall be made to determine that the rotor position signals are properly oriented with respect to stator windings.

10.2 CONVERTER FUNCTIONAL TESTING

10.2.1 Internal power supplies. Power supplies will be tested to determine if power output requirements meet controller power requirements.

10.2.2 Control strategy testing. Tests will be run to verify functional operation of control strategy.

10.2.3 Power control tests. Tests of the power controller and internal power supplies to determine performance characteristics for the following operating modes.

10.2.3.1 Input speed greater than regulated speed.

10.2.3.2 Input speed less than regulated output speed.

10.2.3.3 Input speed is near the straight through speed.

10.3 CONVERTER/MOTOR GENERATOR

10.3.1 System Test. The system loop consisting of motors/generators and controller shall be closed. These tests will not include a differential.

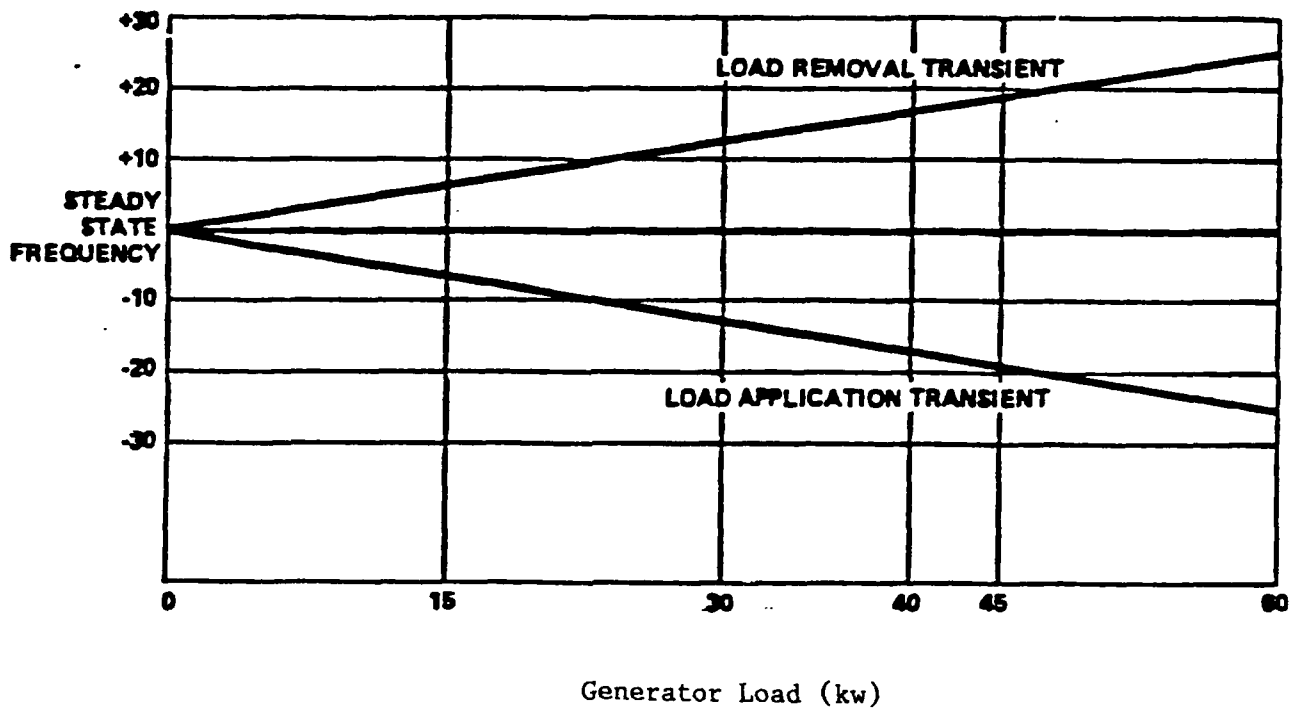
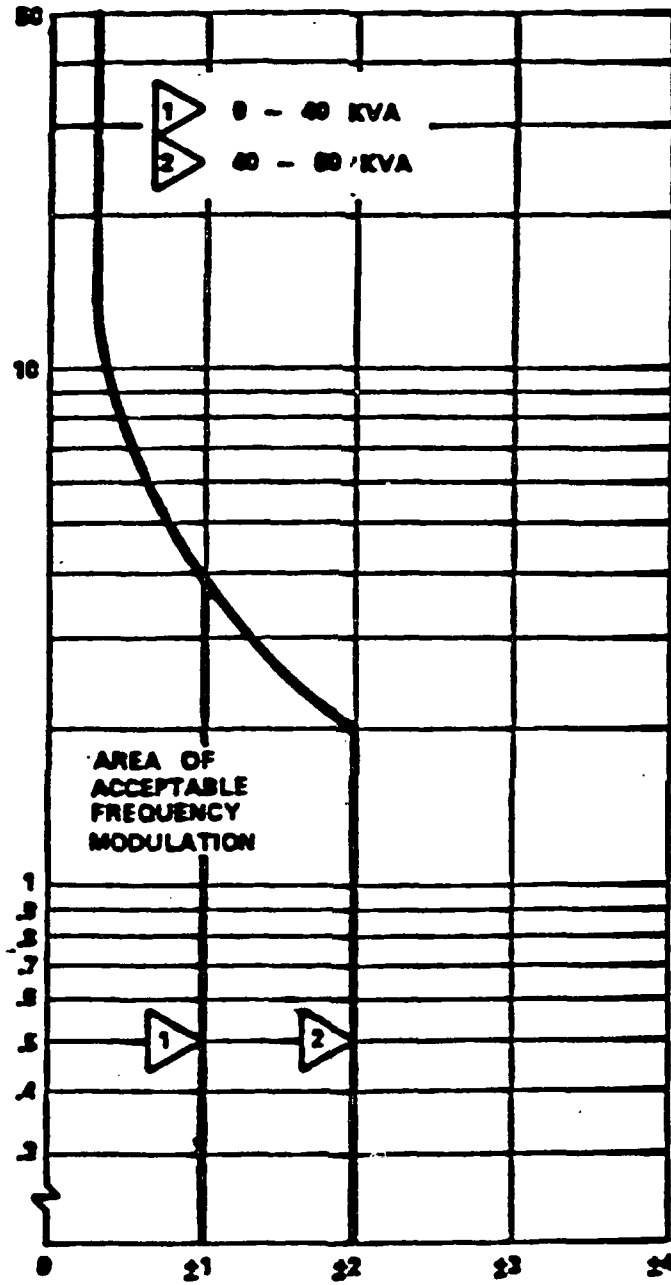


Figure A-1. Transient Frequency Limits

FREQUENCY MODULATION REPETITION RATE - Hz



Frequency Modulation Amplitude - Hz

Figure A-2. Frequency Modulation Limits

APPENDIX B

ELECTROMAGNETIC DESIGN TRADE STUDY

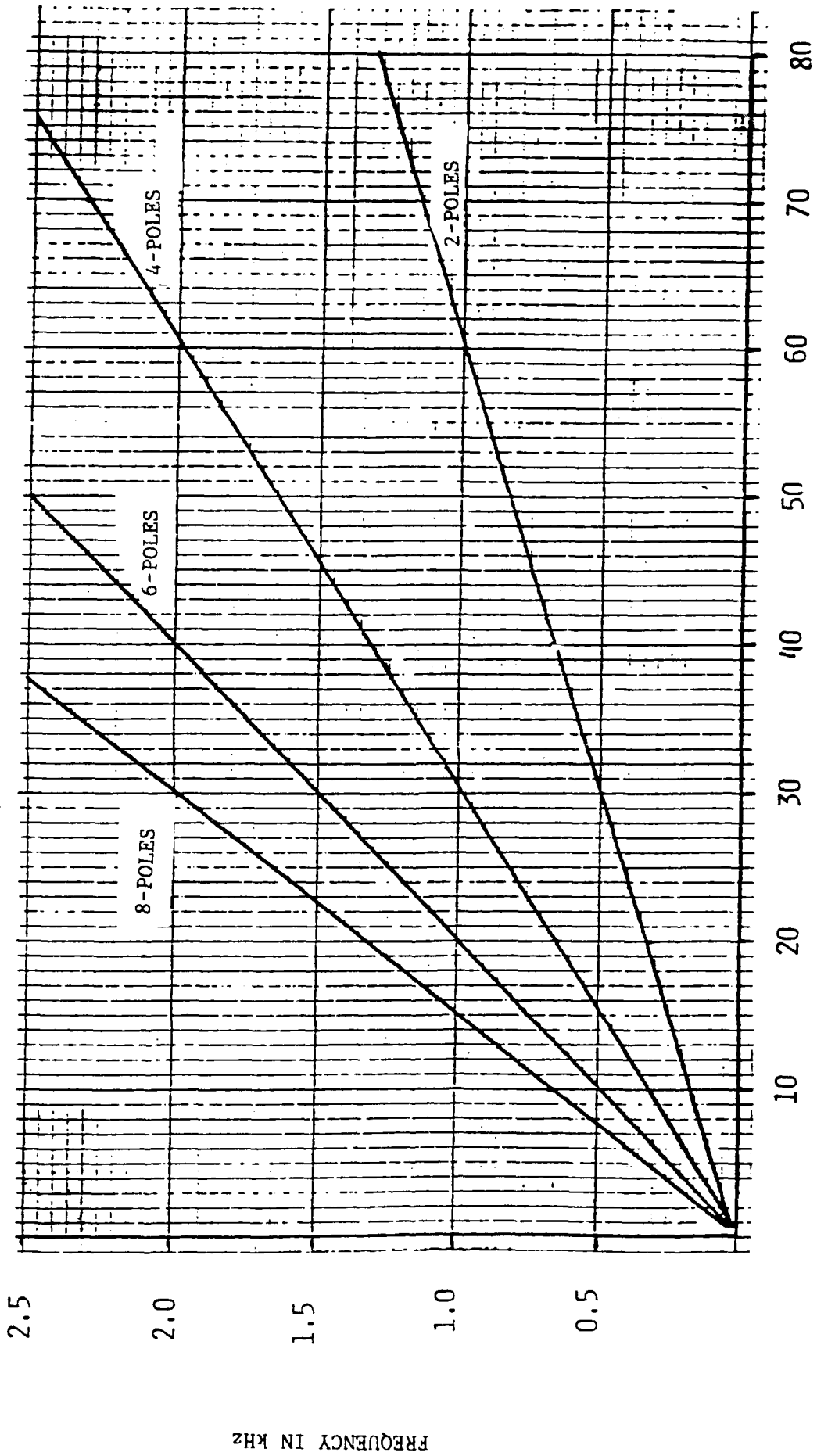
An electromagnetic design trade study was performed to determine optimum machine configuration. The study addressed key design parameters; number of poles, operating speed, and radial/tangential configuration. The objective is to find a combination of the above mentioned parameters which yield the lightest machine within the boundary of our constraints. The recommended design is a six-pole tangential configuration with a maximum operating speed of 50,000 rpm.

OPERATING SPEED

The operating speed along with the number of poles dictate the machine frequency. Figure B-1 shows a plot of frequency versus speed for two, four, six and eight-pole machines. Note that an eight-pole machine reaches 2.5 kHz frequency at a 37.5-KRPM speed. This maximum operating frequency is one of our constraints. It is dictated by the power conversion technique, pulse width modulation, used in designing the power electronics for this project. Consequently, an eight-pole machine must not exceed the 37.5-KRPM speed. This implies that an eight-pole or greater machine is likely to be heavier than a machine with less number of poles operating at a higher speed. Figure B-1 shows that we may go to higher speeds for machines with less number of poles. Therefore, we discard the eight-pole configuration.

NUMBER OF POLES

We now have the option of selecting a two, four, or six-pole machine, and for the moment let us focus on a two-pole configuration. A two-pole machine will be heavier than a four-pole machine with both operating at the same speed. That is to say that a two-pole machine at 70-KRPM will be electromagnetically heavier than a four-pole machine at 70-KRPM. This is due to the fact that a two-pole machine has to carry more electromagnetic flux in the back-iron of its armature. Consequently the armature back-iron has to be thicker in order to maintain the flux density at a proper level. Note that the maximum operating speed of 70-KRPM is one of our design constraints due to the mechanical risk for high reliability and product life. Therefore, we discard a two-pole machine.



Revolutions/Min x 1000

Figure 11.1. Machine Frequency vs Speed for Varying Number of Poles

We are now left with the options of a four or six-pole configuration and any further elimination must be based on rough electromagnetic designs. Start by designing two four-pole machines operating at 40-KRPM and 70-KRPM, respectively. The designs indicate that the 70-KRPM machine is lighter by a factor of roughly 25 percent. This is in line with our expectations. However, we are now sitting right at our maximum speed constraint. With these facts at hand, we may think that a six-pole machine operating at 40-KRPM may be comparable, in terms of weight, to the four-pole 70-KRPM design. The results show that the six-pole 40-KRPM design is comparable to the four-pole 70-KRPM and in addition, allow us to place less stress on the mechanical parts since we are now operating at a lower speed. Therefore, we discard the four-pole machine. The remaining question to be addressed is, should this machine be of radial or tangential direction of magnetization. Again, we must proceed with a design to make a valid conclusion.

DIRECTION OF MAGNETIZATION

Designs were carried out for a six-pole 40-KRPM having radial and tangential direction of magnetization. The results indicate that a tangential configuration will be slightly heavier than a radial configuration in terms of electromagnetic weight. However, the tangential configuration allows for damper bars to be placed in the rotor poles. Damper bars help to reduce switching transients. These transients can cause significant stress on the solid state devices. One of our design goals is to limit excessive stressing of the power electronics in order to achieve high reliability. Consequently we choose the tangential configuration.

Note, however, that we can further optimize the machine total configuration by increasing the operating speed to 50-KRPM without exceeding any constraints. Therefore, we proceed with a six-pole 50-KRPM radial design and obtain the lightest machine within our constraints and assumptions. Finally, the assumption is made that both permanent magnet machines will have the same configuration in terms of number of poles, operating speed and direction of magnetization based on this trade study.